Supporting Information

The Fate of the Contact Ion Pair Determines the Photochemistry of Coumarin-Based Photocleavable Protecting Groups

Albert Marten Schulte,[1,‡] Georgios Alachouzos,[1,‡/*] Wiktor Szymanski,[1,2*] Ben L. Feringa[1*]

[1] Centre for Systems Chemistry, Stratingh Institute for Chemistry, Faculty for Science and Engineering, University of Groningen, Nijenborgh 4, 9747 AG Groningen, The Netherlands;

[2] Department of Radiology, Medical Imaging Center, University Medical Center Groningen, University of Groningen, Hanzeplein 1, 9713 GZ Groningen; The Netherlands

[‡] These authors contributed equally to this work.

Contents

1. General remarks

All reactions were performed without excluding moisture or air, unless stated otherwise. Standard Schlenk techniques were used for reactions requiring an inert atmosphere (using nitrogen as the inert gas). Reagents were purchased from commercial suppliers (Sigma-Aldrich, Combi-Blocks, TCI etc.) and used without further purification. Solvents were purchased from Boom B.V. or Sigma-Aldrich. Flash chromatography was performed on silica gel (Supelco, silica gel 60) with a particle size of 40-64 µm. TLC analysis was conducted on TLC plates with a silica gel matrix (Supelco, silica gel 60) with detection by UV-light (254 or 366 nm).

Nuclear magnetic resonance (NMR) spectra were recorded on an Agilent Technologies 400-MR (400/54 Premium Shielded) spectrometer (400 MHz for ^{1}H nucleus, 101 MHz for ^{13}C nucleus). Deuterated solvents (DMSO-d_6 and $CDCl_3$) were purchased from Sigma-Aldrich. The chemical shift of compound resonances is given in parts per million (ppm, δ) and reported relative to the residual solvent proton or carbon resonance. All spectra were measured at ambient temperature. ^{1}H-NMR data are reported as: chemical shift, multiplicity (s = singlet, d = doublet, t = triplet, q = quartet, m = multiplet, dd = doublet of doublets, dt = doublet of triplets, dq = doublet of quartets, br = broad), coupling constants (J) given in Hz, and integration. ^{13}C-NMR spectra were conducted with proton decoupling and the chemical shifts are reported.

High resolution mass spectra (HRMS) were recorded on a Thermofisher LTQ Orbitrap XL with eluent MeOH (0.1 % TFA) and flow rate of 0.15 mL min^{-1} in positive (ACPI/ESI) mode. UV-vis spectra were recorded with an Agilent 8543 spectrophotometer. Raw data were processed using Agilent UV-vis Chemstation B.02.01 SP1, Spectragryph 1.2, OriginPro 8.5 and MS Excel.

2. Synthetic methods

2.1 Synthetic scheme

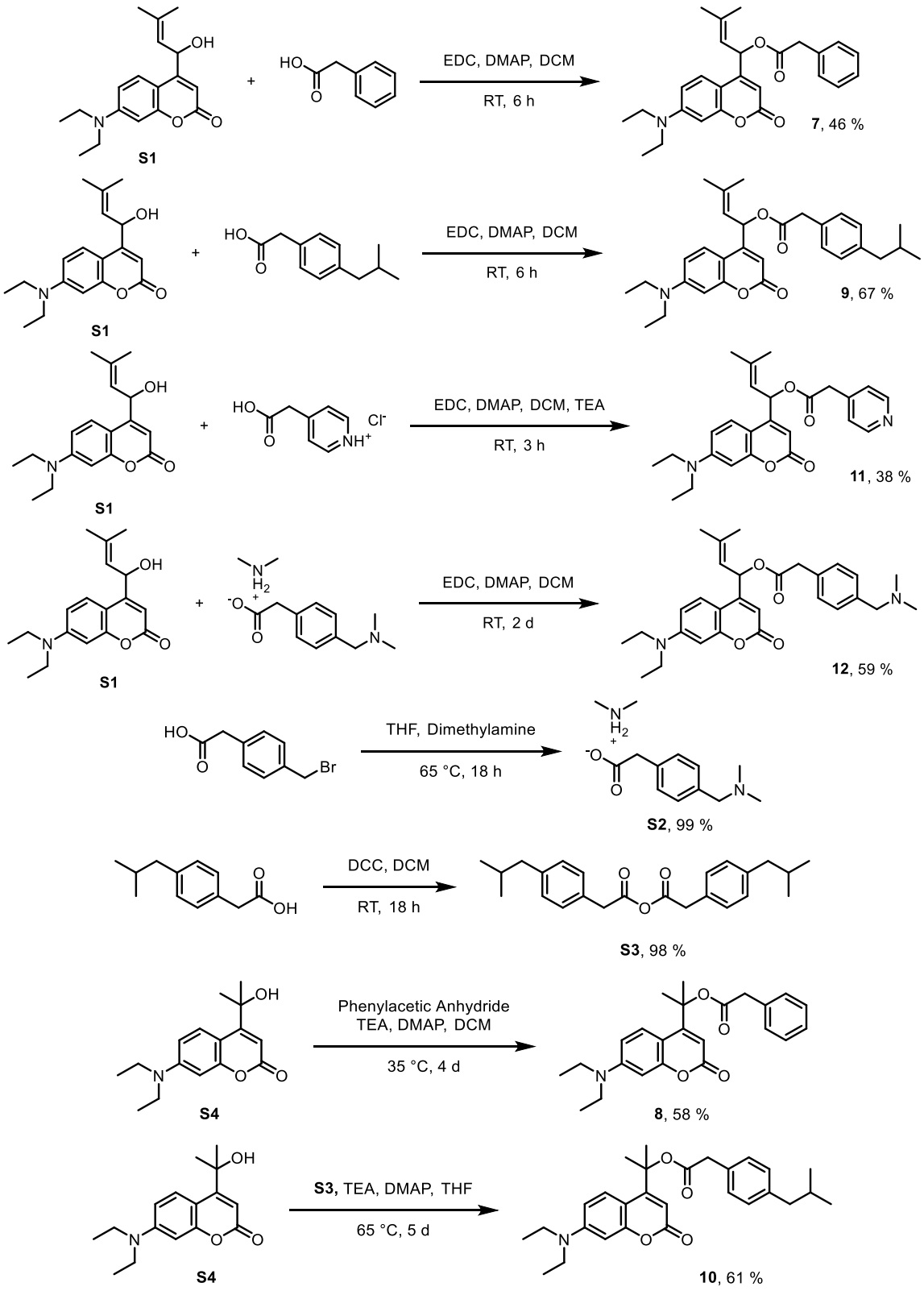

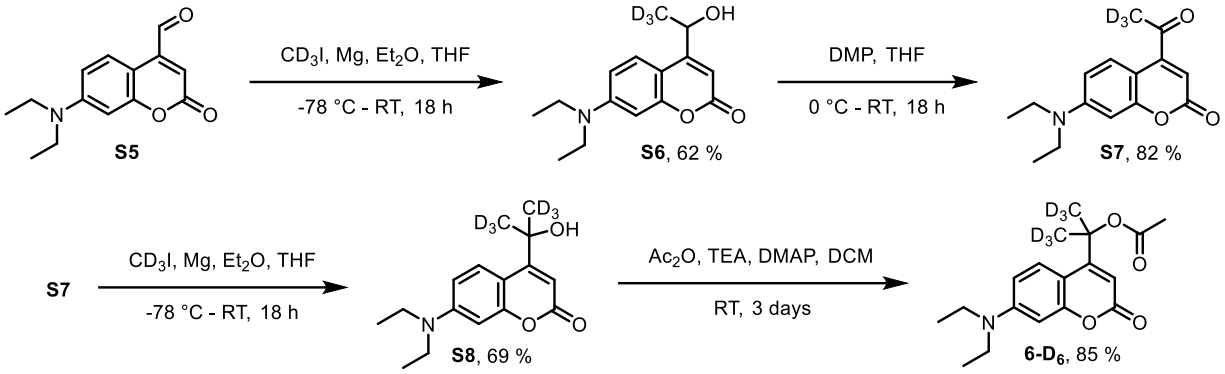
S5
CD3I, Mg, Et2O, THF
-78 °C - RT, 18 h
S6, 62 %
DMP, THF
0 °C - RT, 18 h
S7, 82 %
S7
CD3I, Mg, Et2O, THF
-78 °C - RT, 18 h
S8, 69 %
Ac2O, TEA, DMAP, DCM
RT, 3 days
6-D6, 85 %

2.2 Experimental procedures

2.2.1 Formation of prenyl PPGs **7**, **9**, **11** and **12**

Compound **7** (1-(7-(diethylamino)-2-oxo-2H-chromen-4-yl)-3-methylbut-2-en-1-yl 2-phenylacetate)

To a suspension of Prenyl-Coumarin-Alcohol (prepared as described previously)[1] (**S1**, 110 mg, 0.37 mmol, 1.00 eq.) and phenylacetic acid (99 mg, 0.73 mmol, 2.00 eq.) in DCM (5 mL) under a nitrogen atmosphere was added EDC (140 mg, 0.73 mmol, 2.00 eq.) and DMAP (4 mg, 0.04 mmol, 0.10 eq.). The solution was stirred for 6 h at room temperature in the dark, diluted with DCM (20 mL) and washed with 0.5 M aq. HCl (20 mL) and sat. aq. $NaHCO_3$ (20 mL). The organic layer was dried over $MgSO_4$, filtered, and concentrated under reduced pressure. The crude product was purified by silica gel chromatography (pentane/ethyl acetate 8:1 to 6:1) to give **7** as a yellow oil (70 mg, 46 %). **^{1}H-NMR** (400 MHz, $CDCl_3$) δ 7.33 – 7.22 (m, 6H), 6.59 (d, *J* = 9.3 Hz, 1H), 6.52 – 6.42 (m, 2H), 6.06 (s, 1H), 5.24 (dt, *J* = 9.3, 1.4 Hz, 1H), 3.67 (s, 2H), 3.37 (q, *J* = 7.1 Hz, 4H), 1.85 (d, *J* = 1.3 Hz, 3H), 1.73 (d, *J* = 1.4 Hz, 3H), 1.17 (t, *J* = 7.1 Hz, 6H). **^{13}C-NMR** (101 MHz, $CDCl_3$) δ 170.5, 162.3, 156.6, 153.9, 150.5, 141.1, 133.6, 129.4, 128.7, 127.4, 125.4, 121.0, 108.6, 106.1, 105.8, 98.0, 69.1, 44.8, 41.5, 26.0, 18.9, 12.6. **HRMS** (ESI): calc. for $C_{26}H_{30}NO_4^+$ ($M+H^+$): 420.2169; found: 420.2167.

Compound **9** (1-(7-(diethylamino)-2-oxo-2H-chromen-4-yl)-3-methylbut-2-en-1-yl 2-(4-isobutylphenyl)acetate)

To a suspension of Prenyl-Coumarin-Alcohol (prepared as described previously)[1] (**S1**, 82 mg, 0.27 mmol, 1.00 eq.) and Ibufenac (63 mg, 0.33 mmol, 1.20 eq.) in DCM (4 mL) under a nitrogen atmosphere was added EDC (63 mg, 0.33 mmol, 1.20 eq.) and DMAP (3 mg, 0.03 mmol, 0.10 eq.). The solution was stirred for 6 h at room temperature in the dark, diluted with DCM (20 mL) and washed with sat. aq. $NaHCO_3$ (20 mL). The organic layer was dried over $MgSO_4$, filtered, and concentrated under reduced pressure. The crude product was purified by silica gel chromatography (pentane/Ethyl acetate (9:1 to 6:1) to give **9** as a yellow powder (86 mg, 67 %). **^{1}H-NMR** (400 MHz, $CDCl_3$) δ 7.29 (d, *J* = 9.0 Hz, 1H), 7.17 (d, *J* = 8.0 Hz, 2H), 7.09 (d, *J* = 8.0 Hz, 2H), 6.60 (d, *J* = 9.2 Hz, 1H), 6.51 (dd, *J* = 9.0, 2.6 Hz, 1H), 6.48 (d, *J* = 2.5 Hz, 1H), 6.10 (s, 1H), 5.26 (d, *J* = 9.2 Hz, 1H), 3.66 (s, 2H), 3.39 (q, *J* = 7.1 Hz, 4H), 2.45 (d, *J* = 7.2 Hz, 2H), 1.90 – 1.79 (m, 4H), 1.74 (s, 3H), 1.19 (t, *J* = 7.1 Hz, 6H), 0.89 (d, *J* = 6.6 Hz, 6H). **^{13}C-NMR** (101 MHz, $CDCl_3$) δ 170.7, 162.3, 156.7, 154.0, 150.5, 141.1, 140.8, 130.8, 129.5, 129.1, 125.5, 121.1, 108.6, 106.1, 105.9, 98.0, 69.1, 45.2, 44.8, 41.1, 30.3, 26.0, 22.5, 18.9, 12.6. **HRMS** (ESI): calc. for $C_{30}H_{38}NO_4^+$ ($M+H^+$): 476.2795; found: 476.2794.

Compound **11** (1-(7-(diethylamino)-2-oxo-2H-chromen-4-yl)-3-methylbut-2-en-1-yl 2-(pyridin-4-yl)acetate)

To a suspension of Prenyl-Coumarin-Alcohol (prepared as described previously)[1] (**S1**, 168 mg, 0.56 mmol, 1.00 eq.) and 2-(pyridin-4-yl)acetic acid (193 mg, 1.12 mmol, 2.00 eq.) in DCM (8 mL) under a nitrogen atmosphere was added EDC (214 mg, 1.12 mmol, 2.00 eq.), DMAP (7 mg, 0.06 mmol, 0.10 eq.) and triethylamine (155 µL, 1.12 mmol, 2.00 eq.). The solution was stirred for 3 h at room temperature in the dark, diluted with DCM (50 mL) and washed with sat. aq. $NaHCO_3$ (50 mL). The organic layer was dried over $MgSO_4$, filtered, and concentrated under reduced pressure. The crude product was purified by silica gel chromatography (DCM/acetone (19:1 to 4:1) to give **11** as an orange oil (90 mg, 38 %). **^{1}H-NMR** (400 MHz, $CDCl_3$) δ 8.55 (d, *J* = 6.1 Hz, 2H), 7.25 (d, *J* = 8.5 Hz, 1H), 7.21 (d, *J*

= 6.0 Hz, 2H), 6.61 (d, *J* = 9.3 Hz, 1H), 6.50 (d, *J* = 8.9 Hz, 2H), 6.10 (s, 1H), 5.26 (dt, *J* = 9.3, 1.5 Hz, 1H), 3.69 (s, 2H), 3.38 (q, *J* = 7.1 Hz, 4H), 1.87 (s, 3H), 1.75 (s, 3H), 1.19 (t, *J* = 7.1 Hz, 6H). **^{13}C-NMR** (101 MHz, $CDCl_3$) δ 169.0, 162.3, 156.7, 153.6, 150.6, 150.2, 142.4, 141.6, 125.3, 124.7, 120.7, 108.6, 105.9, 105.8, 98.0, 69.7, 44.8, 40.7, 26.0, 18.9, 12.6. **HRMS** (ESI): calc. for $C_{25}H_{29}N_2O_4^+$ ($M+H^+$): 421.2122; found: 421.2115.

Compound **12** (1-(7-(diethylamino)-2-oxo-2H-chromen-4-yl)-3-methylbut-2-en-1-yl 2-(4-((dimethylamino)methyl)phenyl)acetate)

To a suspension of Prenyl-Coumarin-Alcohol (prepared as described previously)[1] (**S1**, 97 mg, 0.32 mmol, 1.00 eq.) and **S2** (153 mg, 0.64 mmol, 2.00 eq.) in DCM (5 mL) under a nitrogen atmosphere was added EDC (123 mg, 0.64 mmol, 2.00 eq.) and DMAP (4 mg, 0.03 mmol, 0.10 eq.). The solution was stirred for 18 h at room temperature in the dark, and additional amounts of **S2** (150 mg, 0.64 mmol, 2.00 eq.) and EDC (140 mg, 0.73 mmol, 2.27 eq.) were added. After a total reaction time of 42 h, the mixture was diluted with DCM (50 mL) and washed with sat. aq. $NaHCO_3$ (50 mL). The organic layer was dried over $MgSO_4$, filtered, and concentrated under reduced pressure. The crude product was purified by silica gel chromatography (DCM/methanol (24:1 to 9:1) to give **12** as a yellow waxy solid (91 mg, 59 %). **^{1}H-NMR** (400 MHz, $CDCl_3$) δ 7.33 – 7.26 (m, 3H), 7.22 (d, *J* = 8.1 Hz, 2H), 6.60 (d, *J* = 9.3 Hz, 1H), 6.51 (dd, *J* = 9.0, 2.6 Hz, 1H), 6.48 (d, *J* = 2.6 Hz, 1H), 6.06 (s, 1H), 5.25 (dt, *J* = 9.2, 1.5 Hz, 1H), 3.68 (s, 2H), 3.43 (s, 2H), 3.39 (q, *J* = 7.2 Hz, 4H), 2.24 (s, 6H), 1.86 (s, 3H), 1.74 (s, 3H), 1.19 (t, *J* = 7.1 Hz, 6H). **^{13}C-NMR** (101 MHz, $CDCl_3$) δ 170.5, 162.3, 156.7, 154.0, 150.6, 141.2, 137.6, 132.5, 129.6, 129.4, 125.4, 121.1, 108.6, 106.1, 105.8, 98.0, 69.1, 64.0, 45.3, 44.8, 41.2, 26.0, 18.9, 12.6. **HRMS** (ESI): calc. for $C_{29}H_{37}N_2O_4^+$ ($M+H^+$): 477.2748; found: 477.2742.

Compound **S2** (dimethylammonium-2-(4-((dimethylamino)methyl)phenyl)acetate)

To a suspension of 2-(4-(bromomethyl)phenyl)acetic acid (1.20 g, 5.24 mmol, 1.00 eq.) in THF (5 mL) in a pressure tube was added $NHMe_2$ (2 M in THF, 20 mL, 40 mmol, 7.6 eq.). The suspension was stirred at 65 °C for 18 h in a pressure tube. The mixture was filtered while hot, and the filtrate was concentrated under reduced pressure to give **S2** as a brown oil (1.23 g, 99%). **^{1}H-NMR** (400 MHz, DMSO-d_6) δ 7.18 (s, 4H), 3.43 (s, 2H), 3.34 (s, 2H), 2.47 (s, 6H), 2.12 (s, 6H). **^{13}C-NMR** (101 MHz, DMSO-d_6) δ 173.2, 135.7, 134.7, 129.2, 129.0, 62.5, 44.4, 41.2, 34.3. **HRMS** (ESI): calc. for $C_{11}H_{16}NO_2^+$ ($M+H^+$): 194.1176; found: 194.1174.

2.2.2 Formation of tertiary PPGs 8 and 10

Compound **S3** (2-(4-isobutylphenyl)acetic anhydride)

Ibufenac (100 mg, 0.52 mmol, 1.82 eq.) and EDC (55 mg, 0.29 mmol, 1.00 eq.) were dissolved in DCM (2 mL). The mixture was stirred for 18 h at room temperature, and DCM was evaporated under reduced pressure. The crude material was suspended in heptane (2 mL) and filtered. The residue was washed with heptane (2 mL). The filtrate was concentrated under reduced pressure to yield **S3** as a white powder (70 mg, ~90 % purity, 60%). **^{1}H-NMR** (400 MHz, $CDCl_3$) δ 7.12 (d, *J* = 2.1 Hz, 4H), 3.70 (s, 2H), 2.48 (d, *J* = 7.2 Hz, 2H), 1.87 (hept, *J* = 13.5, 6.7 Hz, 1H), 0.92 (d, *J* = 6.6 Hz, 6H). **^{13}C-NMR** (101 MHz, $CDCl_3$) δ 167.3, 141.2, 129.6, 129.3, 129.3, 45.2, 41.8, 30.3, 22.5. **HRMS** (ESI): calc. for $C_{24}H_{30}O_3Na^+$ ($M+Na^+$): 389.2087; found: 389.2087.

Compound **8** (2-(7-(diethylamino)-2-oxo-2H-chromen-4-yl)propan-2-yl 2-phenylacetate)

To a solution of Tertiary-Coumarin-Alcohol (prepared as described previously)[1] (**S4**, 72 mg, 0.26 mmol, 1.00 eq.) and phenylacetic-anhydride (133 mg, 0.52 mmol, 2.00 eq.) in DCM (3 mL) was added triethylamine (40 µL, 0.29 mmol, 1.10 eq.) and DMAP (3 mg, 0.03 mmol, 0.10 eq.). The mixture was stirred for 4 d at 35 °C in a sealed tube in the dark, diluted with DCM (20 mL), washed with sat. aq. $NaHCO_3$ (20 mL), dried over $MgSO_4$, and the volatiles were evaporated under reduced pressure. The crude product was purified by silica gel chromatography (pentane/ethyl acetate 8:1 to 7:1 to yield a product that was still contaminated with phenylacetic-anhydride. Following another column chromatography (Et_2O/pentane 1:1) pure **8** was obtained as a yellow solid (60 mg, 58%).**^{1}H-NMR** (400 MHz, $CDCl_3$) δ 7.51 (d, *J* = 9.2 Hz, 1H), 7.34 – 7.26 (m, 3H), 7.20 (dd, *J* = 7.8, 1.8 Hz, 2H), 6.46 (d, *J* = 2.7 Hz, 1H), 6.25 (dd, *J* = 9.3, 2.7 Hz, 1H), 6.05 (s, 1H), 3.57 (s, 2H), 3.36 (q, *J* = 7.1 Hz, 4H), 1.76 (s, 6H), 1.18 (t, *J* = 7.1 Hz, 6H). **^{13}C-NMR** (101 MHz, $CDCl_3$) δ 169.6, 162.5, 158.1, 156.8, 149.9, 133.6, 129.6, 128.7, 127.3, 126.8, 108.2, 106.2, 105.8, 98.5, 81.0, 44.7, 42.2, 27.6, 12.7. **HRMS** (ESI): calc. for $C_{24}H_{28}NO_4^+$ ($M+H^+$): 394.2013; found: 394.2010.

Compound **10** (2-(7-(diethylamino)-2-oxo-2H-chromen-4-yl)propan-2-yl 2-(4-isobutylphenyl)acetate)

To a solution of Tertiary-Coumarin-Alcohol (prepared as described previously)[1] (**S4**, 47 mg, 0.17 mmol, 1.00 eq.) and **S3** (313 mg, 0.85 mmol, 5.00 eq.) in dry THF (1 mL) under a nitrogen atmosphere was added DMAP (5 mg, 0.04 mmol, 0.24 eq.). The mixture was stirred for 3 d at 65 °C in a Schlenk tube in the dark, and an additional amount of **S3** was added (100 mg, 0.27 mmol, 1.60 eq.). The mixture was stirred for two more days at 65 °C in a Schlenk tube, concentrated under reduced pressure, and purified by silica gel chromatography (Et_2O/pentane 1:3 to 1:2) to yield **10** as a yellow oil (47 mg, 61%). **^{1}H-NMR** (400 MHz, $CDCl_3$) δ 7.56 (d, *J* = 9.3 Hz, 1H), 7.09 (q, *J* = 8.2 Hz, 4H), 6.47 (d, *J* = 2.7 Hz, 1H), 6.31 (dd, *J* = 9.3, 2.7 Hz, 1H), 6.06 (s, 1H), 3.55 (s, 2H), 3.37 (q, *J* = 7.1 Hz, 4H), 2.44 (d, *J* = 7.2 Hz, 2H), 1.89 – 1.79 (m, 1H), 1.76 (s, 6H), 1.19 (t, *J* = 7.1 Hz, 6H), 0.89 (d, *J* = 6.6 Hz, 6H). **^{13}C-NMR** (101 MHz, $cdcl_3$) δ 169.9, 162.5, 158.2, 156.8, 149.9, 140.6, 130.8, 129.4, 129.3, 126.9, 108.3, 106.1, 105.9, 98.4, 80.8, 45.2, 44.7, 41.7, 30.4, 27.6, 22.5, 12.6. **HRMS** (ESI): calc. for $C_{28}H_{36}NO_4^+$ ($M+H^+$): 450.2639; found: 450.2631.

2.2.3 Formation of deuterated coumarin 6-D_6

Compound **S6** (7-(diethylamino)-4-(1-hydroxyethyl-2,2,2-d3)-2H-chromen-2-one)

Preparation of the Grignard reagent (D_3-methyl-magnesium-iodide): a Schlenk-flask containing Mg turnings (93 mg, 3.81 mmol, 5.00 eq.) was dried with a heatgun. Under nitrogen, an iodine crystal was added, and the flask was heated until a purple vapor was observed. Dry Et_2O (3 mL) was added, and the mixture was cooled in a water bath, followed by the addition of CD_3I (190 µL, 3.05 mmol, 4.00 eq.). The mixture was heated to 35 °C for 30 min.

To a solution of coumarin-aldehyde **S5** (prepared according to a literature procedure)[2] (1.00 g, 4.08 mmol, 1.00 eq.) in dry THF (28 mL) at -78 °C under a nitrogen atmosphere was slowly added the prepared Grignard solution (5.10 mL, 5.10 mmol, 1.25 eq.). The mixture was stirred for 18 h, during which it was allowed to warm up to room temperature. Sat. aq. NH_4Cl was added (50 mL) and the mixture was extracted with ethyl acetate (70 mL). The organic layer was washed with brine, dried over $MgSO_4$, and the volatiles were evaporated under reduced pressure. The crude product was purified by silica gel chromatography (DCM/acetone 24:1 to 19:1) to yield **S6** as a brown oil (663 mg, 62 %). **^{1}H-NMR** (400 MHz, $CDCl_3$) δ 7.41 (d, *J* = 9.0 Hz, 1H), 6.56 (dd, *J* = 9.1, 2.6 Hz, 1H), 6.48 (d, *J* = 2.6 Hz, 1H), 6.27 (s, 1H), 5.13 (s, 1H), 3.40 (q, *J* = 7.1 Hz, 4H), 1.20 (t, *J* = 7.1 Hz, 6H). **^{13}C-NMR** (101 MHz, $CDCl_3$) δ 163.1, 159.7, 156.6, 150.4, 125.1, 108.6, 106.3, 104.5, 98.0, 66.0, 44.8, 12.6 (deuterated carbon not observed). **HRMS** (ESI): calc. for $C_{15}H_{17}D_3NO_3^+$ ($M+H^+$): 265.1626; found: 265.1628.

Compound **S7** (4-(acetyl-d3)-7-(diethylamino)-2H-chromen-2-one)

To a solution of **S6** (496 mg, 1.88 mmol, 1.00 eq.) in THF (6 mL) at 0 °C was added DMP (955 mg, 2.25 mmol, 1.20 eq.). The solution was stirred at RT for 18 h and diluted with sat. aq. $NaHCO_3$. The aqueous mixture was extracted with DCM (2x), and the combined organic layers were washed with water (1x), brine (1x) dried over $MgSO_4$ and concentrated under reduced pressure. The crude product was purified by silica gel chromatography (DCM/acetone 99:1 to 98:2) to yield **S7** as a light brown solid (403 mg, 82 %). **^{1}H-NMR** (400 MHz, $CDCl_3$) δ 7.69 (d, *J* = 9.2 Hz, 1H), 6.57 (dd, *J* = 9.2, 2.6 Hz, 1H), 6.49 (d, *J* = 2.6 Hz, 1H), 6.25 (s, 1H), 3.41 (q, *J* = 7.1 Hz, 4H), 1.20 (t, *J* = 7.1 Hz, 6H). **^{13}C-NMR** (101 MHz, $CDCl_3$) δ 200.2, 162.1, 157.3, 151.0, 149.9, 127.7, 109.4, 108.9, 104.2, 97.9, 44.9, 28.9 (multiplet), 12.5. **HRMS** (ESI): calc. for $C_{15}H_{15}D_3NO_3^+$ ($M+H^+$): 263.1470; found: 263.1471.

Compound **S8** (7-(diethylamino)-4-(2-hydroxypropan-2-yl-1,1,1,3,3,3-d6)-2H-chromen-2-one)

The Grignard reagent was prepared freshly as described above (synthesis of **S6**)

To a solution of **S7** (200 mg, 0.76 mmol, 1.00 eq.) in THF (5 mL) at -78 °C under a nitrogen atmosphere was slowly added the prepared Grignard solution (0.95 mL, 0.95 mmol, 1.25 eq.). The mixture was stirred for 18 h during which it warmed to room temperature. Sat. aq. NH_4Cl was added (20 mL) and the mixture was extracted with ethyl acetate (20 mL). The organic layer was washed with brine, dried over $MgSO_4$, and evaporated under reduced pressure. The crude product was purified by silica gel chromatography (DCM/acetone 24:1 to 19:1) to yield **S8** as a light brown powder (148 mg, 69 %). **^{1}H-NMR** (400 MHz, $CDCl_3$) δ 8.07 (d, *J* = 9.2 Hz, 1H), 6.53 (dd, *J* = 9.3, 2.7 Hz, 1H), 6.40 (d, *J* = 2.7 Hz, 1H), 6.08 (s, 1H), 3.36 (q, *J* = 7.1 Hz, 4H), 3.02 (s, 1H), 1.16 (t, *J* = 7.1 Hz, 6H). **^{13}C-NMR** (101 MHz, $CDCl_3$) δ

163.1, 161.8, 156.8, 149.8, 128.9, 108.2, 106.4, 105.4, 97.9, 72.4, 44.6, 29.3 (multiplet), 12.5. **HRMS** (ESI): calc. for $C_{16}H_{16}D_6NO_3^+$ ($M+H^+$): 282.1971; found: 282.1972.

Compound **6-D$_6$** (2-(7-(diethylamino)-2-oxo-2H-chromen-4-yl)propan-2-yl-1,1,1,3,3,3-d6 acetate)

To a solution of compound **S8** (69 mg, 0.24 mmol, 1.00 eq.) in DCM (2.5 mL) was added acetic anhydride (37 µL, 0.39 mmol, 1.60 eq.), triethylamine (54 µL, 0.39 mmol, 1.60eq.) and DMAP (2 mg, 0.02 mmol, 0.07 eq.). The mixture was stirred at room temperature in the dark for 3 d, diluted with DCM (20 mL) and washed with 0.5 M aqueous HCl (20 mL) and brine (20 mL). The organic layer was dried over $MgSO_4$, filtered, and concentrated under reduced pressure. The crude product was purified by silica gel chromatography (DCM/ethyl acetate 97:3) to yield **6-D$_6$** as a yellow powder (67 mg, 85 %). **^{1}H-NMR** (400 MHz, $CDCl_3$) δ 7.79 (d, *J* = 9.2 Hz, 1H), 6.52 (dd, *J* = 9.3, 2.2 Hz, 1H), 6.47 (d, *J* = 2.2 Hz, 1H), 6.04 (s, 1H), 3.37 (q, *J* = 7.1 Hz, 4H), 1.98 (s, 3H), 1.17 (t, *J* = 7.1 Hz, 6H). **^{13}C-NMR** (101 MHz, $CDCl_3$) δ 169.3, 162.4, 158.3, 156.8, 149.9, 126.7, 108.4, 106.0, 105.9, 98.4, 80.6, 44.6, 26.8, 21.6, 12.5. **HRMS** (ESI): calc. for $C_{18}H_{18}D_6N_1O_4^+$ ($M+H^+$): 324.2077; found: 324.2076.

2.3 NMR spectra

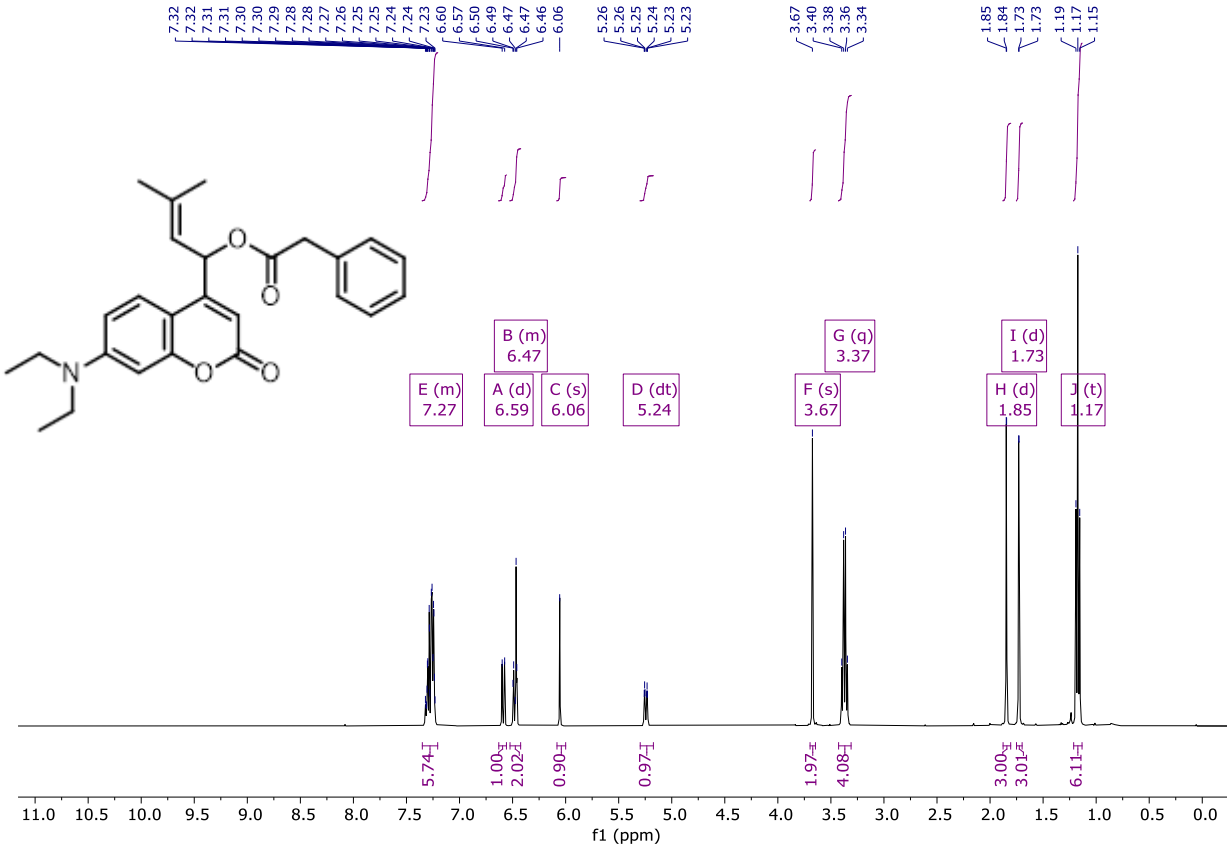

Figure S1. ^{1}H-NMR spectrum of compound **7** ($CDCl_3$).

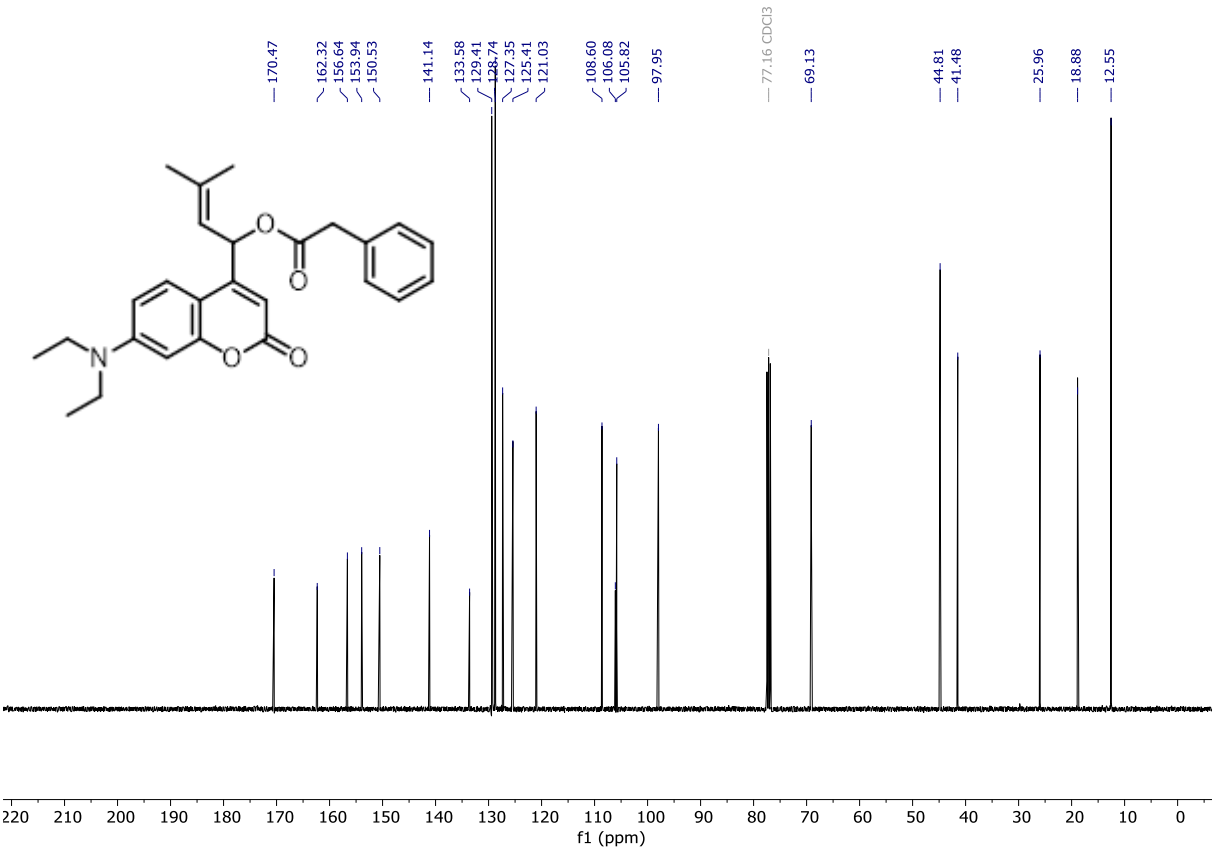

Figure S2. ^{13}C-NMR spectrum of compound **7** ($CDCl_3$).

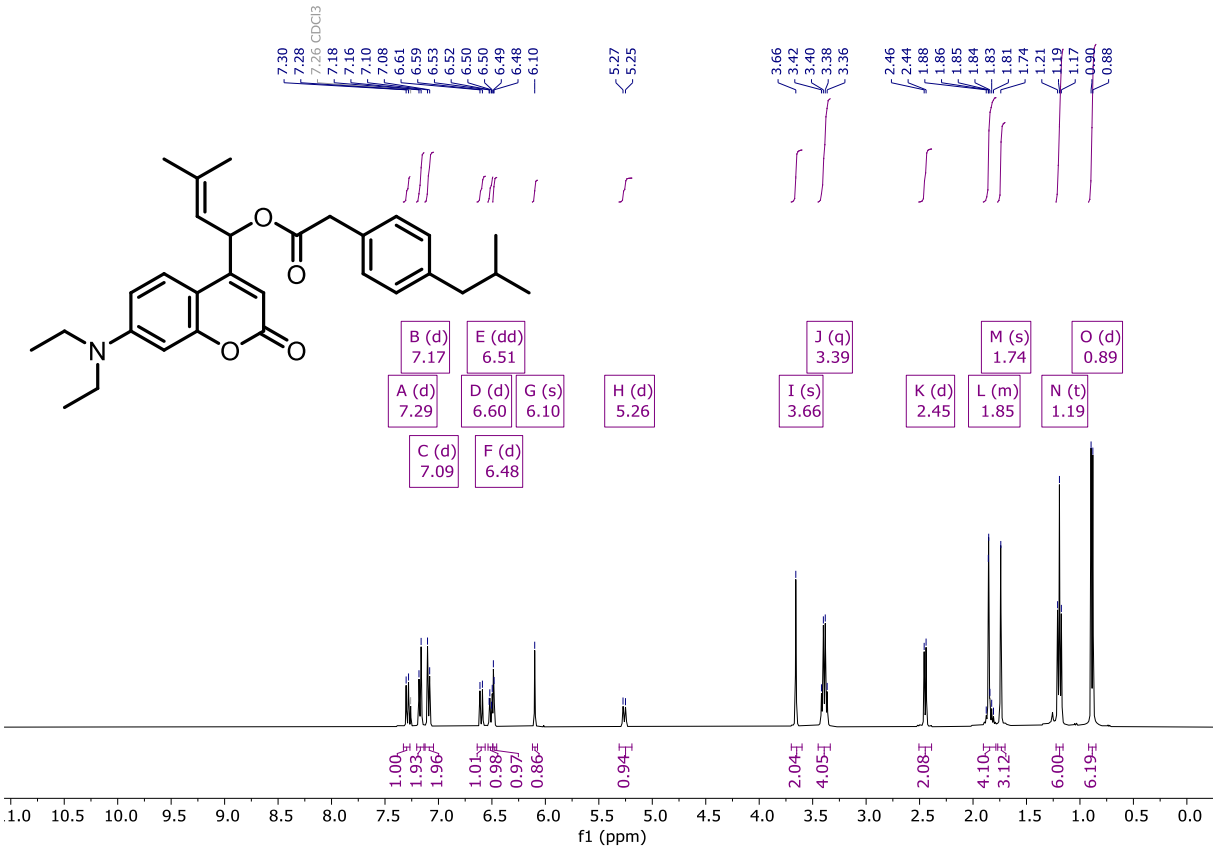

Figure S 3. ^{1}H-NMR spectrum of compound **9** ($CDCl_3$).

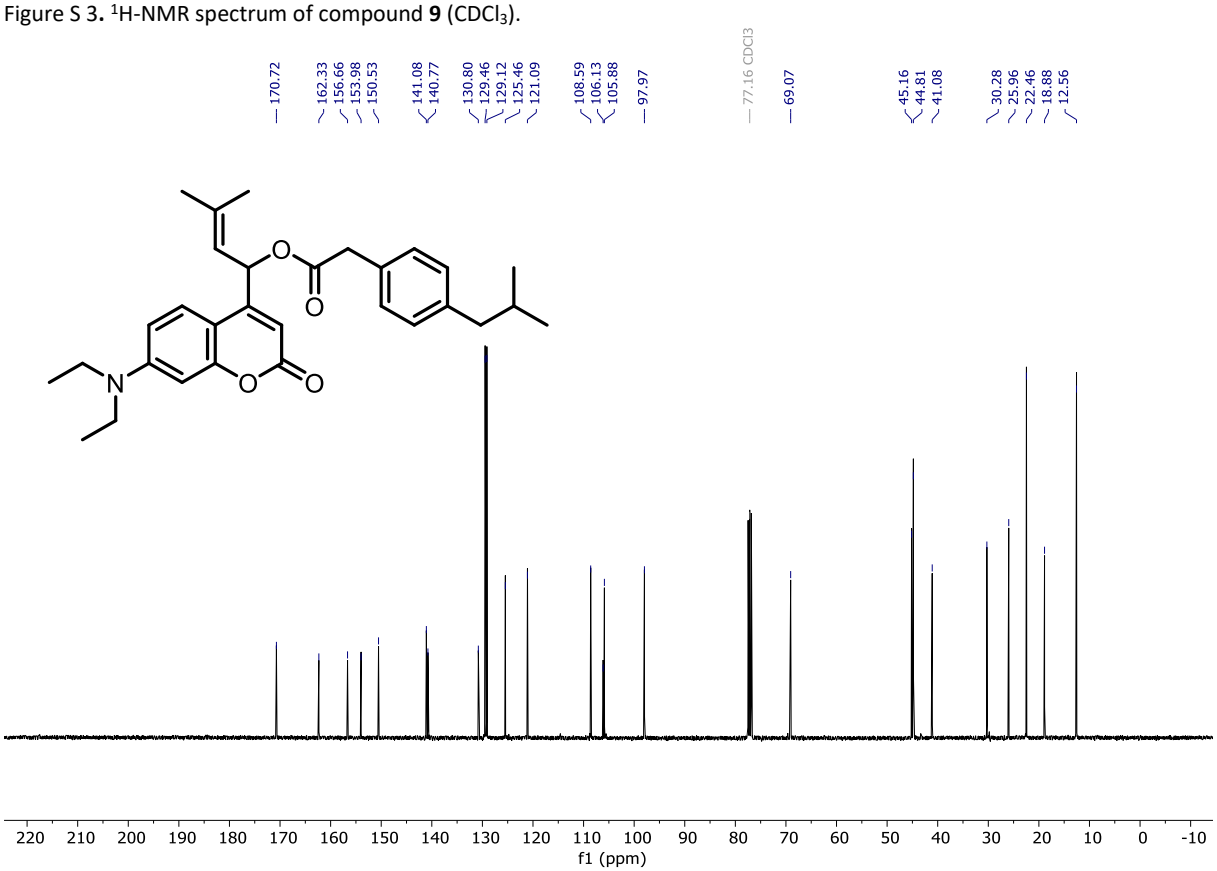

Figure S 4. ^{13}C-NMR spectrum of compound **9** ($CDCl_3$).

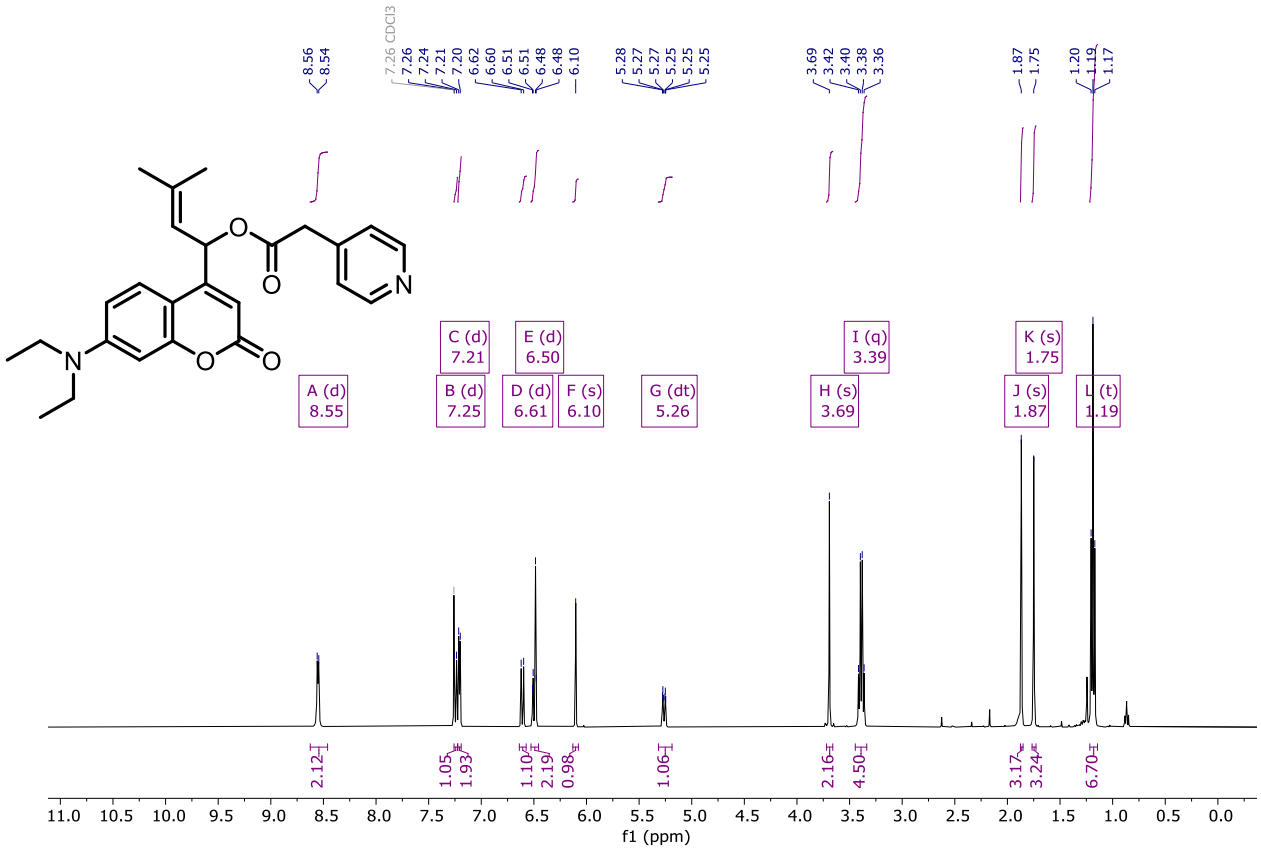

Figure S 5**.** ^{1}H-NMR spectrum of compound **11** ($CDCl_3$).

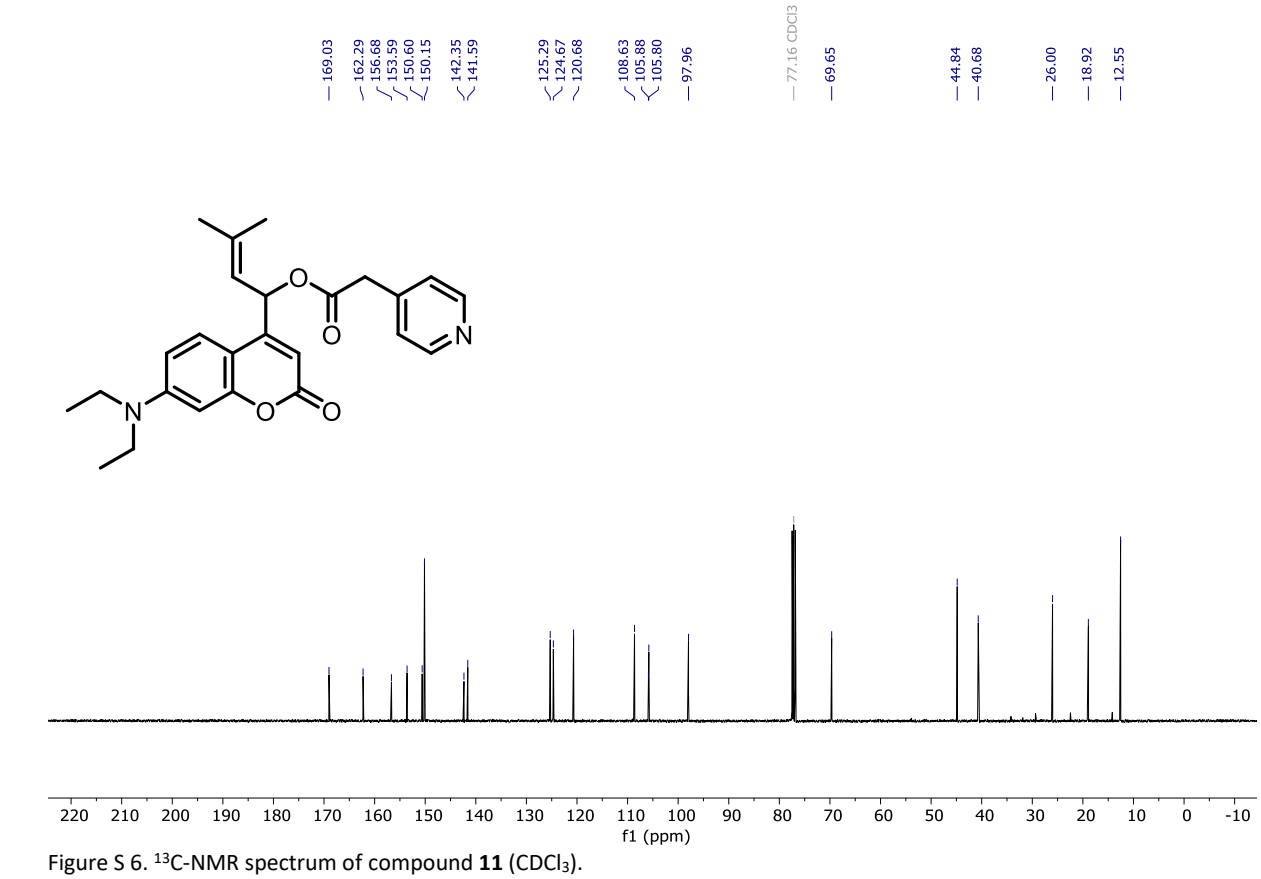

Figure S 6. ^{13}C-NMR spectrum of compound **11** ($CDCl_3$).

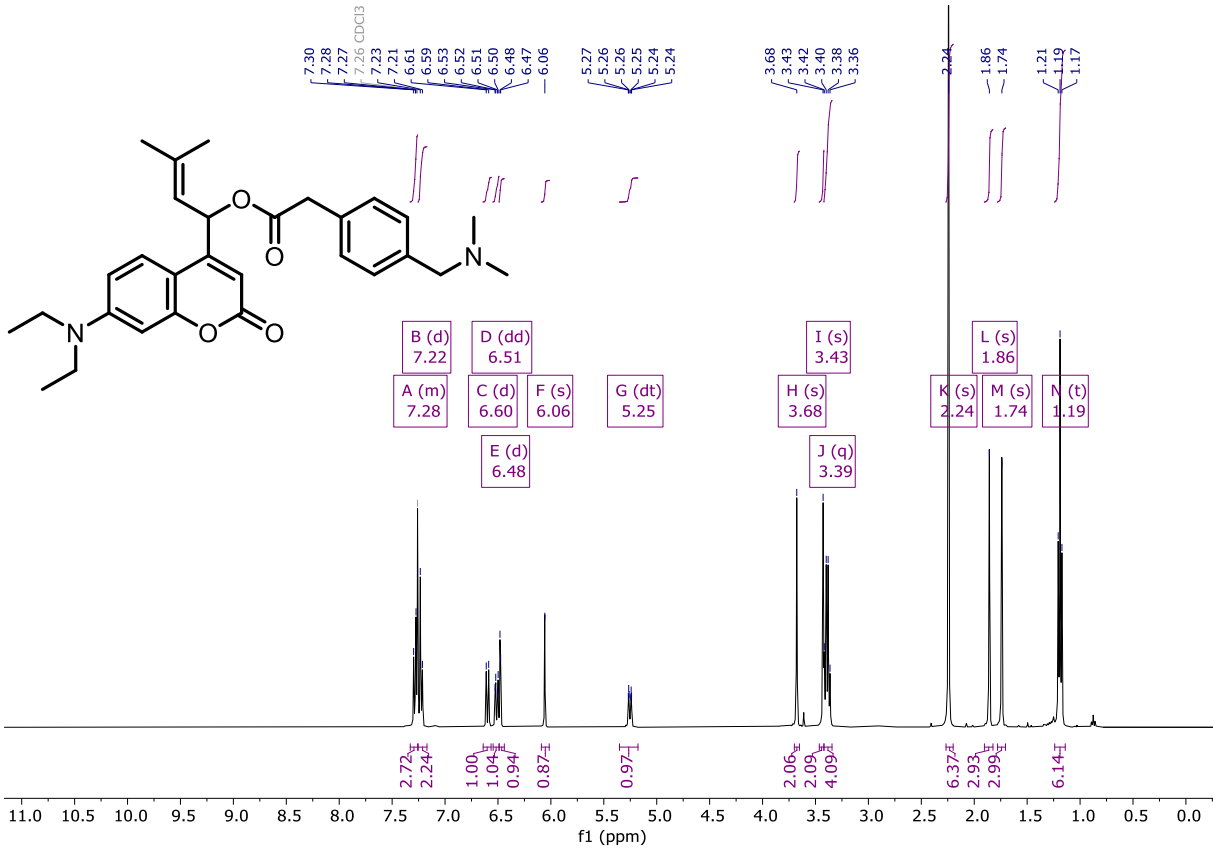

Figure S 7. ^{1}H-NMR spectrum of compound **12** ($CDCl_3$).

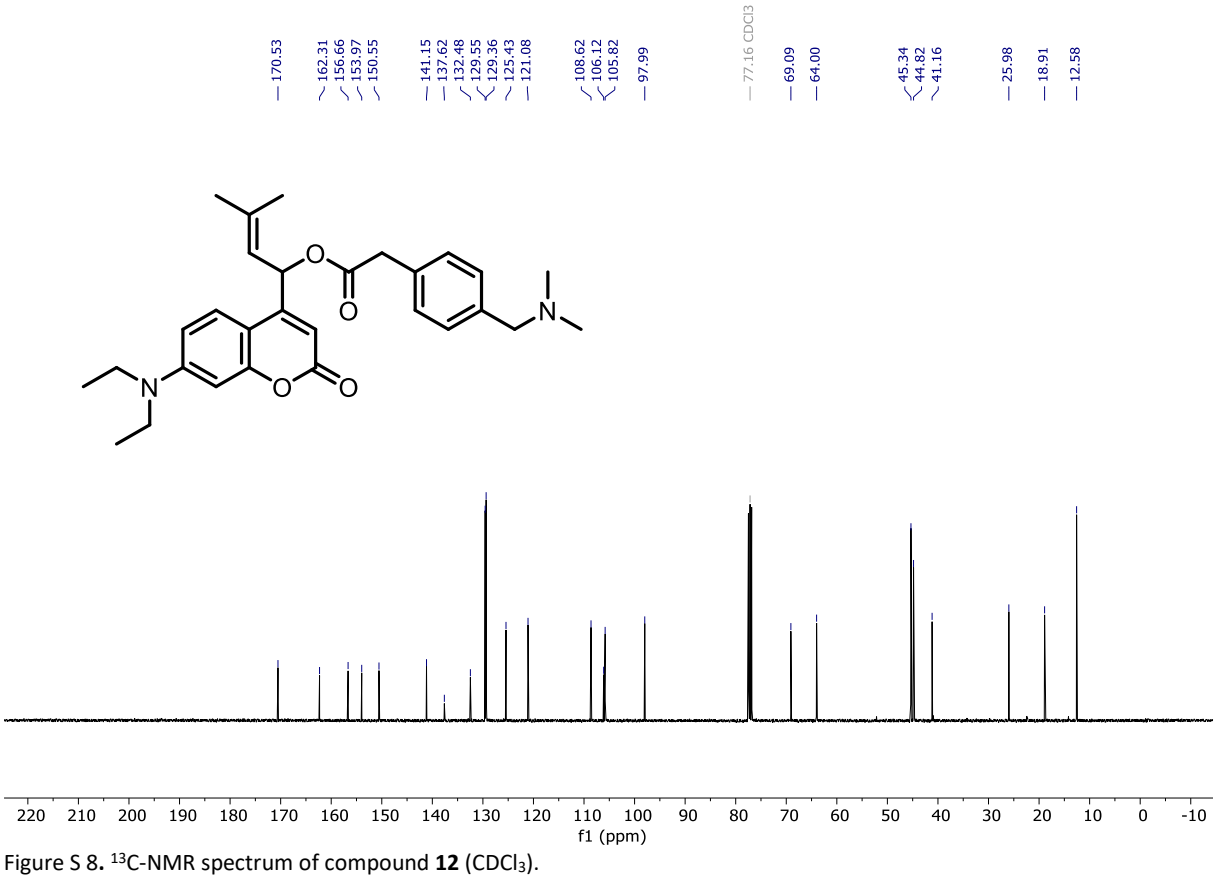

Figure S 8. ^{13}C-NMR spectrum of compound **12** ($CDCl_3$).

Figure S 9. ^{1}H-NMR spectrum of compound **S2** (DMSO-d_6).

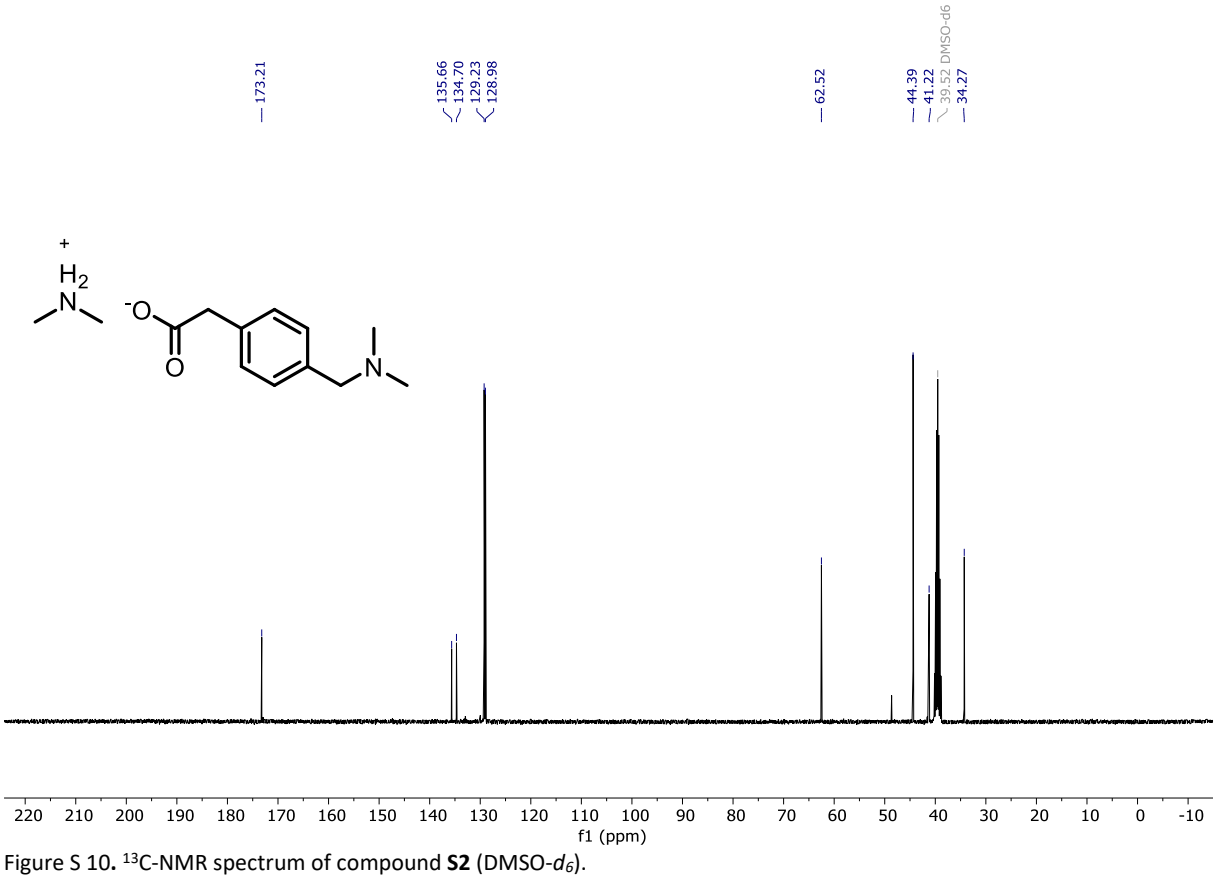

Figure S 10. ^{13}C-NMR spectrum of compound **S2** (DMSO-d_6).

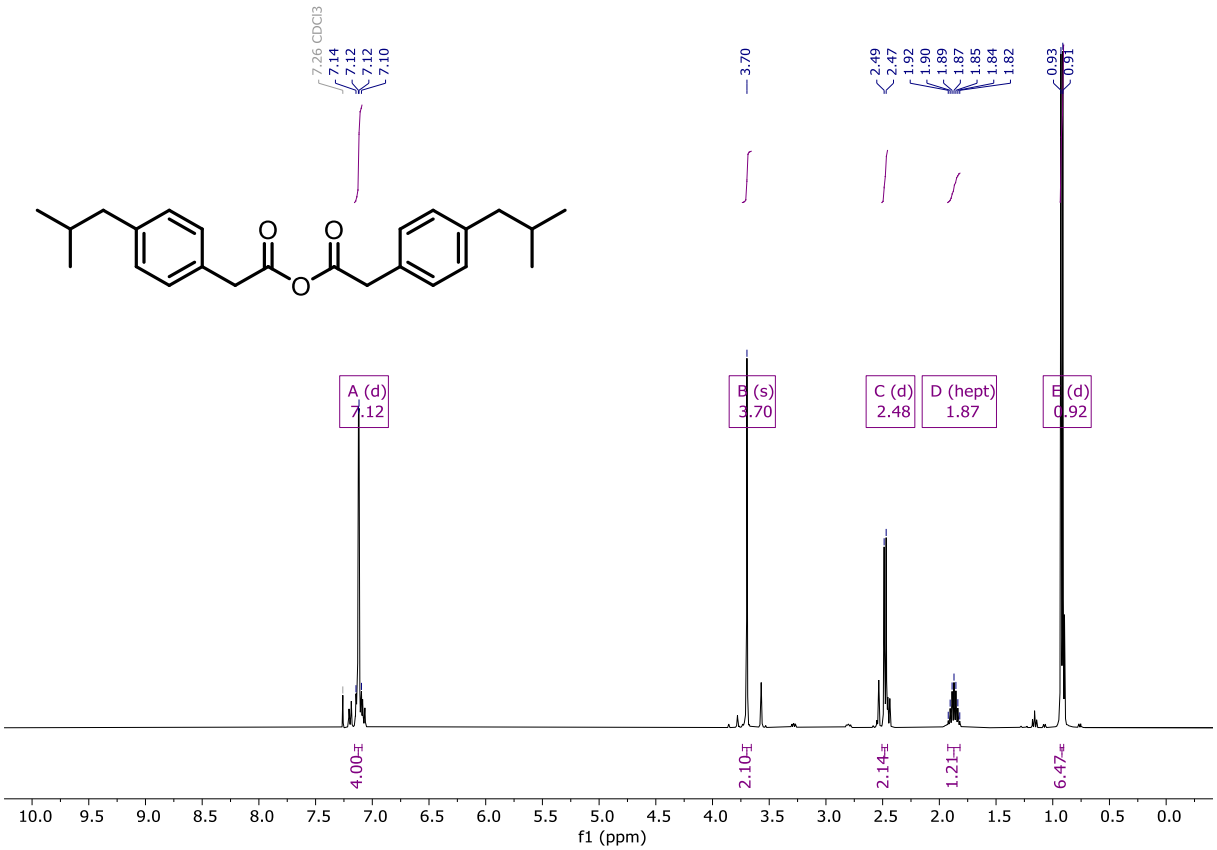

Figure S 11. ^{1}H-NMR spectrum of compound **S3** (~90% purity, $CDCl_3$).

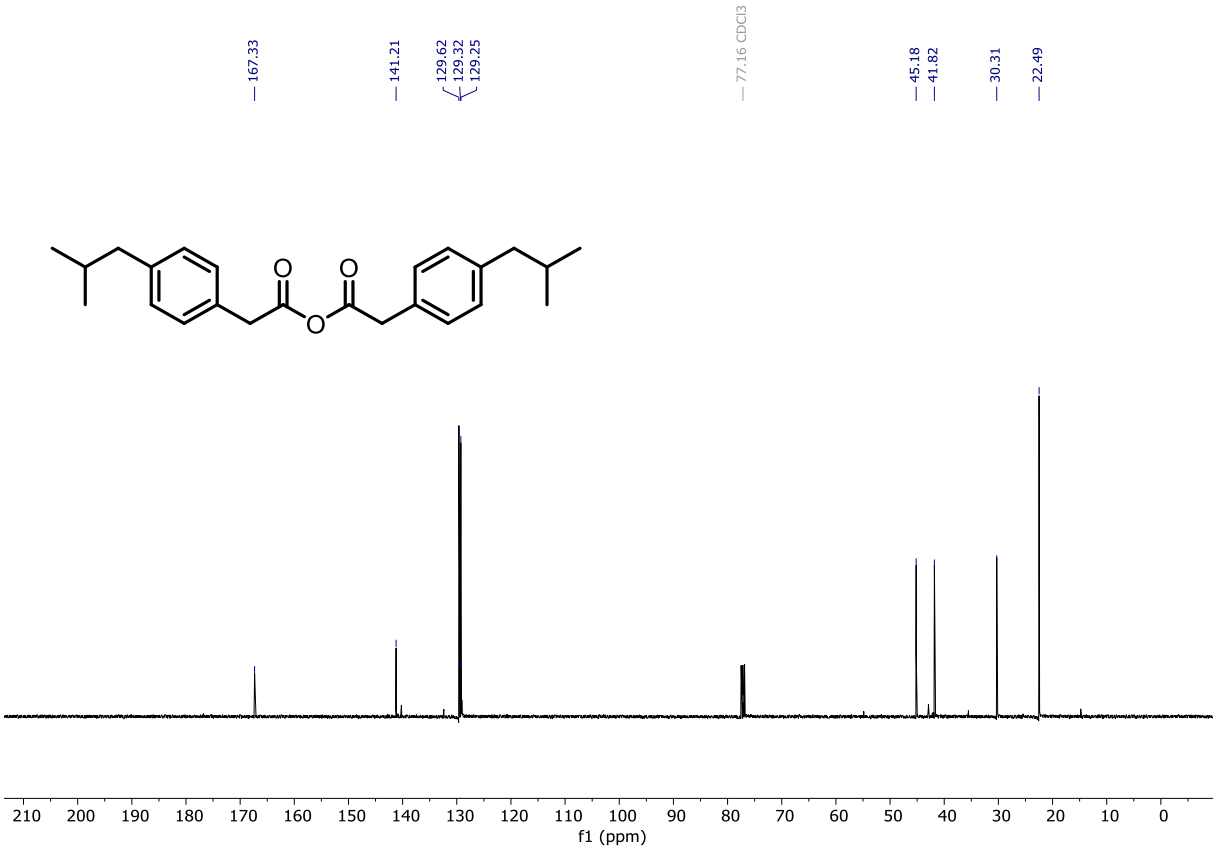

Figure S 12. ^{13}C-NMR spectrum of compound **S3** (~90% purity, $CDCl_3$).

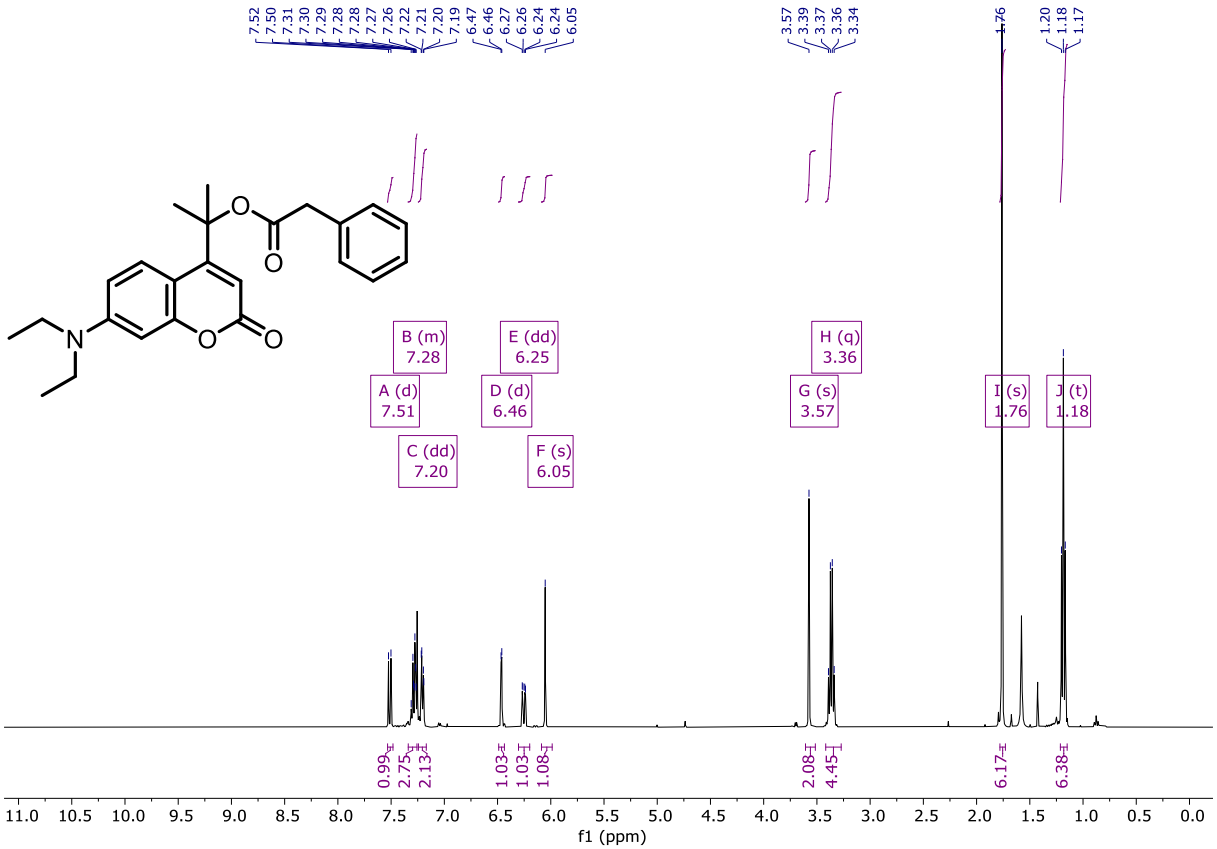

Figure S 13. ^{1}H-NMR spectrum of compound **8** ($CDCl_3$).

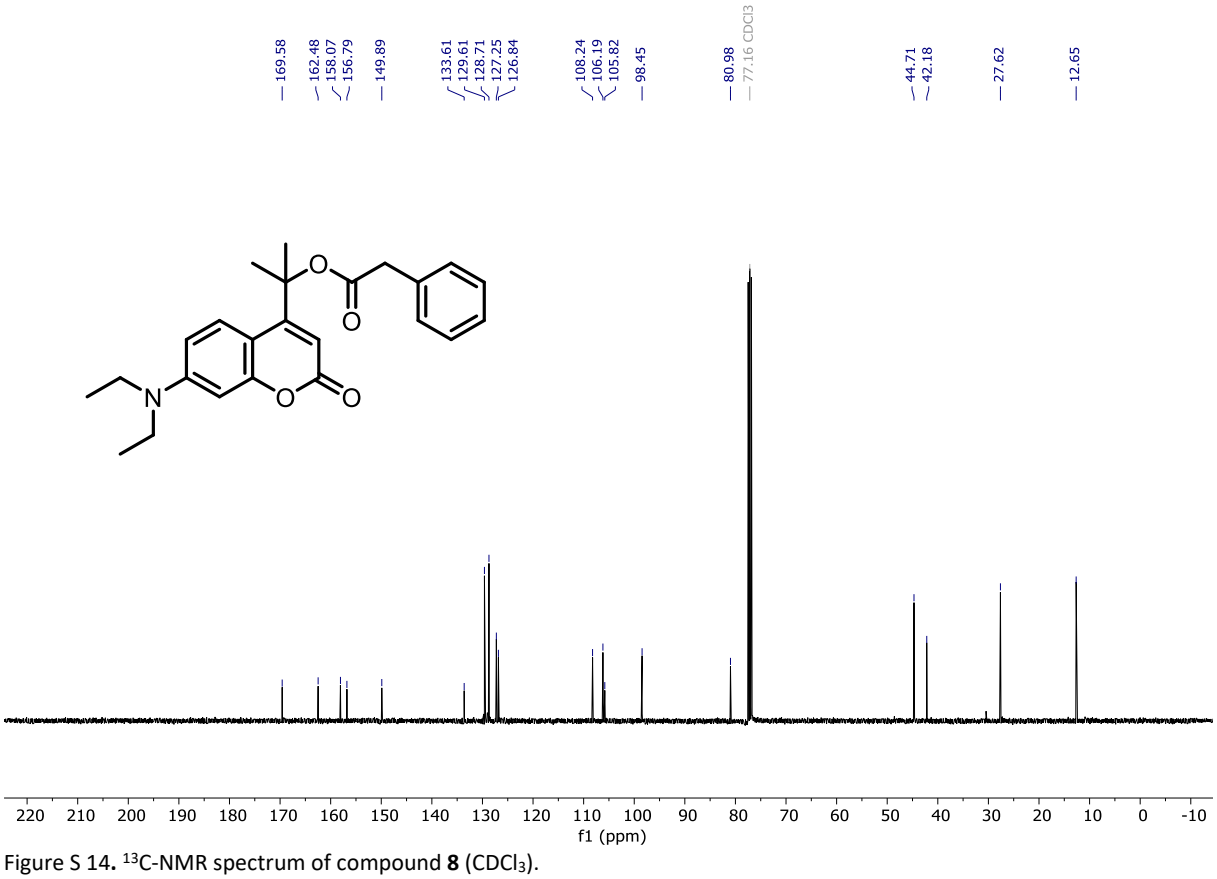

Figure S 14. ^{13}C-NMR spectrum of compound **8** ($CDCl_3$).

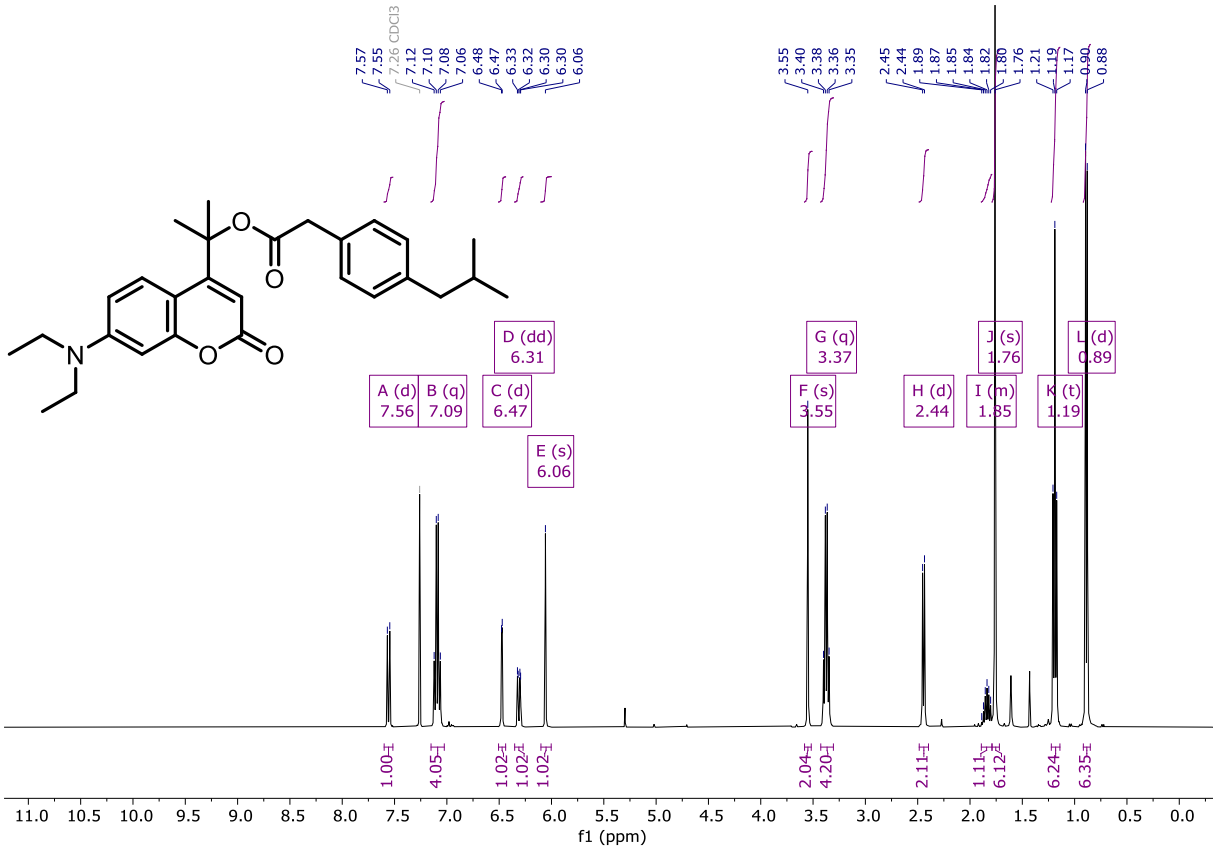

Figure S 15. ^{1}H-NMR spectrum of compound **10** ($CDCl_3$).

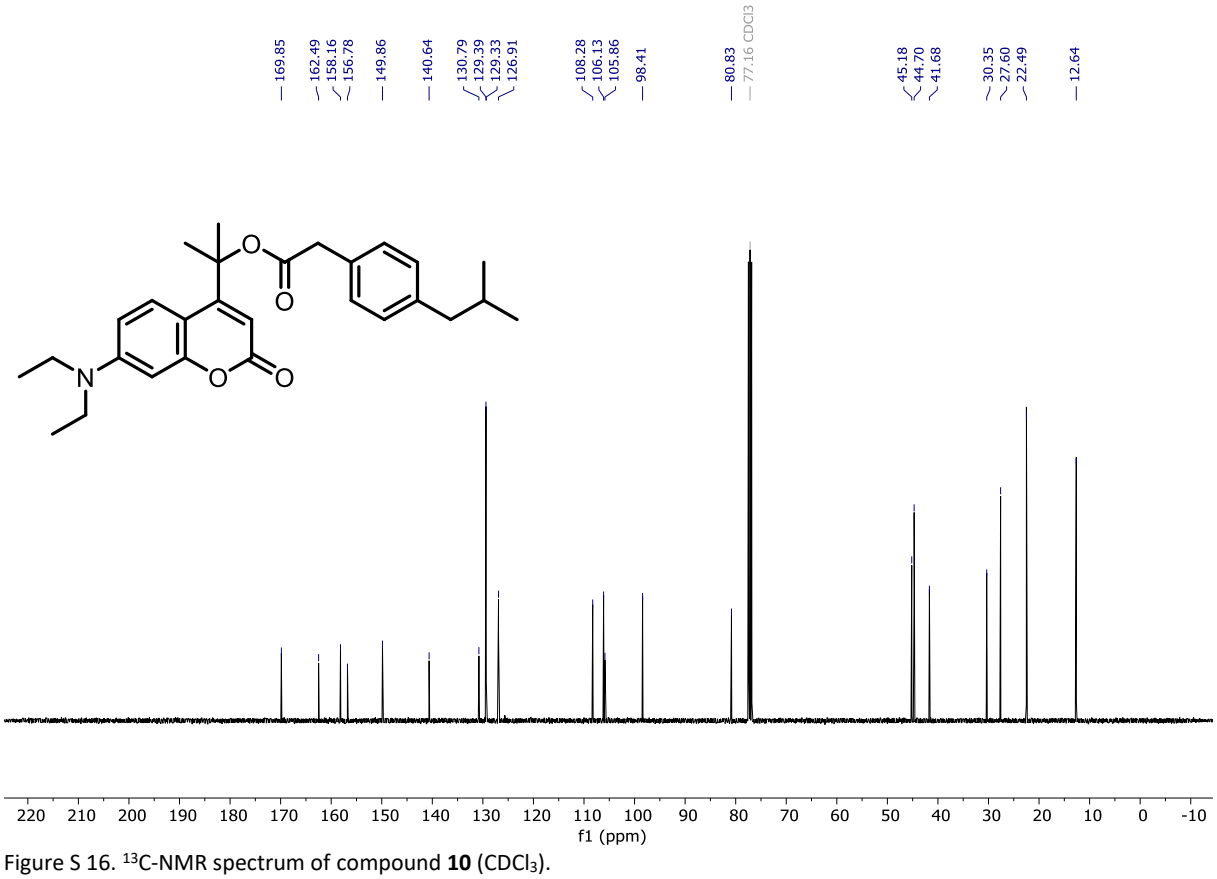

Figure S 16. ^{13}C-NMR spectrum of compound **10** ($CDCl_3$).

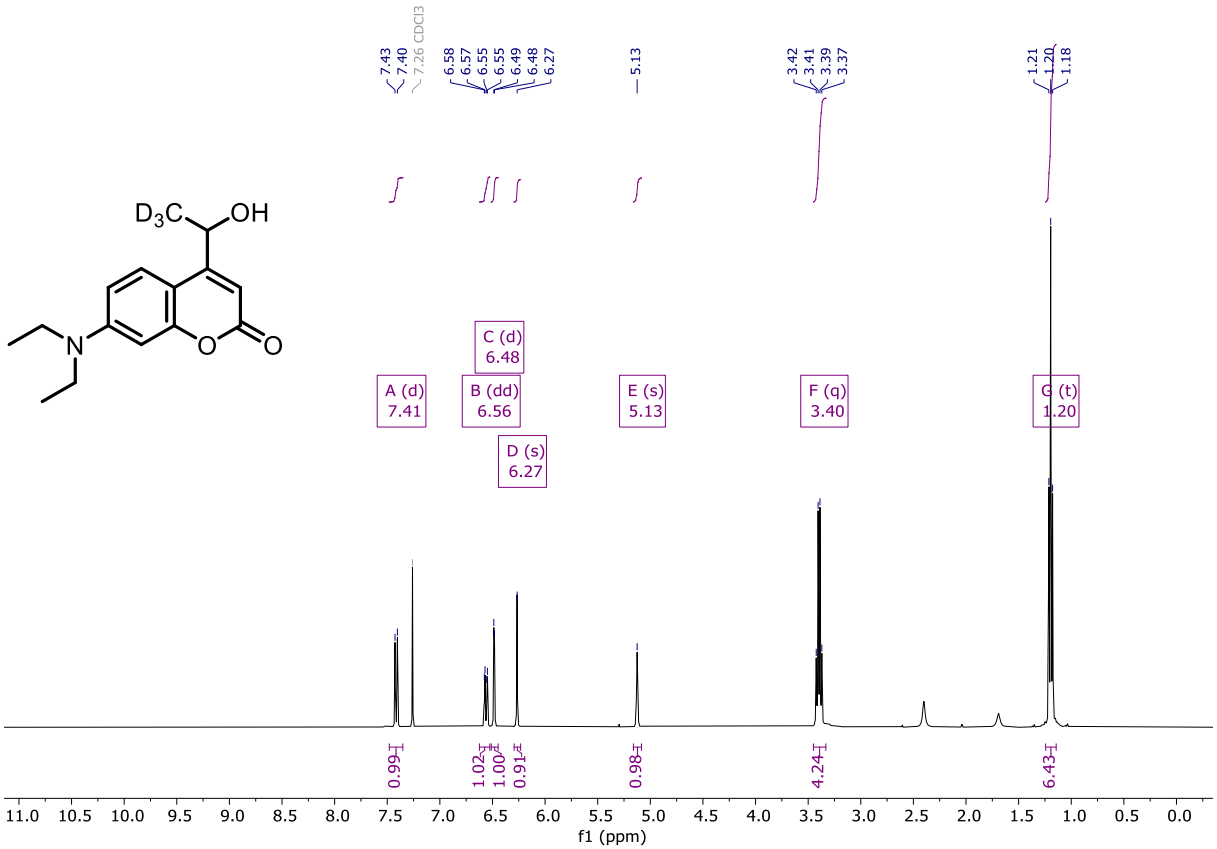

Figure S 17. ^{1}H-NMR spectrum of compound **S6** ($CDCl_3$).

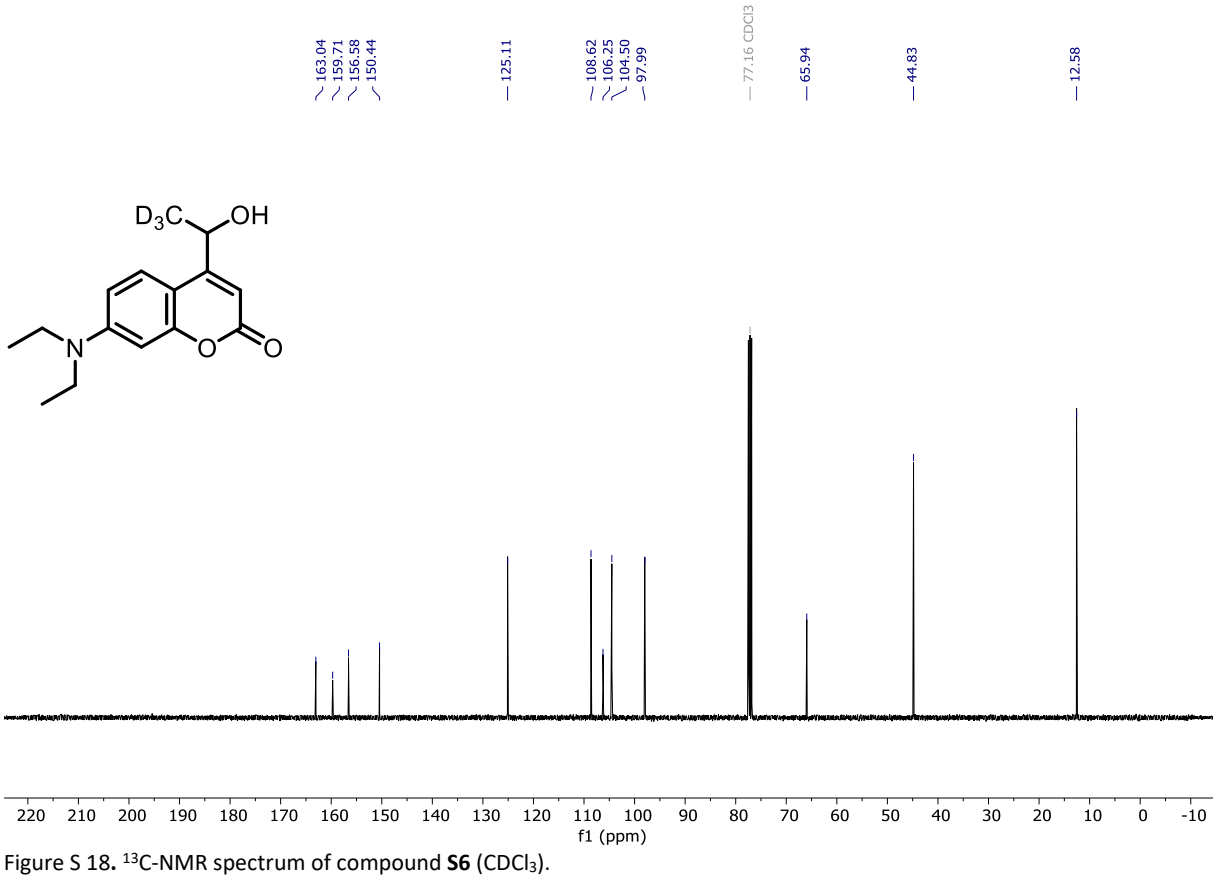

Figure S 18. ^{13}C-NMR spectrum of compound **S6** ($CDCl_3$).

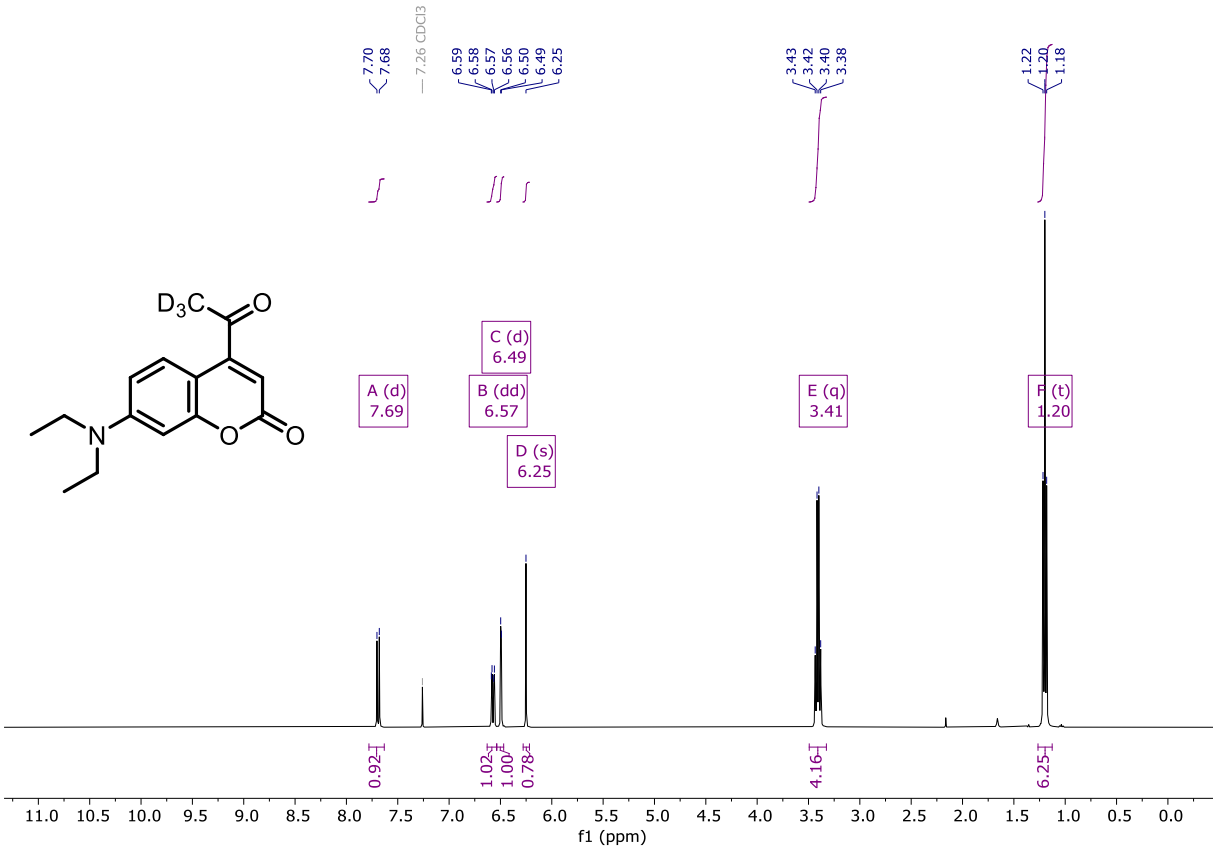

Figure S 19. ^{1}H-NMR spectrum of compound **S7** ($CDCl_3$).

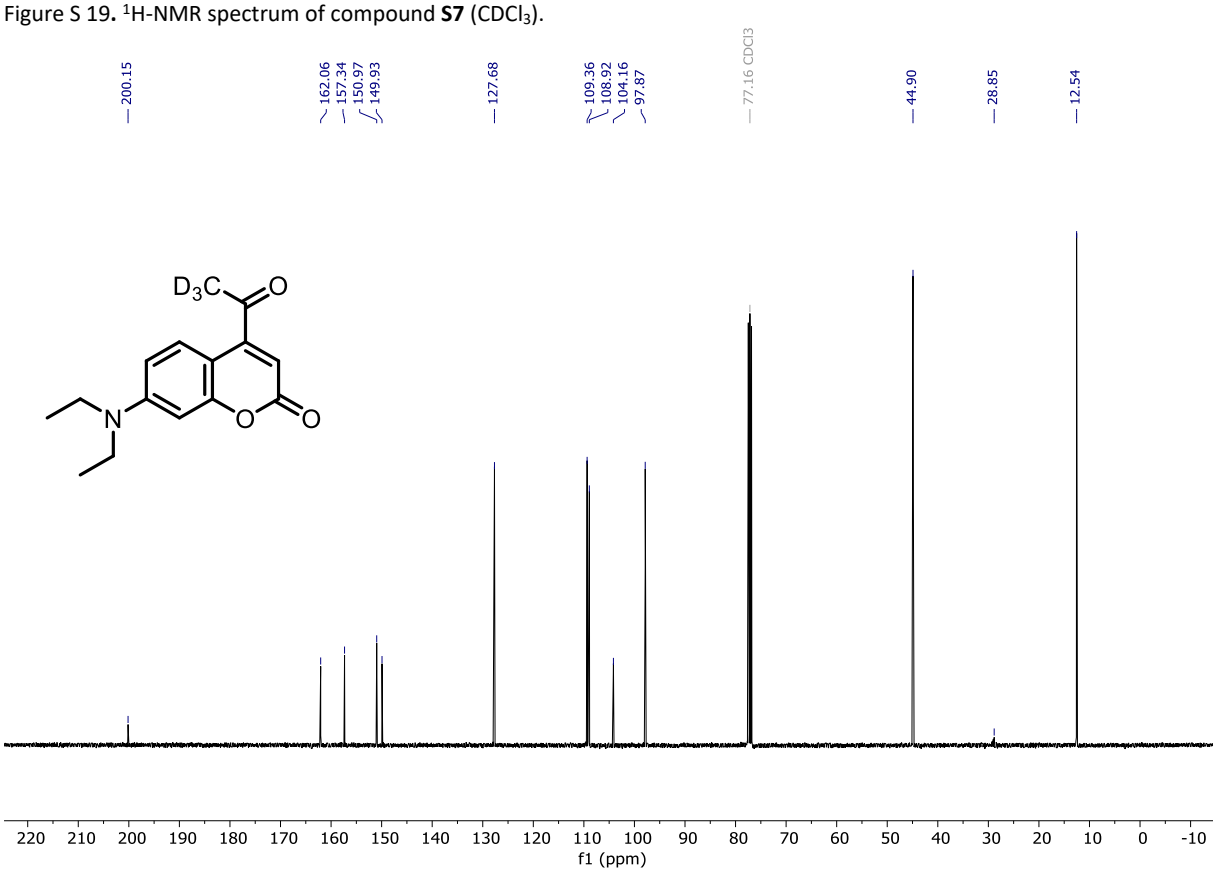

Figure S 20. ^{13}C-NMR spectrum of compound **S7** ($CDCl_3$).

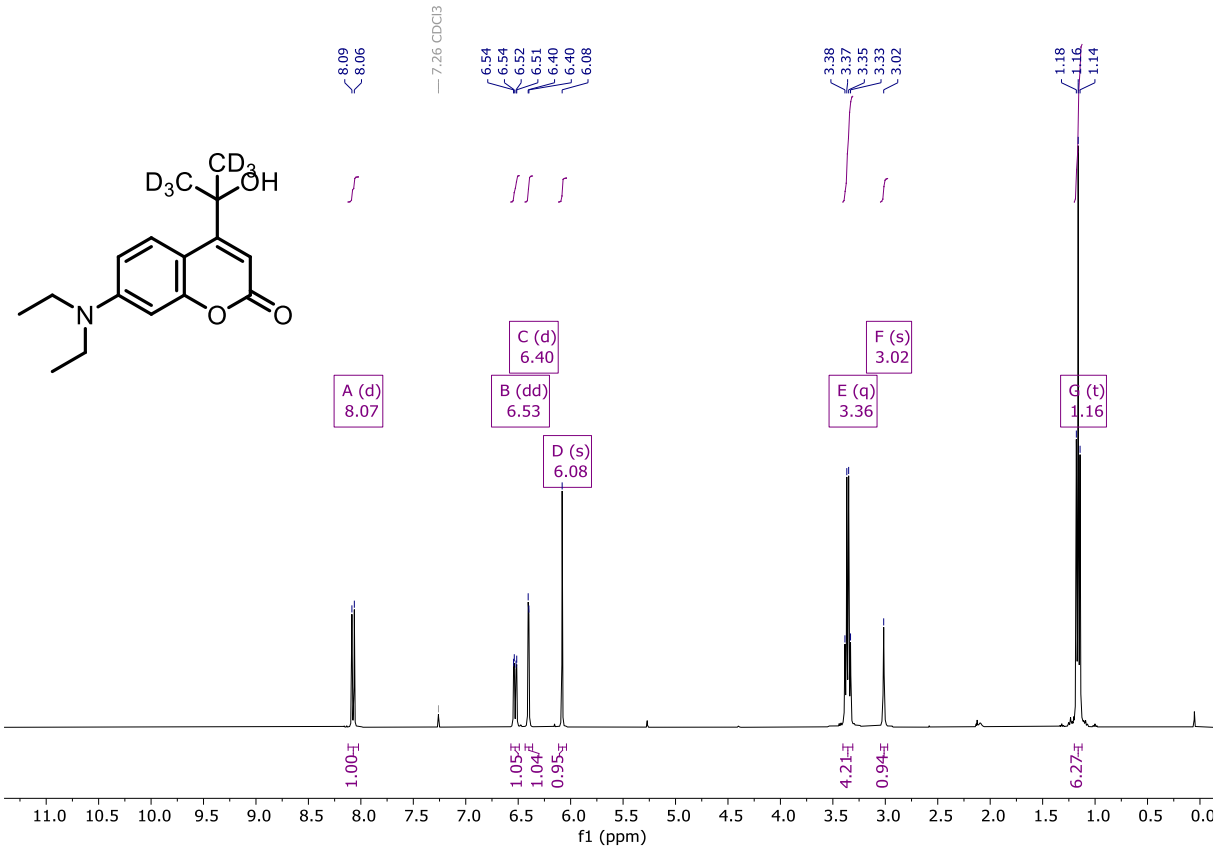

Figure S 21. ^{1}H-NMR spectrum of compound **S8** ($CDCl_3$).

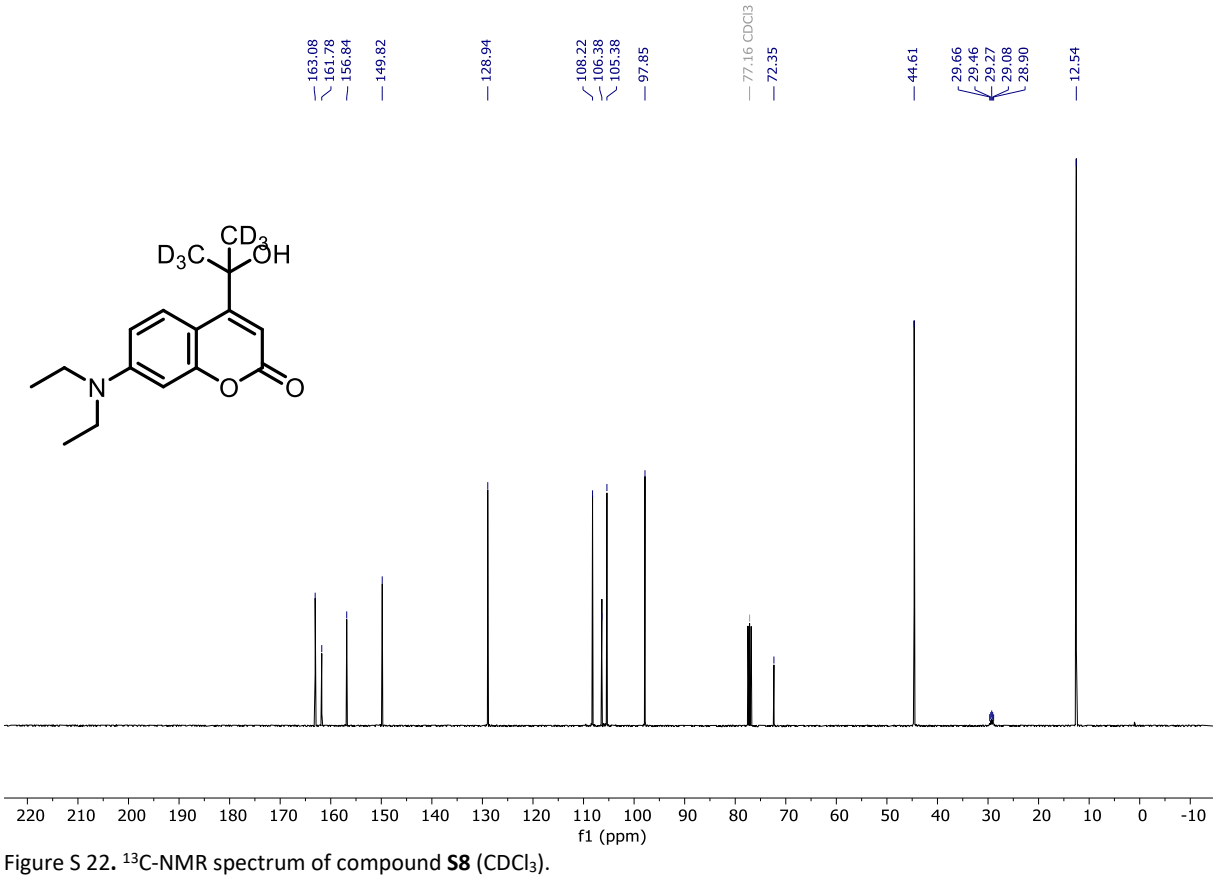

Figure S 22. ^{13}C-NMR spectrum of compound **S8** ($CDCl_3$).

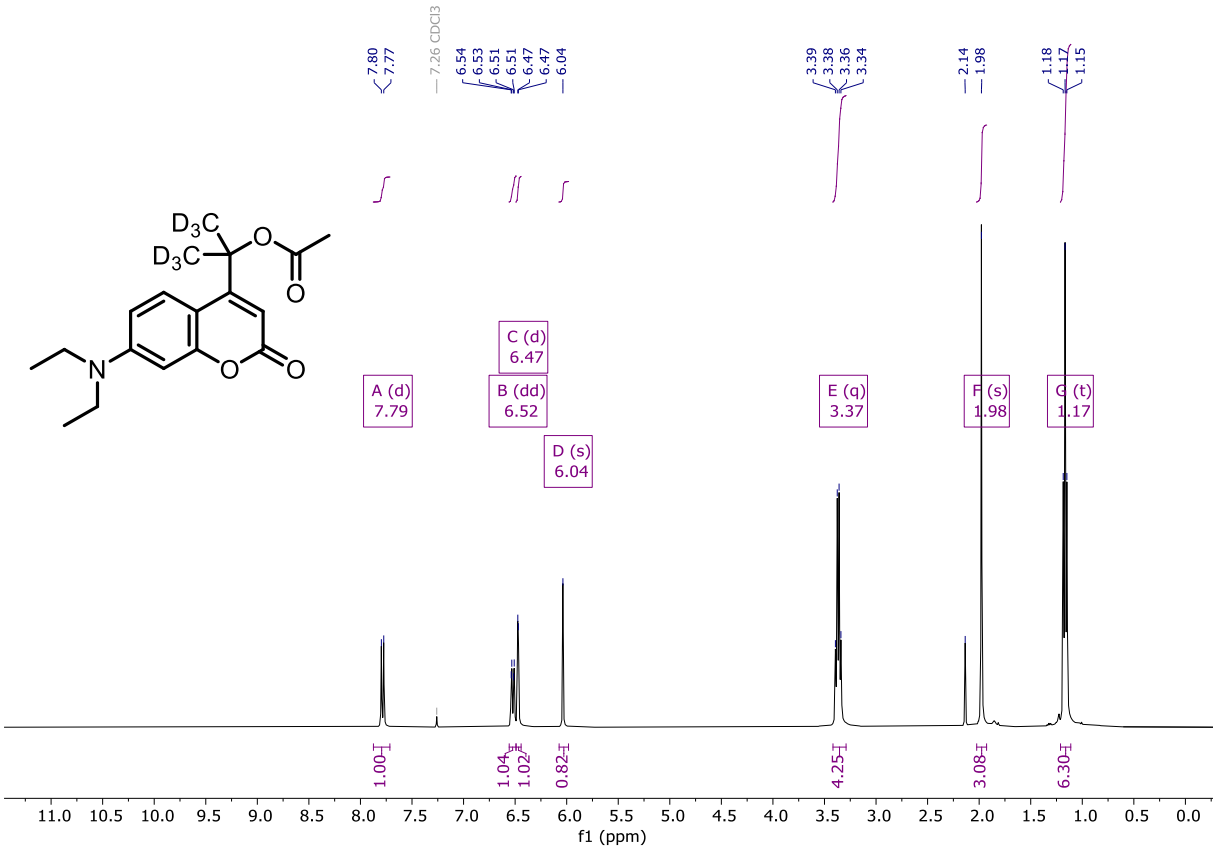

Figure S 23. ^{1}H-NMR spectrum of compound **6-D$_6$** ($CDCl_3$).

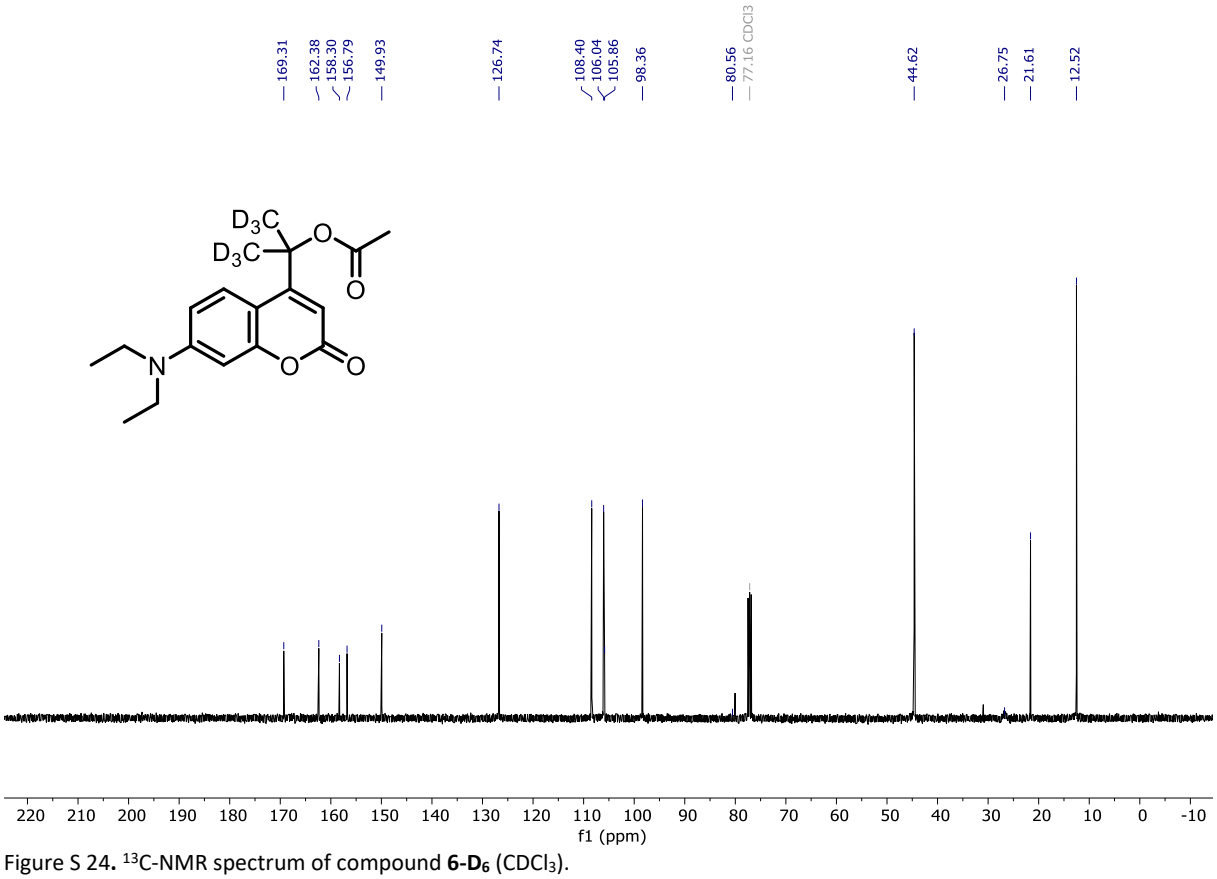

Figure S 24. ^{13}C-NMR spectrum of compound **6-D$_6$** ($CDCl_3$).

3. Photochemistry

3.1 ^{1}H-NMR study on the uncaging of compounds **7-12**

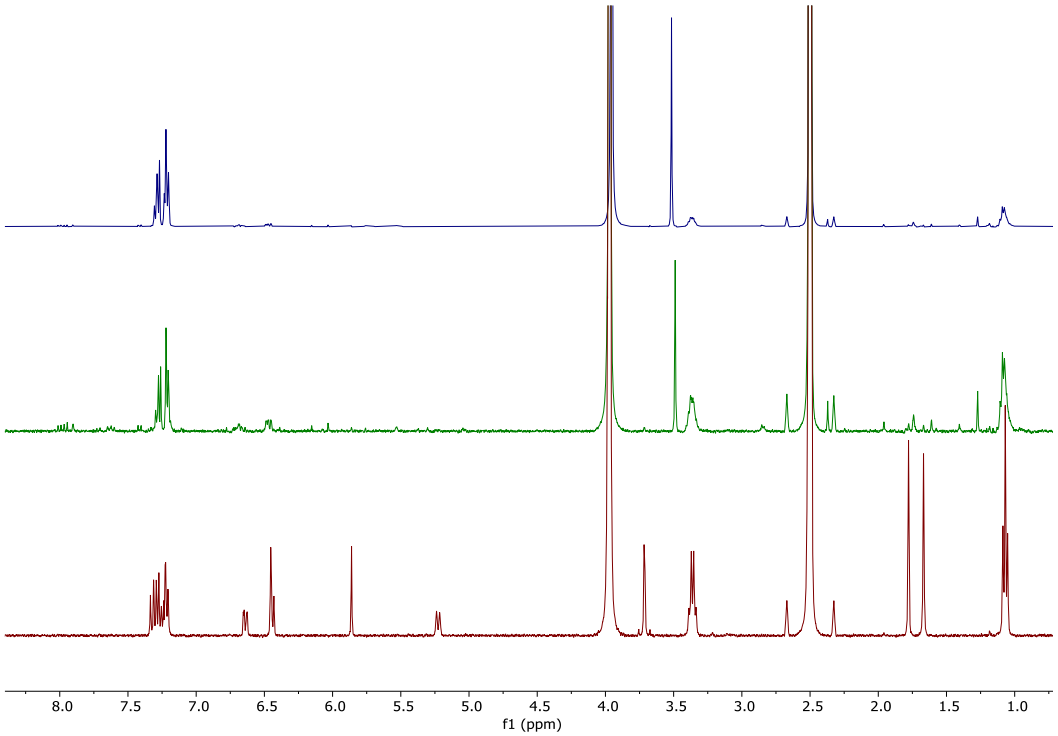

Figure S 25. ^{1}**H-NMR** spectra of compound **7** (1 mM, DMSO-d_6/D_2O 4:1) in the dark (red spectrum) and after 5 min of irradiation (green spectrum, λ = 400 nm). Phenylacetic acid release was confirmed by the addition of phenylacetic acid standard (blue spectrum). Signals reported relative to DMSO-d_6 at 2.50 ppm.

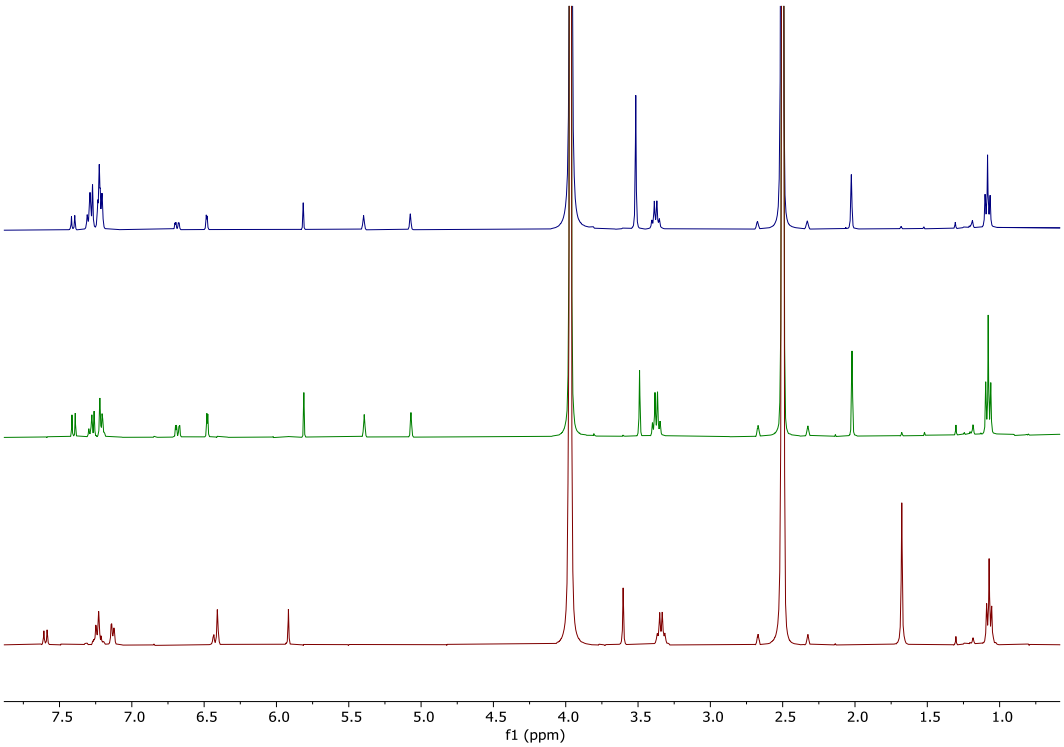

Figure S 26. ^{1}**H-NMR** spectra of compound **8** (1 mM, DMSO-d_6/D_2O 4:1) in the dark (red spectrum) and after 5 min of irradiation (green spectrum, λ = 400 nm). The formation of the coumarin-alkene can be observed. Phenylacetic acid release was confirmed by the addition of phenylacetic acid standard (blue spectrum). Signals reported relative to DMSO-d_6 at 2.50 ppm.

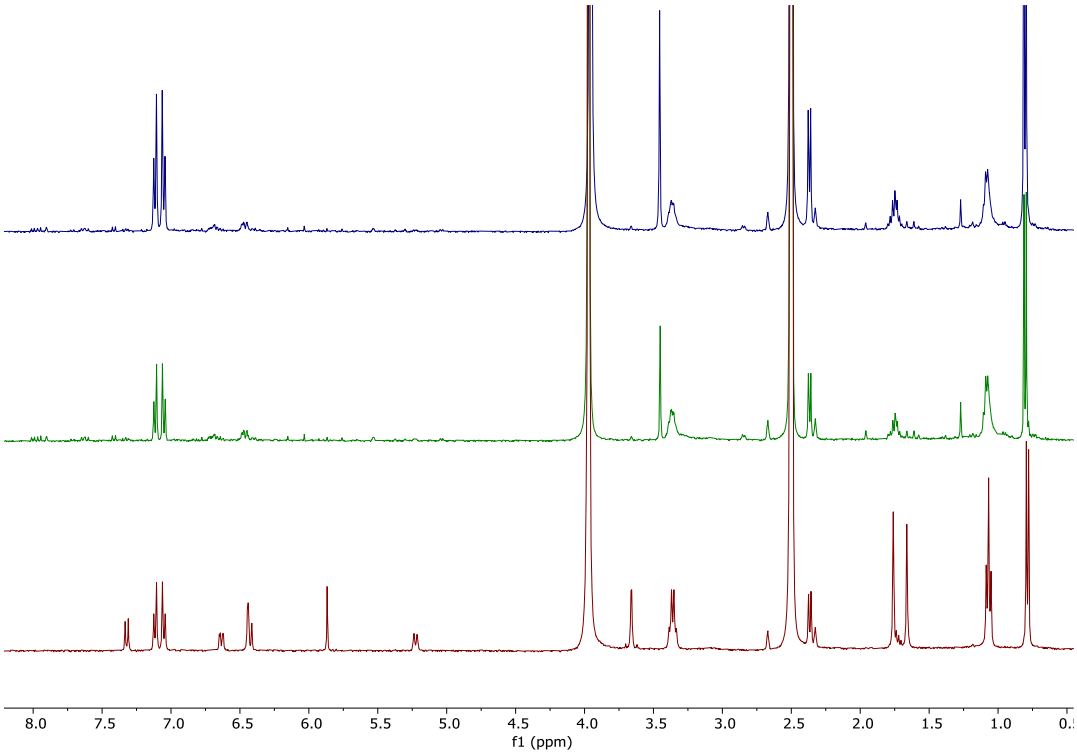

Figure S 27. ^{1}**H-NMR** spectra of compound **9** (1 mM, DMSO-d_6/D_2O 4:1) in the dark (red spectrum) and after 5 min of irradiation (green spectrum, λ = 400 nm). Ibufenac release was confirmed by the addition of ibufenac standard (blue spectrum). Signals reported relative to DMSO-d_6 at 2.50 ppm.

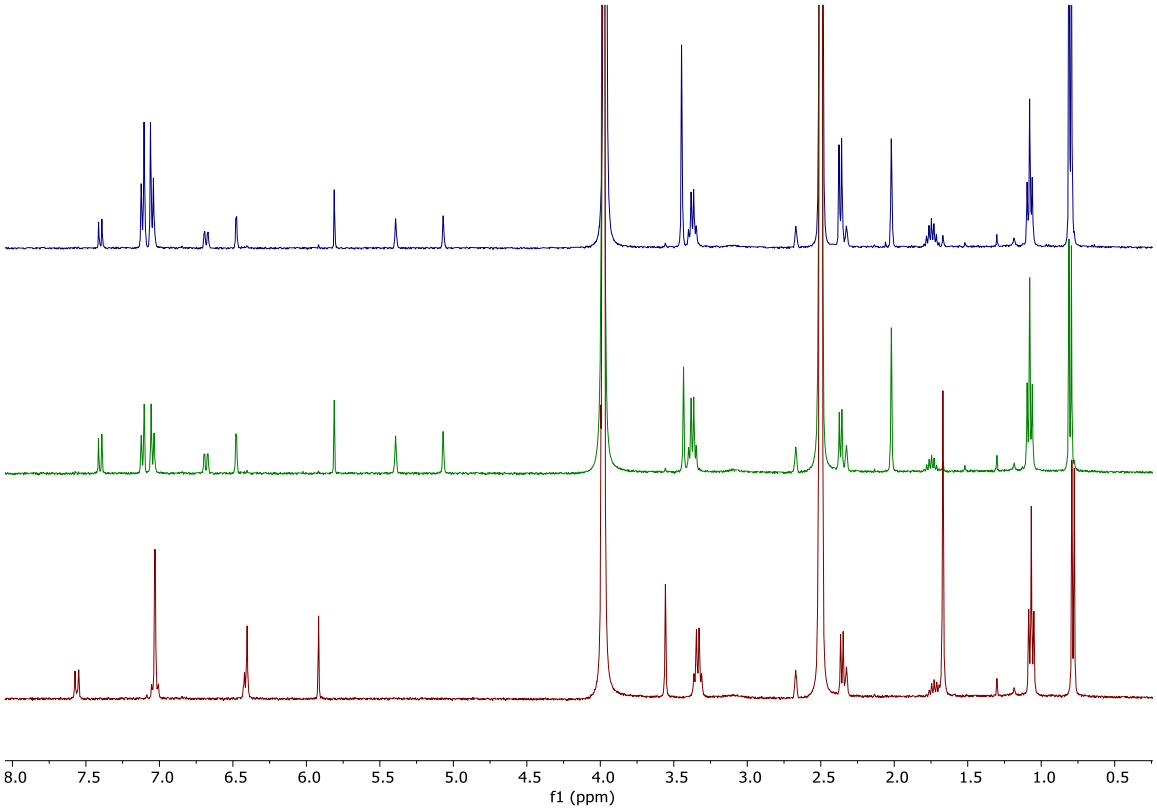

Figure S 28.^{1}**H-NMR** spectra of compound **10** (1 mM, DMSO-d_6/D_2O 4:1) in the dark (red spectrum) and after 5 min of irradiation (green spectrum, λ = 400 nm). The formation of the coumarin-alkene can be observed. Ibufenac release was confirmed by the addition of ibufenac standard (blue spectrum). Signals reported relative to DMSO-d_6 at 2.50 ppm.

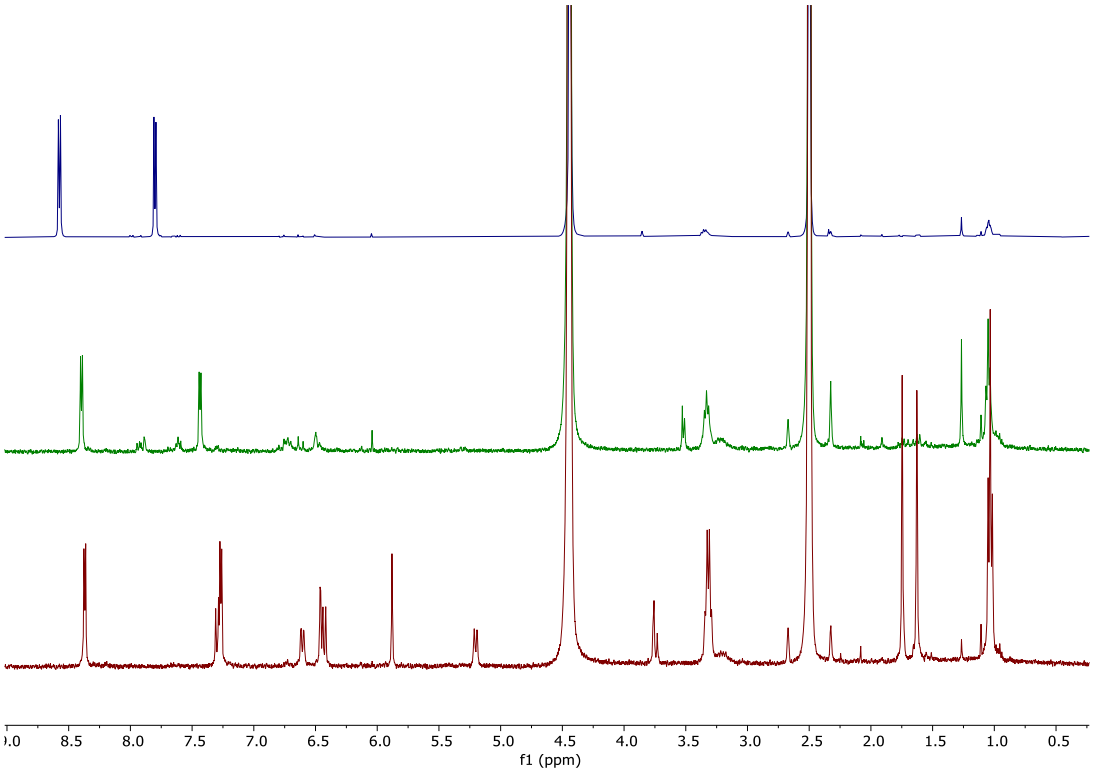

Figure S 29. ^{1}**H-NMR** spectra of compound **11** (1 mM, DMSO-d_6/D_2O 1:1) in the dark (red spectrum) and after 5 min of irradiation (green spectrum, λ = 400 nm). 2-(pyridin-4-yl)acetic acid release was confirmed by the addition of 2-(pyridin-4-yl)acetic acid hydrochloride standard (blue spectrum). The signals shift due to the addition of an HCl salt. Signals reported relative to DMSO-d_6 at 2.50 ppm.

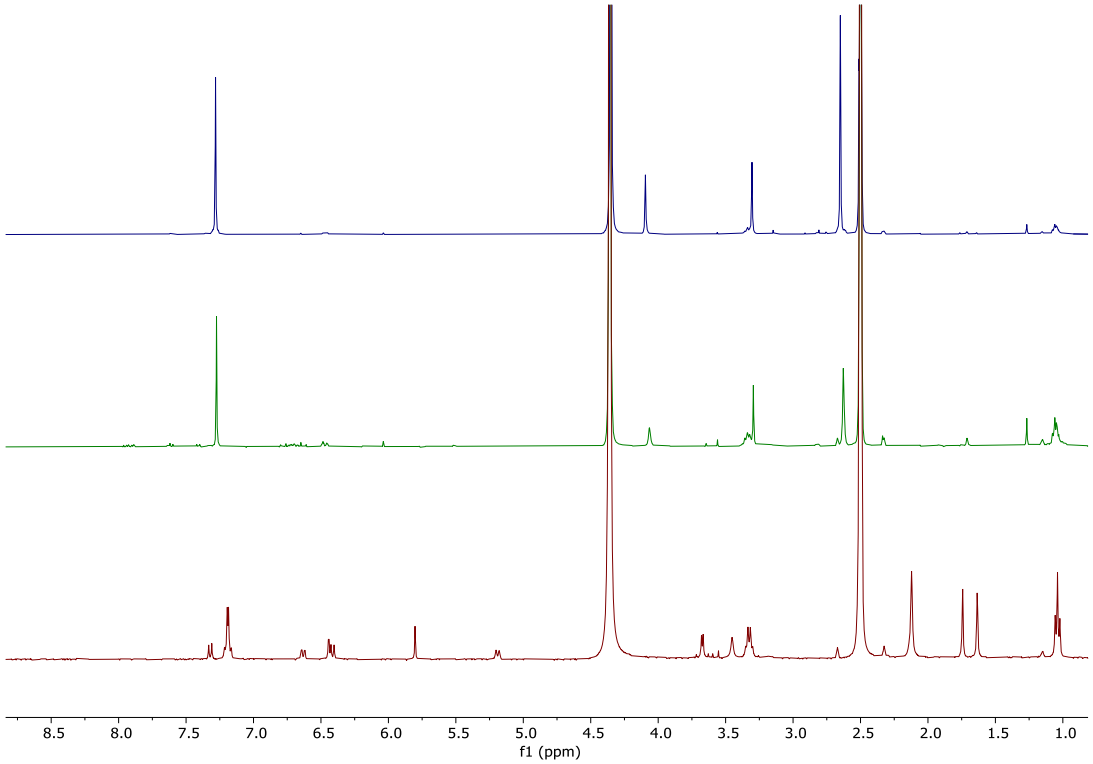

Figure S 30. ^{1}**H-NMR** spectra of compound **12** (0.8 mM, DMSO-d_6/D_2O 35:25) in the dark (red spectrum) and after 5 min of irradiation (green spectrum, λ = 400 nm). Payload release was confirmed by the addition of **S2** (blue spectrum). Signals reported relative to DMSO-d_6 at 2.50 ppm.

3.2 Solvent Effect

3.2.1 Irradiation-dependent absorption spectra of compounds **5** and **6** in water/THF mixtures

*Compound **5***

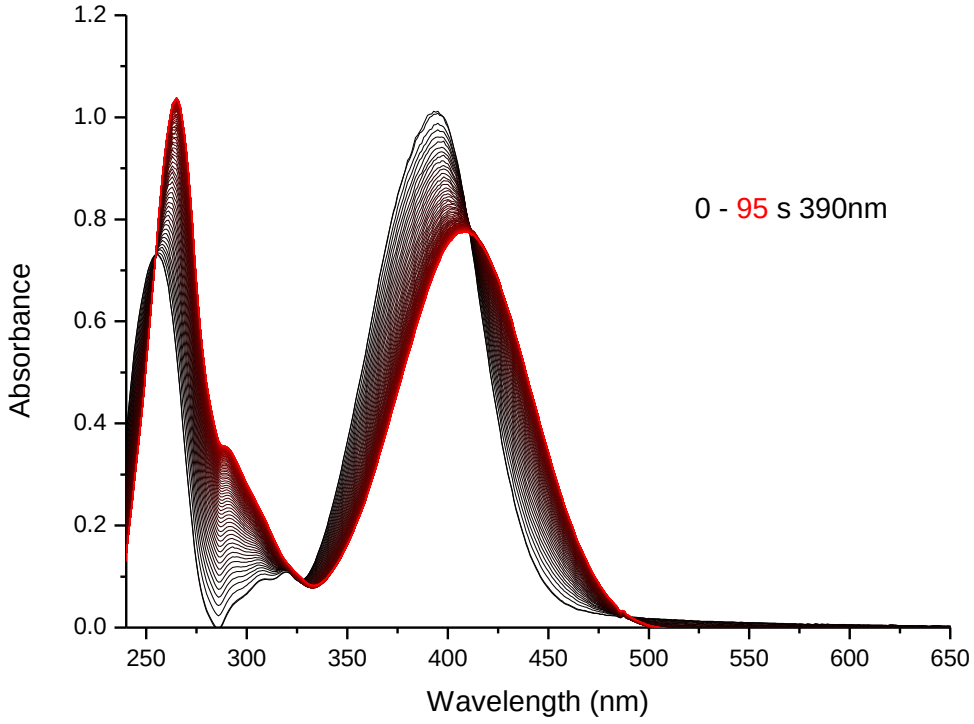

Figure S 31. UV-vis absorption spectra of compound **5** solution (60 µM, water/THF 95:5). A freshly prepared solution (black) and solution after irradiation (λ = 390 nm, red line).

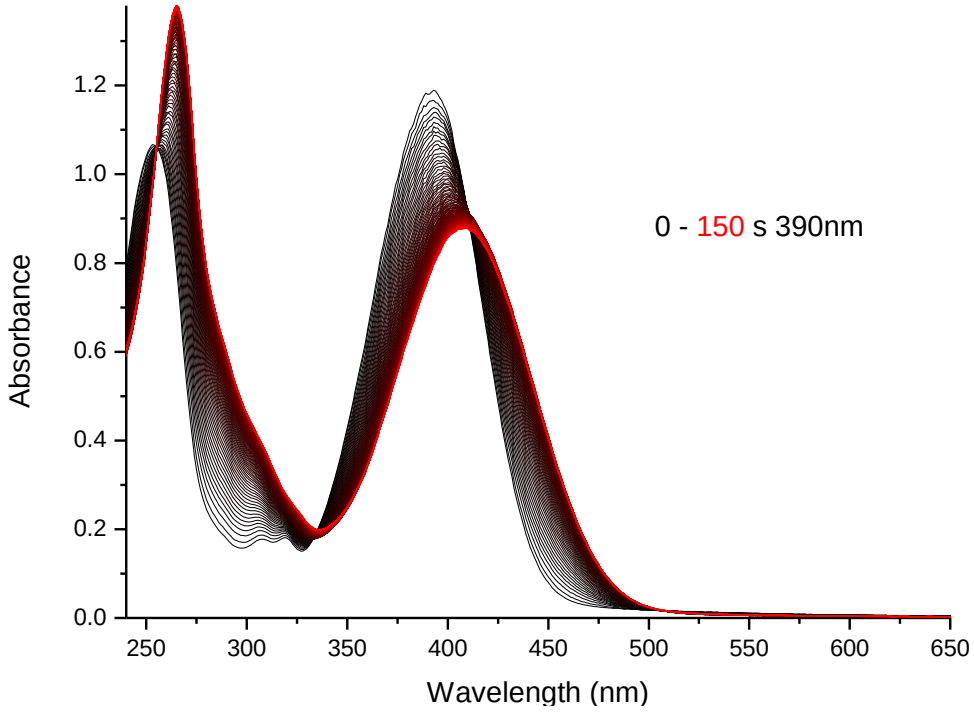

Figure S 32. UV-vis absorption spectra of compound **5** solution (60 µM, water/THF 9:1). A freshly prepared solution (black) and solution after irradiation (λ = 390 nm, red line).

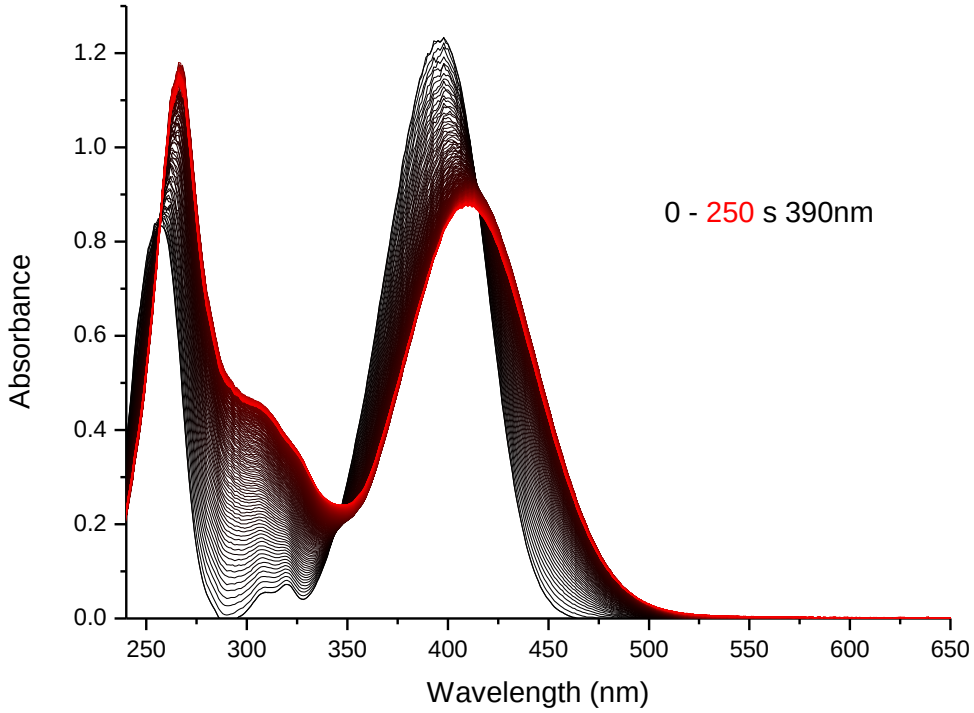

Figure S 33. UV-vis absorption spectra of compound **5** solution (60 µM, water/THF 8:2). A freshly prepared solution (black) and solution after irradiation (λ = 390 nm, red line).

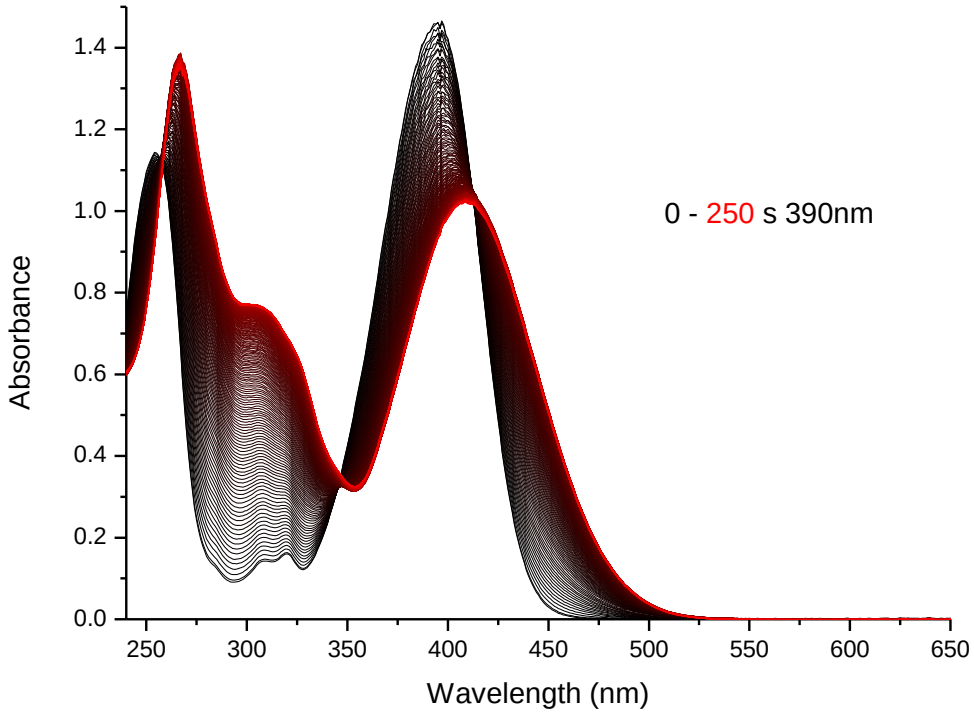

Figure S 34. UV-vis absorption spectra of compound **5** solution (60 µM, water/THF 7:3). A freshly prepared solution (black) and solution after irradiation (λ = 390 nm, red line).

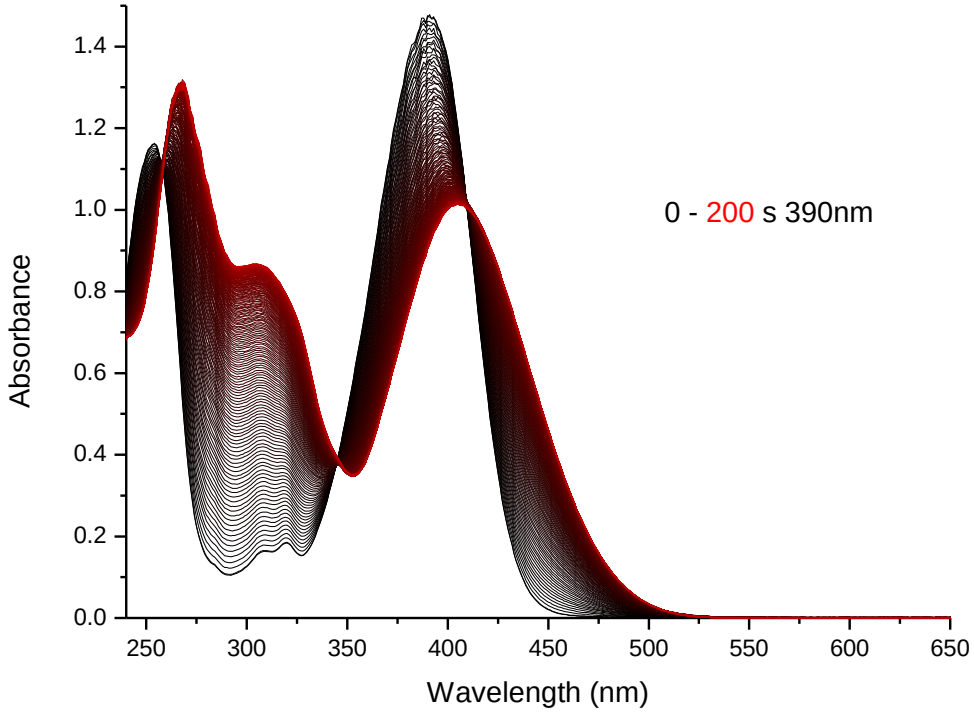

Figure S 35. UV-vis absorption spectra of compound **5** solution (60 µM, water/THF 6:4). A freshly prepared solution (black) and solution after irradiation (λ = 390 nm, red line).

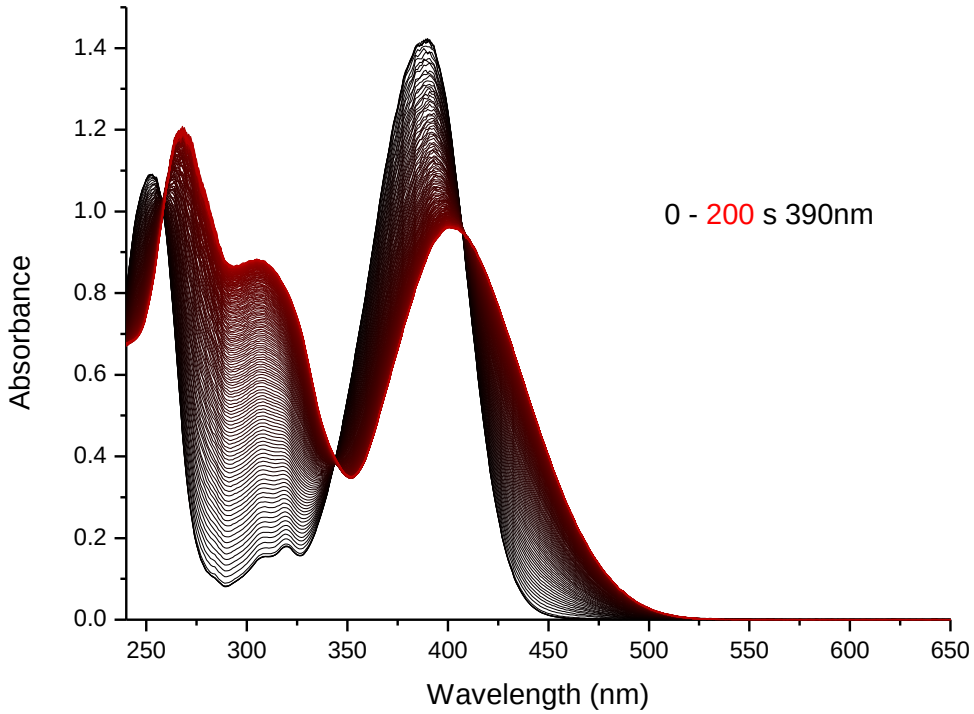

Figure S 36. UV-vis absorption spectra of compound **5** solution (60 µM, water/THF 1:1). A freshly prepared solution (black) and solution after irradiation (λ = 390 nm, red line).

*Compound **6***

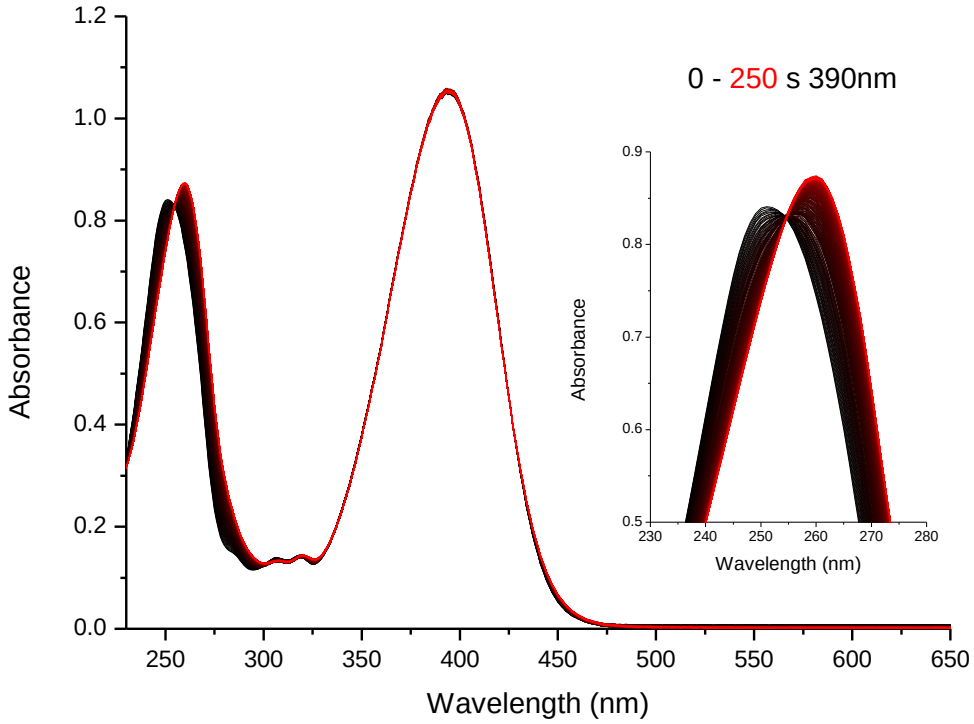

Figure S 37. UV-vis absorption spectra of compound **6** solution (60 µM, water/THF 95:5). A freshly prepared solution (black) and solution after irradiation (λ = 390 nm, red line). The insert highlights the isosbestic point.

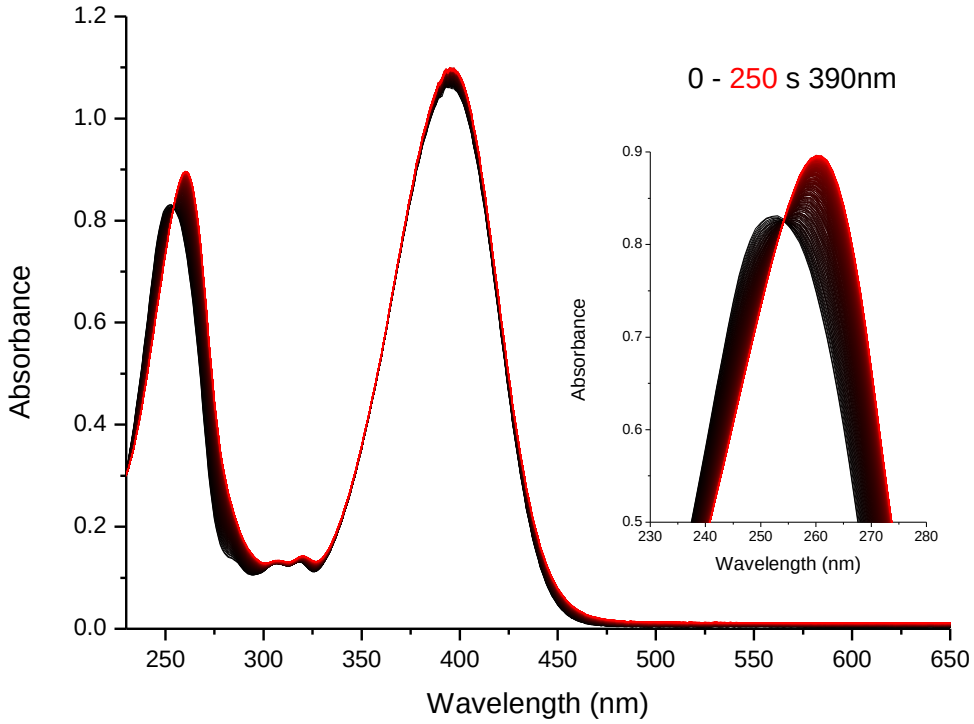

Figure S 38. UV-vis absorption spectra of compound **6** solution (60 µM, water/THF 9:1). A freshly prepared solution (black) and solution after irradiation (λ = 390 nm, red line). The insert highlights the isosbestic point.

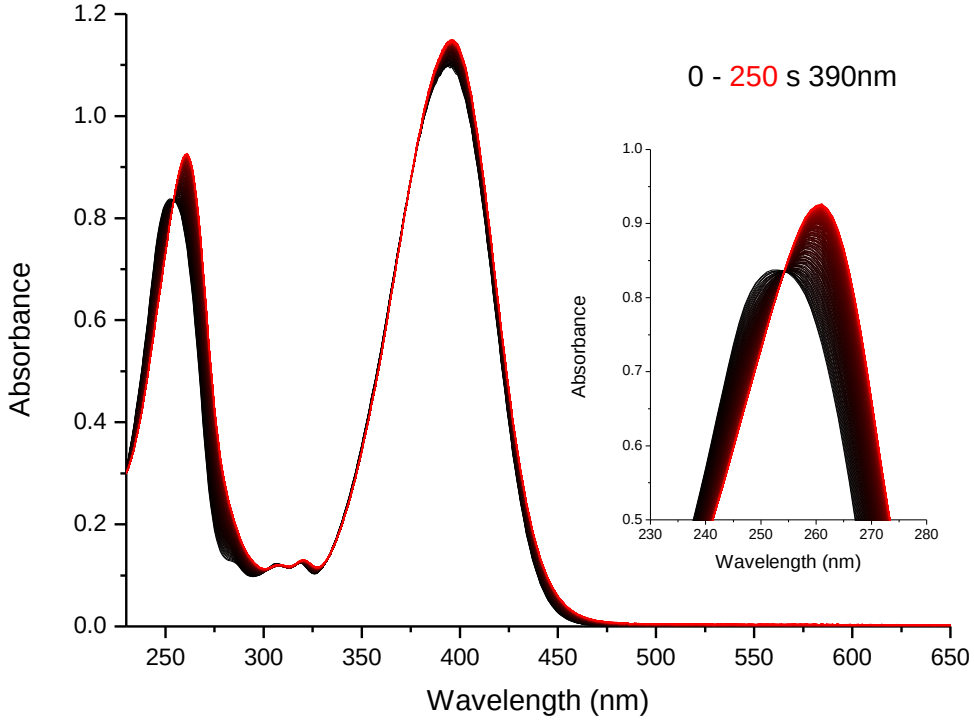

Figure S 39. UV-vis absorption spectra of compound **6** solution (60 µM, water/THF 8:2). A freshly prepared solution (black) and solution after irradiation (λ = 390 nm, red line). The insert highlights the isosbestic point.

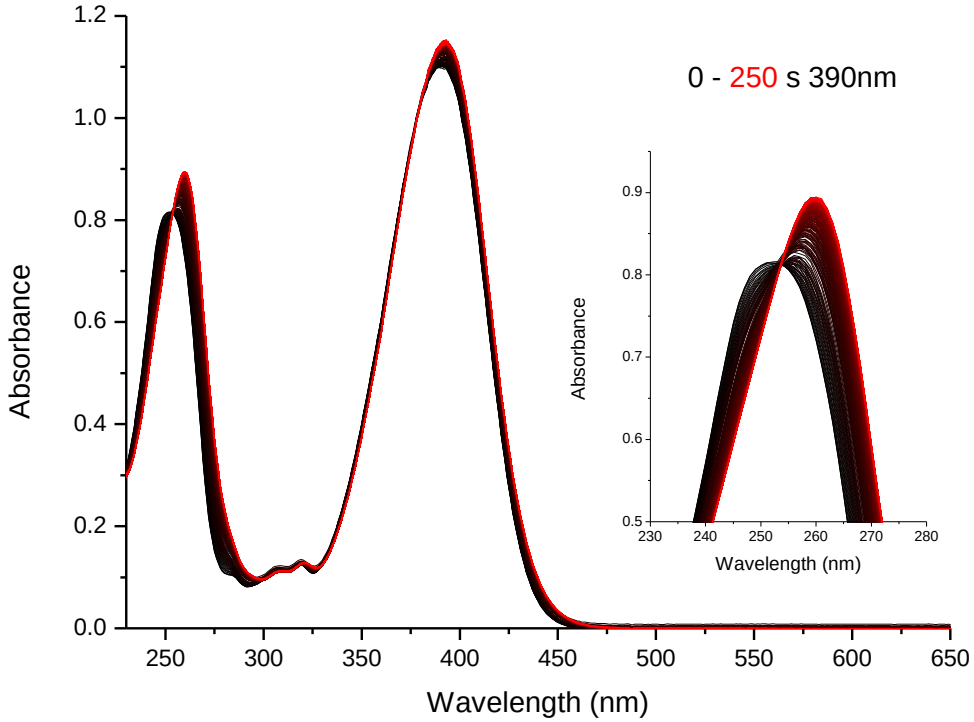

Figure S 40. UV-vis absorption spectra of compound **6** solution (60 µM, water/THF 7:3). A freshly prepared solution (black) and solution after irradiation (λ = 390 nm, red line). The insert highlights the isosbestic point.

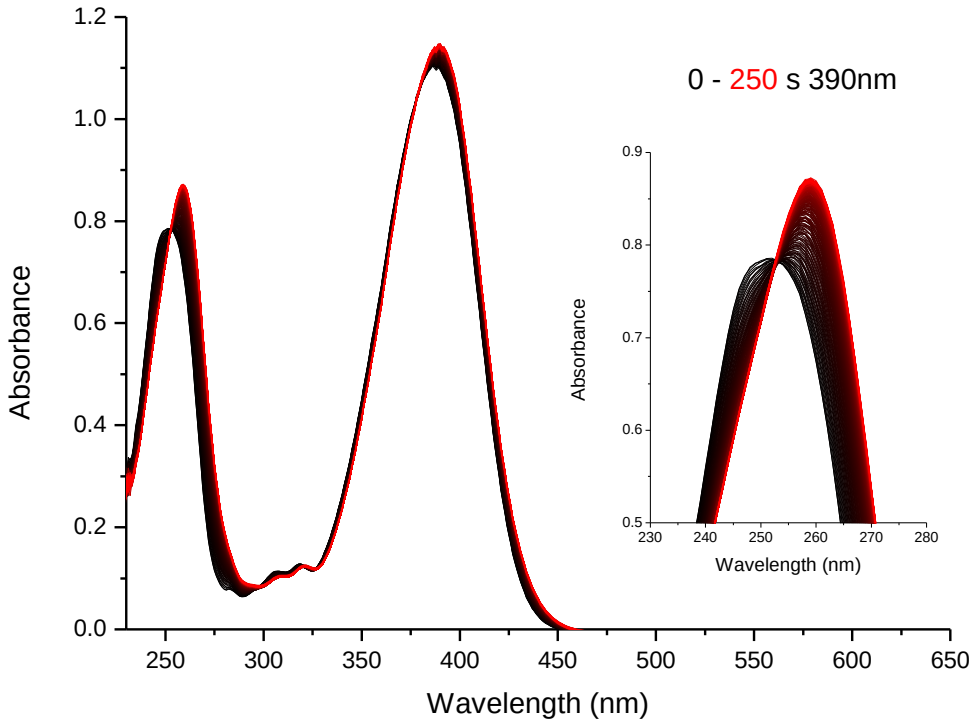

Figure S 41. UV-vis absorption spectra of compound **6** solution (60 µM, water/THF 6:4). A freshly prepared solution (black) and solution after irradiation (λ = 390 nm, red line). The insert highlights the isosbestic point.

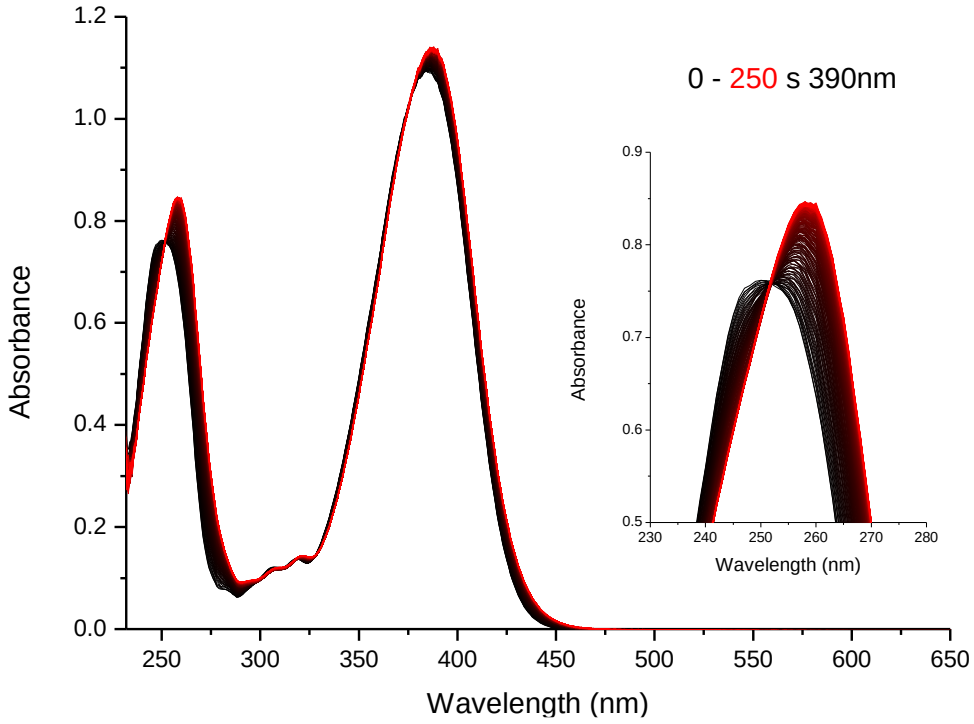

Figure S 42. UV-vis absorption spectra of compound **6** solution (60 µM, water/THF 1:1). A freshly prepared solution (black) and solution after irradiation (λ = 390 nm, red line). The insert highlights the isosbestic point.

3.2.2 Quantum Yields of compounds 5 and 6 in water/THF mixtures

The QY of PPG photolysis was determined using the following formula:

$$\frac{conversion\ rate\ (s^{-1}) \times concentration\ (mM) \times volume\ (L)}{corrected\ photon\ flux\ (mmol \times s^{-1})}$$

The normalized conversion rate was determined by UV-vis spectroscopy through following PPG consumption at a fixed wavelength upon irradiation (λ = 390 nm). The average rate over the first 10 % of conversion was determined through fitting a trend-line and multiplied by the concentration and volume of the sample to reach a PPG consumption rate in mmol · s^{-1}. This rate was divided by the photon flux at λ = 390 nm ($2.84 \cdot 10^{-5}$ mmol · s^{-1} or $2.98 \cdot 10^{-5}$ mmol · s^{-1}, determined by ferrioxalate actinometry[3]) that was corrected for the specific absorbance of each sample at the irradiation wavelength (A ≈ 1, values reported, λ = 390 nm). All measurements were performed in triplicate and averages and standard deviations are reported for all QYs.

A Prizmatix FC6-LED Multi channel fiber coupled LED source was used. For irradiation of the coumarin PPGs, the 390 nm channel was used which consists of a LED with a peak wavelength at 389.67 nm, FWHM 14.28 nm and -depending on when the measurement was taken- a photon flux as reported in the caption of every figure that reports a QY. 2 mL solutions were irradiated in a quartz cuvette (10 x 10 mm) from the side.

To accurately measure the QY, we first start recording absorption spectra before turning on the LED irradiation source and starting the photochemical reaction. This way, we capture the initial rate of uncaging and don't miss it through first turning on the LED and afterwards start recording spectra. A result of this technique is that we always have to omit the first spectrum that's recorded by our spectrophotometer because the irradiation LED was turned on somewhere between this first measurement and the second measurement. This means that substrate conversion between measurement 1 and 2 will be less than the conversion between the later measurements, because the LED was only turned on for part of the time between these first 2 measurements. If we didn't omit the first measurement, our QY values will be slightly off. Because of this, the conversion plots always start slightly above zero, caused by the conversion that is achieved between measurement 1 and measurement 2.

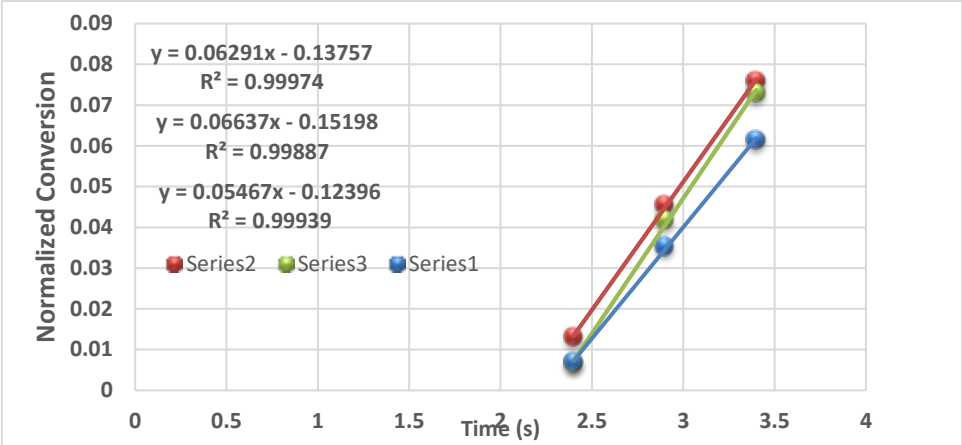

water/THF 95:5	Compound 5	rate	A_{390}	QY
	#1	0,06291	1,00	0,296
	#2	0,06637	1,00	0,312
	#3	0,05467	1,03	0,255
			Av. QY	**0,288**
			SD	**0,024**

Figure S 43. Normalized conversion of compound **5** (60 µM, 2mL water/THF 95:5, 25 °C) (y-axis) vs time (x-axis). Shown are the measurements taken after the start of irradiation (λ = 390 nm). A linear trendline allowed for the determination of the average rate over the first 10% of PPG consumption. Conversion followed at λ = 450 nm (photon flux 2,837*10^{-5} mmol/s). Normalization of the absorbance values was performed from data collection start (t=0) to the maximum achieved absorbance value at full deprotection.

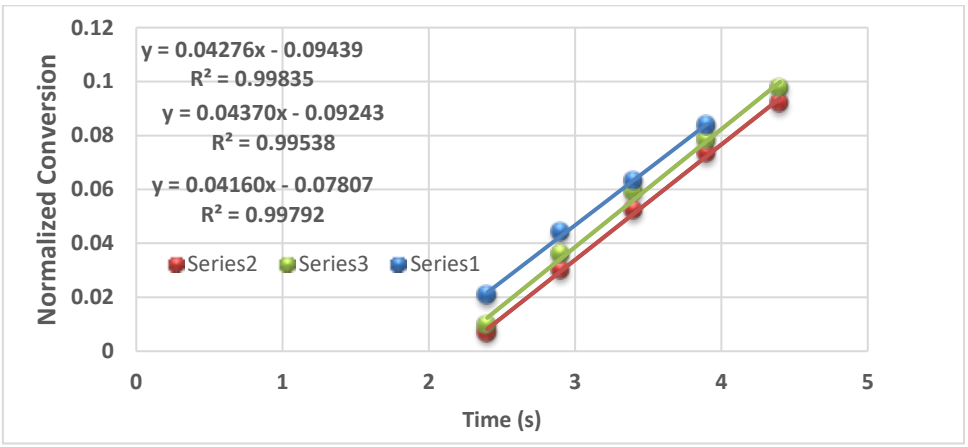

water/THF 9:1	compound 5	rate	A_{390}	QY
	#1	0,04276	1,21	0,193
	#2	0,04370	1,18	0,198
	#3	0,04160	1,20	0,188
			Av. QY	**0,193**
			SD	0,004

Figure S 44. Normalized conversion of compound **5** (60 µM, 2mL water/THF 9:1, 25 °C) (y-axis) vs time (x-axis). Shown are the measurements taken after the start of irradiation (λ = 390 nm). A linear trendline allowed for the determination of the average rate over the first 10% of PPG consumption. Conversion followed at λ = 450 nm (photon flux 2,837*10^{-5} mmol/s). Normalization of the absorbance values was performed from data collection start (t=0) to the maximum achieved absorbance value at full deprotection.

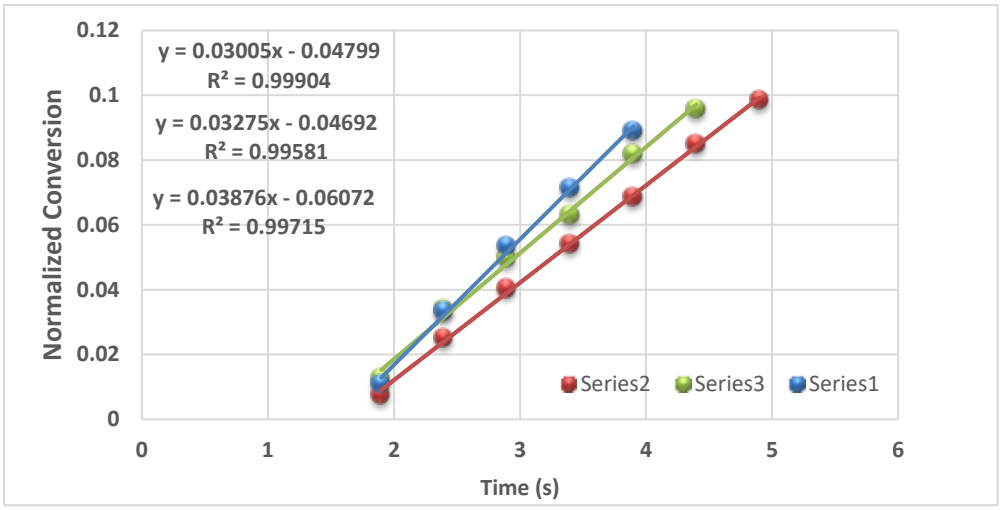

water/THF 8:2	compound 5	rate	A_{390}	QY
	#1	0,03005	1,26	0,135
	#2	0,03275	1,21	0,148
	#3	0,03876	1,20	0,175
			Av. QY	**0,153**
			SD	0,017

Figure S 45. Normalized conversion of compound **5** (60 µM, 2mL water/THF 8:2, 25 °C) (y-axis) vs time (x-axis). Shown are the measurements taken after the start of irradiation (λ = 390 nm). A linear trendline allowed for the determination of the average rate over the first 10% of PPG consumption. Conversion followed at λ = 450 nm (photon flux 2,837*10^{-5} mmol/s). Normalization of the absorbance values was performed from data collection start (t=0) to the maximum achieved absorbance value at full deprotection.

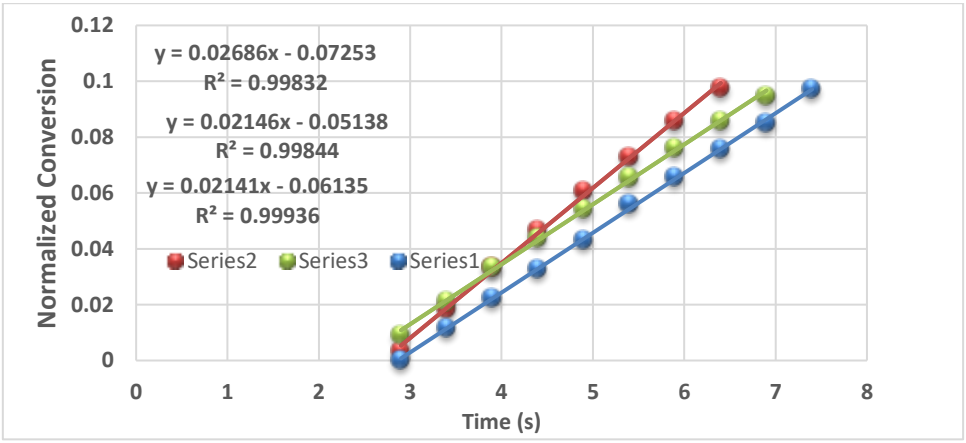

water/THF 7:3	compound 5	rate	A_{390}	QY
	#1	0,02686	1,39	0,118
	#2	0,02146	1,43	0,094
	#3	0,02141	1,41	0,094
			Av. QY	**0,102**
			SD	0,011

Figure S 46. Normalized conversion of compound **5** (60 µM, 2mL water/THF 7:3, 25 °C) (y-axis) vs time (x-axis). Shown are the measurements taken after the start of irradiation (λ = 390 nm). A linear trendline allowed for the determination of the average rate over the first 10% of PPG consumption. Conversion followed at λ = 450 nm (photon flux 2,837*10^{-5} mmol/s). Normalization of the absorbance values was performed from data collection start (t=0) to the maximum achieved absorbance value at full deprotection.

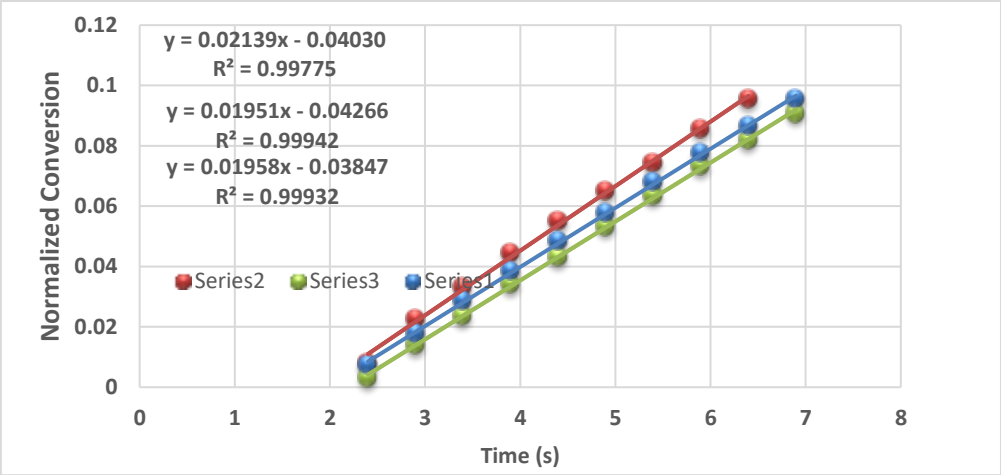

water/THF 6:4	compound 5	rate	A_{390}	QY
	#1	0,02139	1,46	0,094
	#2	0,01951	1,47	0,085
	#3	0,01958	1,47	0,086
			Av. QY	**0,088**
			SD	0,004

Figure S 47**.** Normalized conversion of compound **5** (60 µM, 2mL water/THF 6:4, 25 °C) (y-axis) vs time (x-axis). Shown are the measurements taken after the start of irradiation (λ = 390 nm). A linear trendline allowed for the determination of the average rate over the first 10% of PPG consumption. Conversion followed at λ = 450 nm (photon flux 2,837*10^{-5} mmol/s). Normalization of the absorbance values was performed from data collection start (t=0) to the maximum achieved absorbance value at full deprotection.

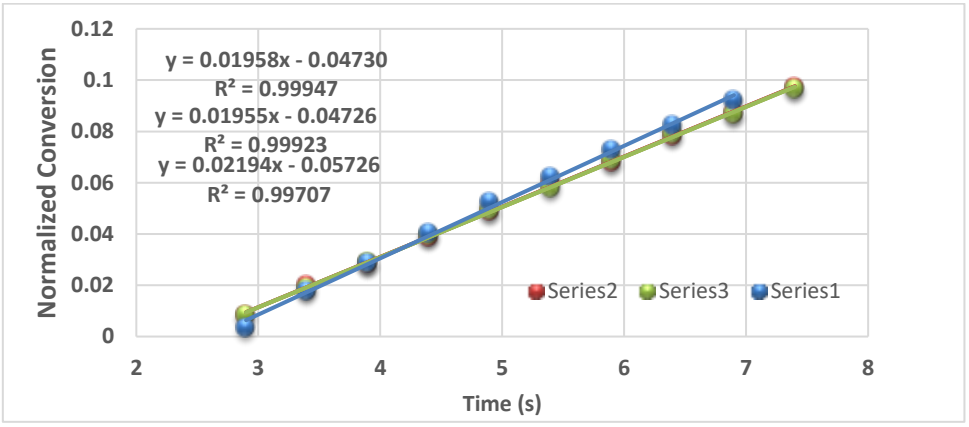

water/THF 1:1	compound 5	rate	A_{390}	QY
	#1	0,01958	1,42	0,086
	#2	0,01955	1,40	0,086
	#3	0,02194	1,43	0,096
			Av. QY	**0,090**
			SD	0,005

Figure S 48**.** Normalized conversion of compound **5** (60 µM, 2mL water/THF 1:1, 25 °C) (y-axis) vs time (x-axis). Shown are the measurements taken after the start of irradiation (λ = 390 nm). A linear trendline allowed for the determination of the average rate over the first 10% of PPG consumption. Conversion followed at λ = 450 nm (photon flux 2,837*10^{-5} mmol/s). Normalization of the absorbance values was performed from data collection start (t=0) to the maximum achieved absorbance value at full deprotection.

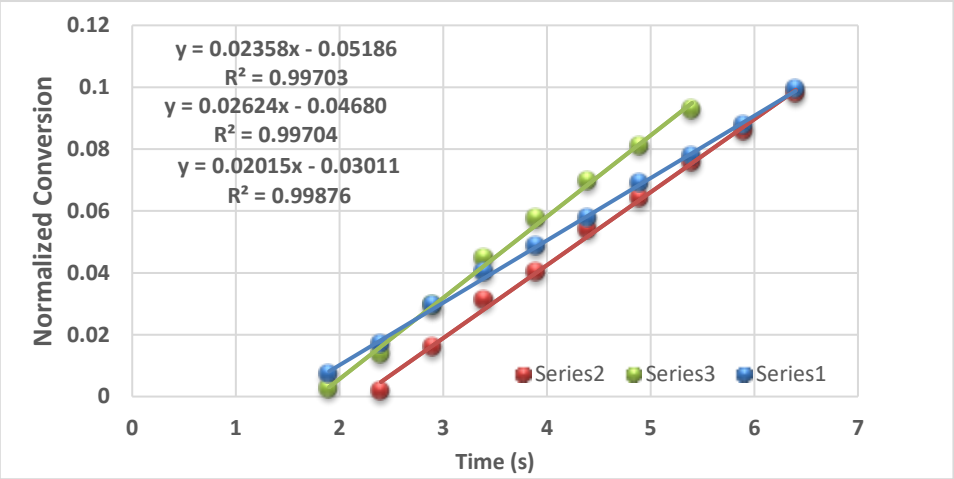

water/THF 95:5	compound 6	rate	A_{390}	QY
	#1	0,02358	1,00	0,111
	#2	0,02624	1,01	0,123
	#3	0,02015	1,04	0,094
			Av. QY	**0,109**
			SD	0,012

Figure S 49**.** Normalized conversion of compound **6** (60 µM, 2mL water/THF 95:5, 25 °C) (y-axis) vs time (x-axis). Shown are the measurements taken after the start of irradiation (λ = 390 nm). A linear trendline allowed for the determination of the average rate over the first 10% of PPG consumption. Conversion followed at λ = 270 nm (photon flux 2,837*10^{-5} mmol/s). Normalization of the absorbance values was performed from data collection start (t=0) to the maximum achieved absorbance value at full deprotection.

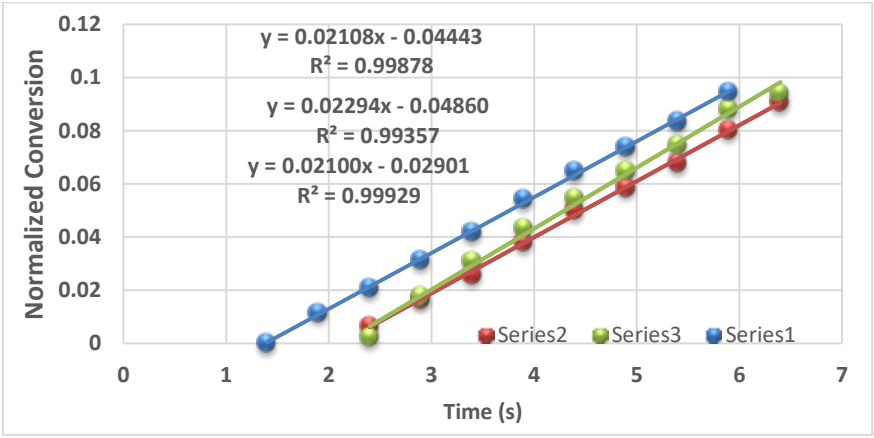

water/THF 9:1	compound 6	rate	A_{390}	QY
	#1	0,02108	1,02	0,099
	#2	0,02294	1,03	0,107
	#3	0,02100	1,03	0,098
			Av. QY	**0,101**
			SD	0,004

Figure S 50**.** Normalized conversion of compound **6** (60 µM, 2mL water/THF 9:1, 25 °C) (y-axis) vs time (x-axis). Shown are the measurements taken after the start of irradiation (λ = 390 nm). A linear trendline allowed for the determination of the average rate over the first 10% of PPG consumption. Conversion followed at λ = 270 nm (photon flux 2,837*10^{-5} mmol/s). Normalization of the absorbance values was performed from data collection start (t=0) to the maximum achieved absorbance value at full deprotection.

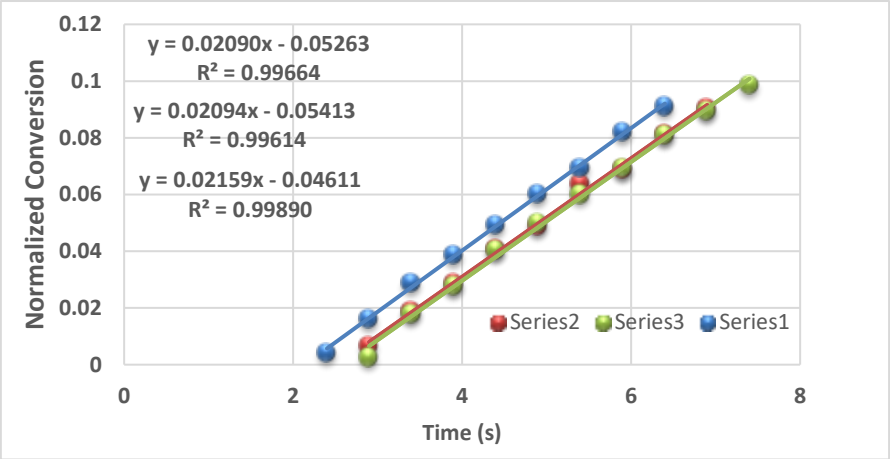

water/THF 8:2	compound 6	rate	A_{390}	QY
	#1	0,02090	1,06	0,097
	#2	0,02094	1,08	0,097
	#3	0,02159	1,08	0,100
			Av. QY	**0,098**
			SD	0,001

Figure S 51. Normalized conversion of compound **6** (60 µM, 2mL water/THF 8:2, 25 °C) (y-axis) vs time (x-axis). Shown are the measurements taken after the start of irradiation (λ = 390 nm). A linear trendline allowed for the determination of the average rate over the first 10% of PPG consumption. Conversion followed at λ = 270 nm (photon flux 2,837*10^{-5} mmol/s). Normalization of the absorbance values was performed from data collection start (t=0) to the maximum achieved absorbance value at full deprotection.

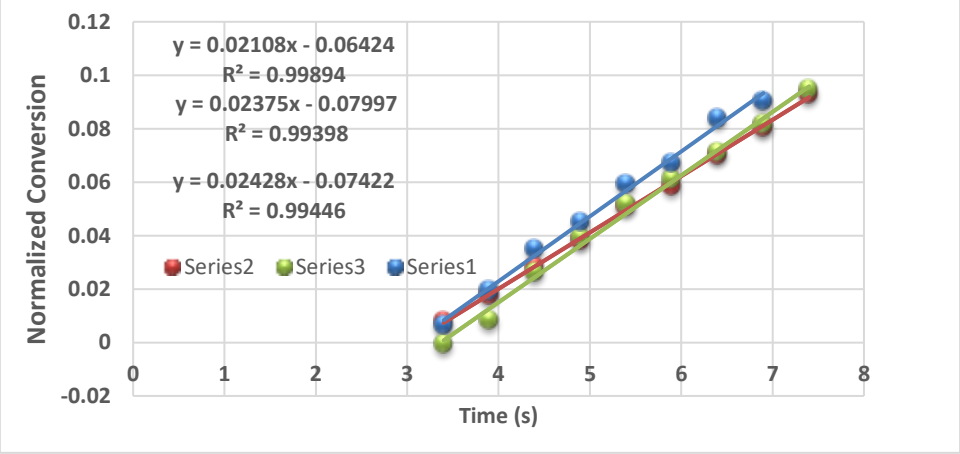

water/THF 7:3	compound 6	rate	A_{390}	QY
	#1	0,02108	1,10	0,097
	#2	0,02375	1,13	0,109
	#3	0,02428	1,12	0,111
			Av. QY	**0,106**
			SD	0,006

Figure S 52. Normalized conversion of compound **6** (60 µM, 2mL water/THF 7:3, 25 °C) (y-axis) vs time (x-axis). Shown are the measurements taken after the start of irradiation (λ = 390 nm). A linear trendline allowed for the determination of the average rate over the first 10% of PPG consumption. Conversion followed at λ = 270 nm (photon flux 2,837*10^{-5} mmol/s). Normalization of the absorbance values was performed from data collection start (t=0) to the maximum achieved absorbance value at full deprotection.

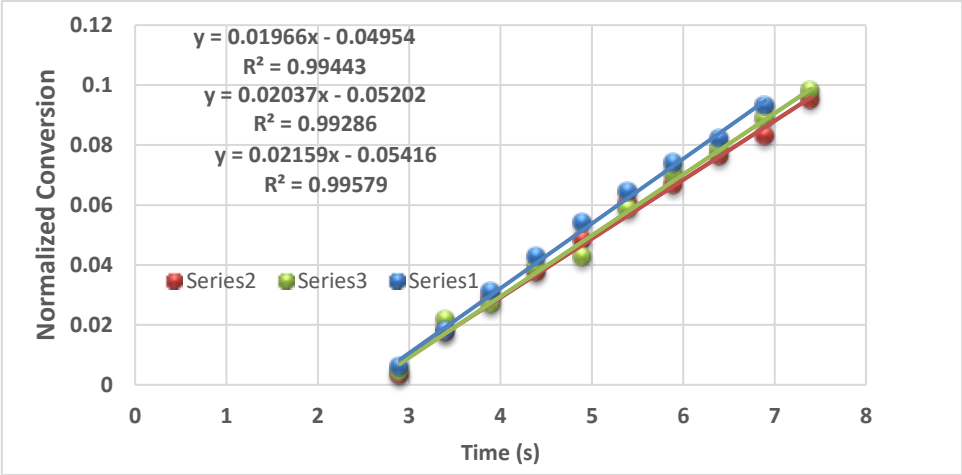

water/THF 6:4	compound 6	rate	A_{390}	QY
	#1	0,01966	1,10	0,090
	#2	0,02037	1,12	0,093
	#3	0,02159	1,12	0,099
			Av. QY	**0,094**
			SD	0,004

Figure S 53**.** Normalized conversion of compound **6** (60 µM, 2mL water/THF 6:4, 25 °C) (y-axis) vs time (x-axis). Shown are the measurements taken after the start of irradiation (λ = 390 nm). A linear trendline allowed for the determination of the average rate over the first 10% of PPG consumption. Conversion followed at λ = 270 nm (photon flux 2,837*10^{-5} mmol/s). Normalization of the absorbance values was performed from data collection start (t=0) to the maximum achieved absorbance value at full deprotection.

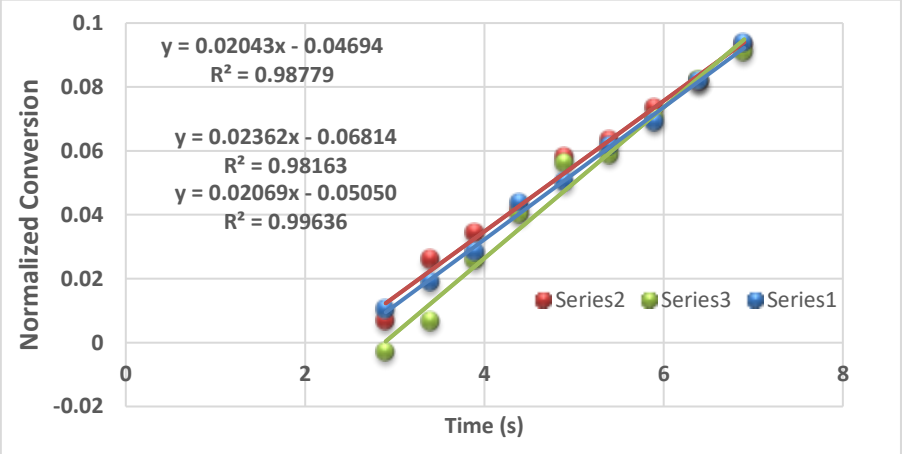

water/THF 1:1	compound 6	rate	A_{390}	QY
	#1	0,02043	1,07	0,094
	#2	0,02362	1,08	0,109
	#3	0,02069	1,09	0,095
			Av. QY	**0,100**
			SD	0,007

Figure S 54**.** Normalized conversion of compound **6** (60 µM, 2mL water/THF 1:1, 25 °C) (y-axis) vs time (x-axis). Shown are the measurements taken after the start of irradiation (λ = 390 nm). A linear trendline allowed for the determination of the average rate over the first 10% of PPG consumption. Conversion followed at λ = 270 nm (photon flux 2,837*10^{-5} mmol/s). Normalization of the absorbance values was performed from data collection start (t=0) to the maximum achieved absorbance value at full deprotection.

3.2.3 Irradiation-dependent absorption spectra of compounds **5** and **6** in various solvent mixtures

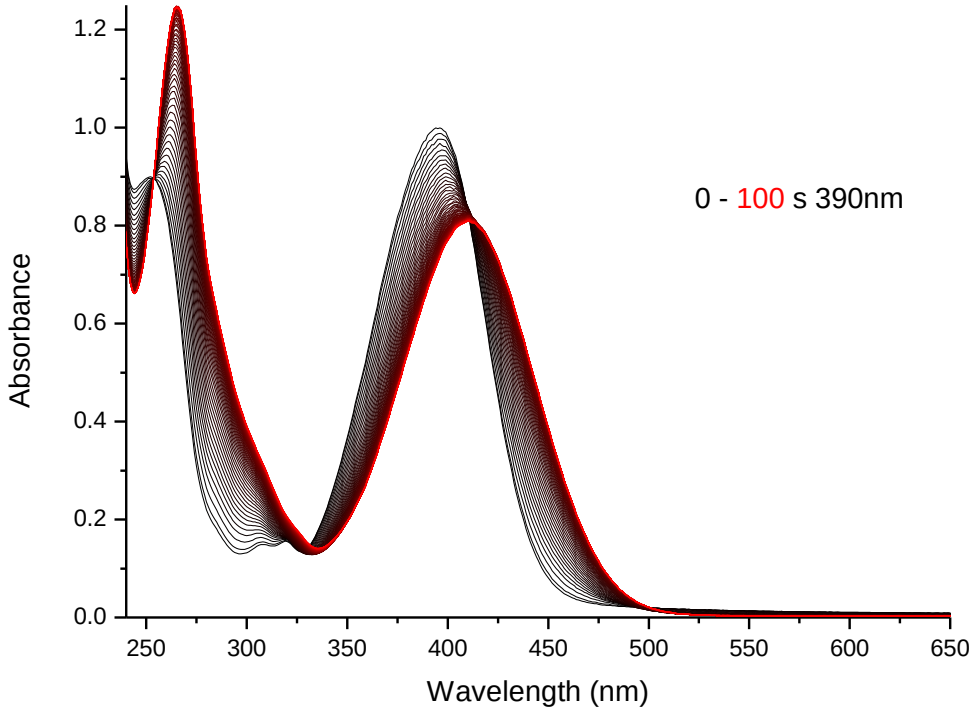

Figure S 55. UV-vis absorption spectra of compound **5** solution (50 µM, water/DMSO 95:5). A freshly prepared solution (black) and solution after irradiation (λ = 390 nm, red line).

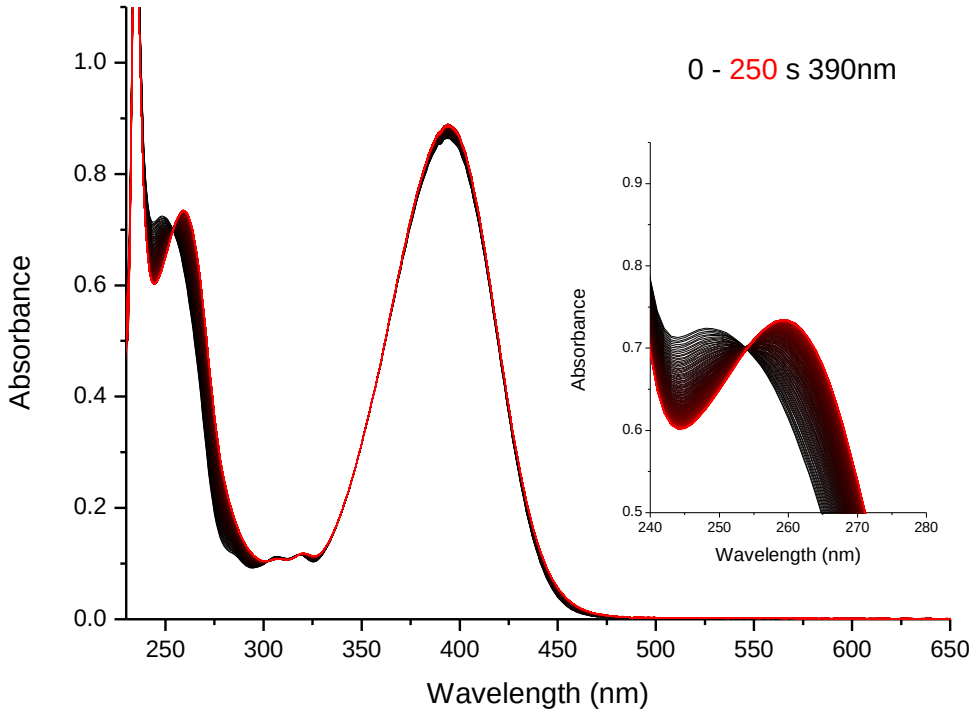

Figure S 56. UV-vis absorption spectra of compound **6** solution (50 µM, water/DMSO 95:5). A freshly prepared solution (black) and solution after irradiation (λ = 390 nm, red line). The insert highlights the isosbestic point.

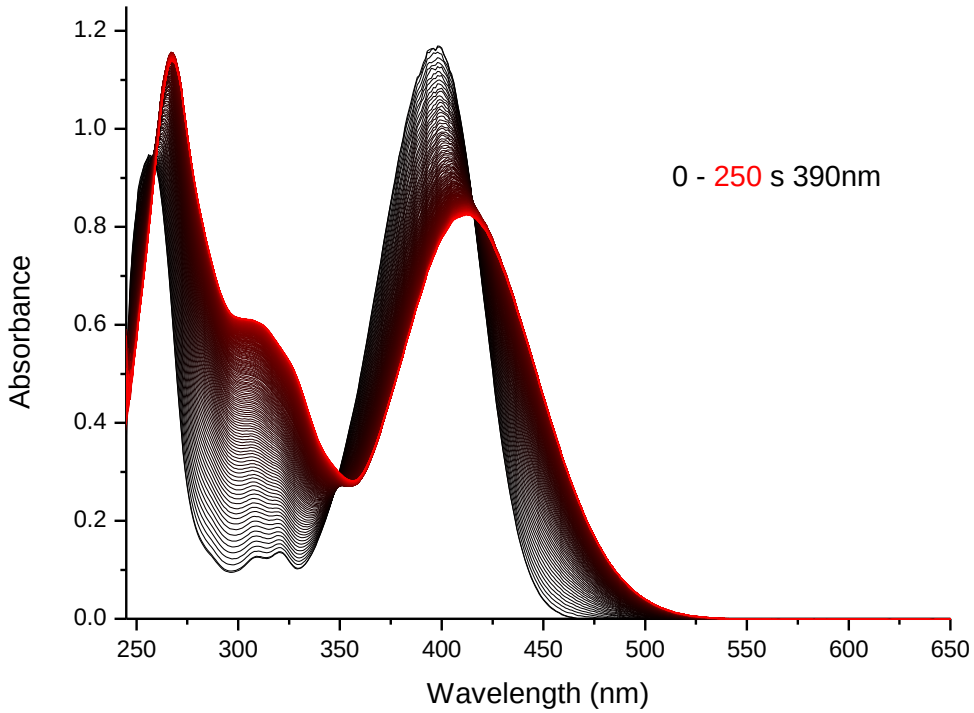

Figure S 57. UV-vis absorption spectra of compound **5** solution (50 µM, water/DMSO 1:1). A freshly prepared solution (black) and solution after irradiation (λ = 390 nm, red line).

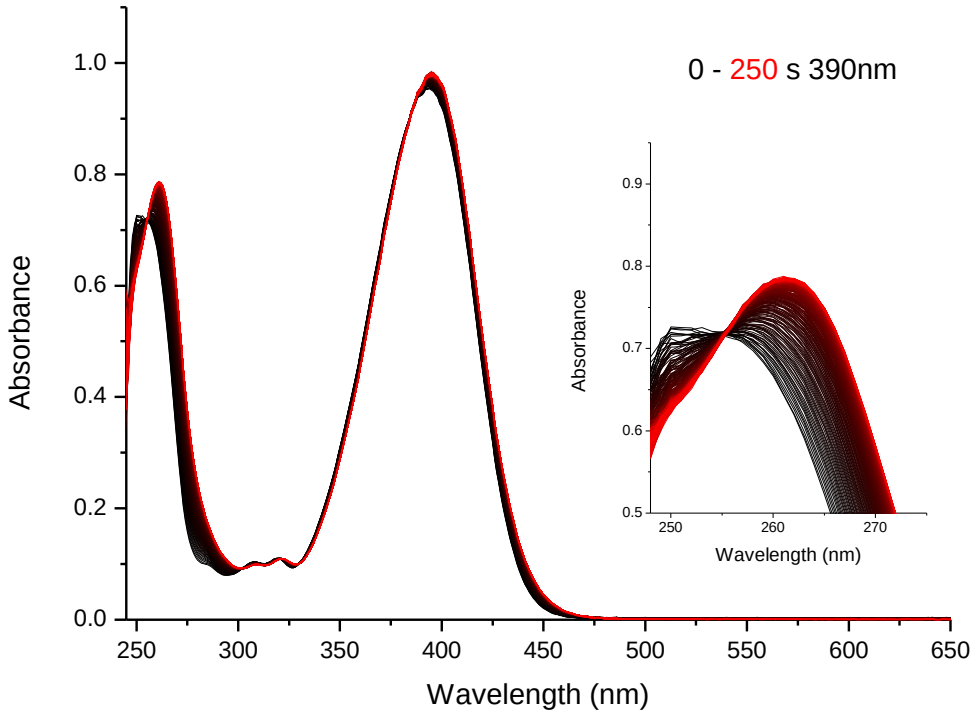

Figure S 58. UV-vis absorption spectra of compound **6** solution (50 µM, water/DMSO 1:1). A freshly prepared solution (black) and solution after irradiation (λ = 390 nm, red line). The insert highlights the isosbestic point.

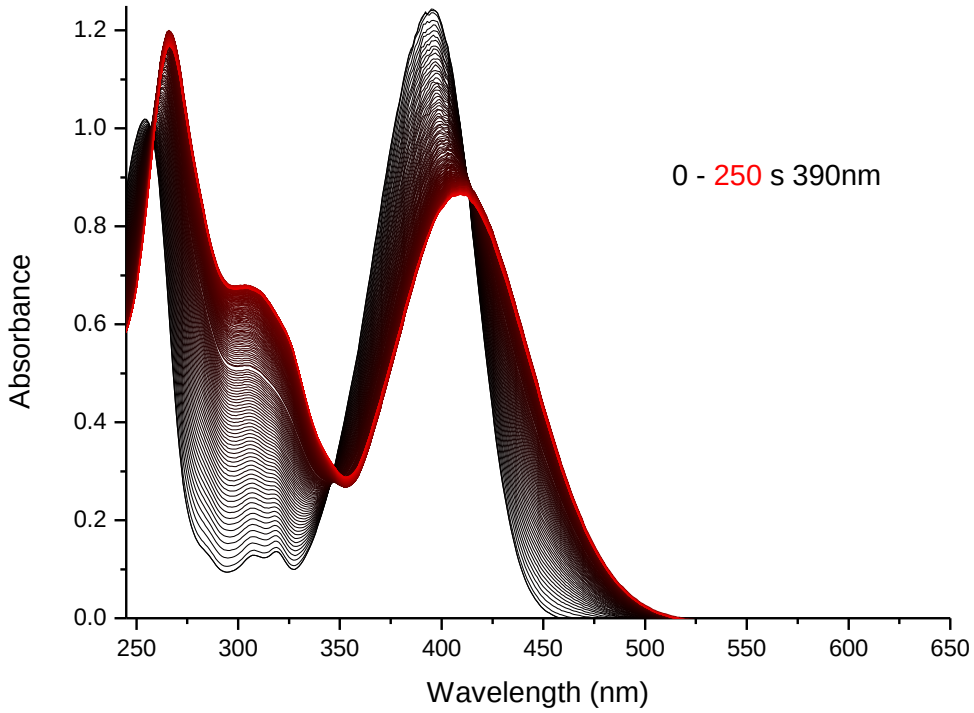

Figure S 59. UV-vis absorption spectra of compound **5** solution (50 µM, water/EtOH 1:1). A freshly prepared solution (black) and solution after irradiation (λ = 390 nm, red line).

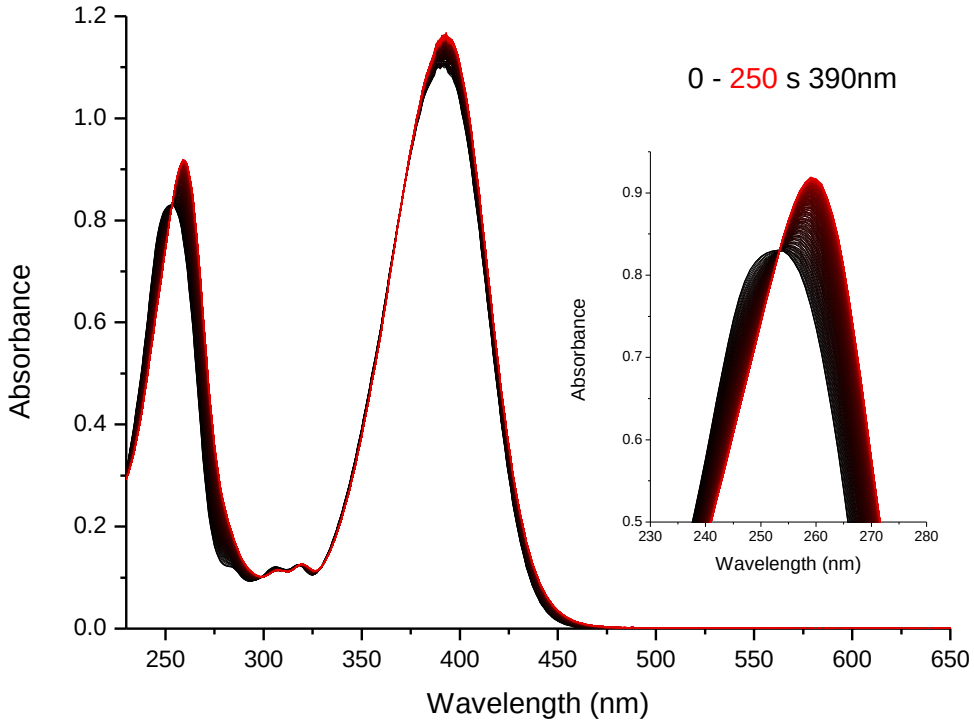

Figure S 60. UV-vis absorption spectra of compound **6** solution (50 µM, water/EtOH 1:1). A freshly prepared solution (black) and solution after irradiation (λ = 390 nm, red line). The insert highlights the isosbestic point.

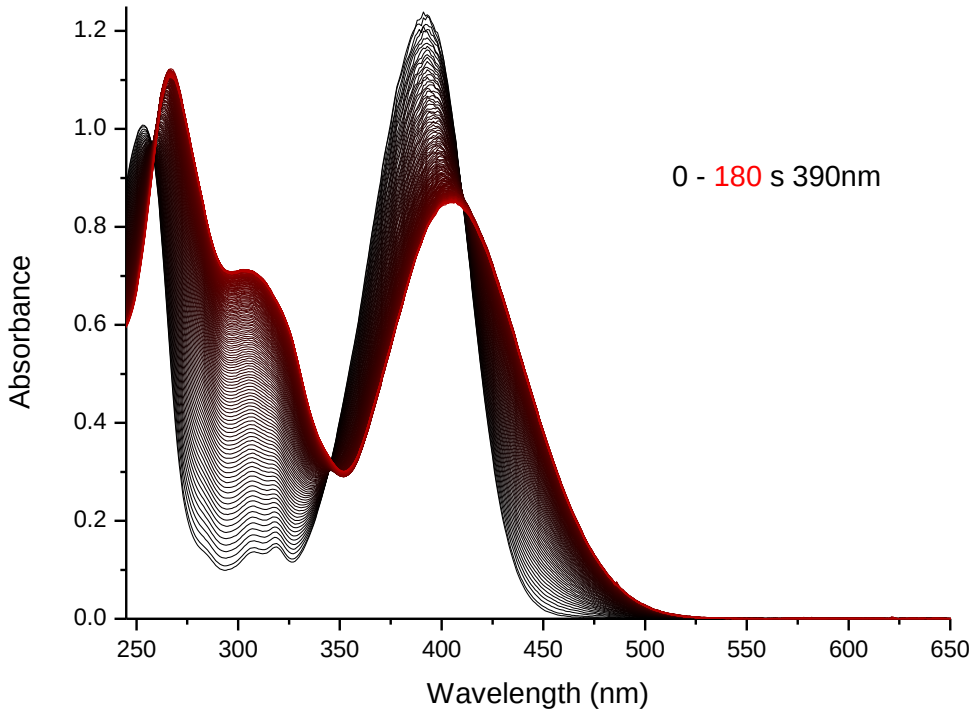

Figure S 61. UV-vis absorption spectra of compound **5** solution (50 µM, water/PrOH 1:1). A freshly prepared solution (black) and solution after irradiation (λ = 390 nm, red line).

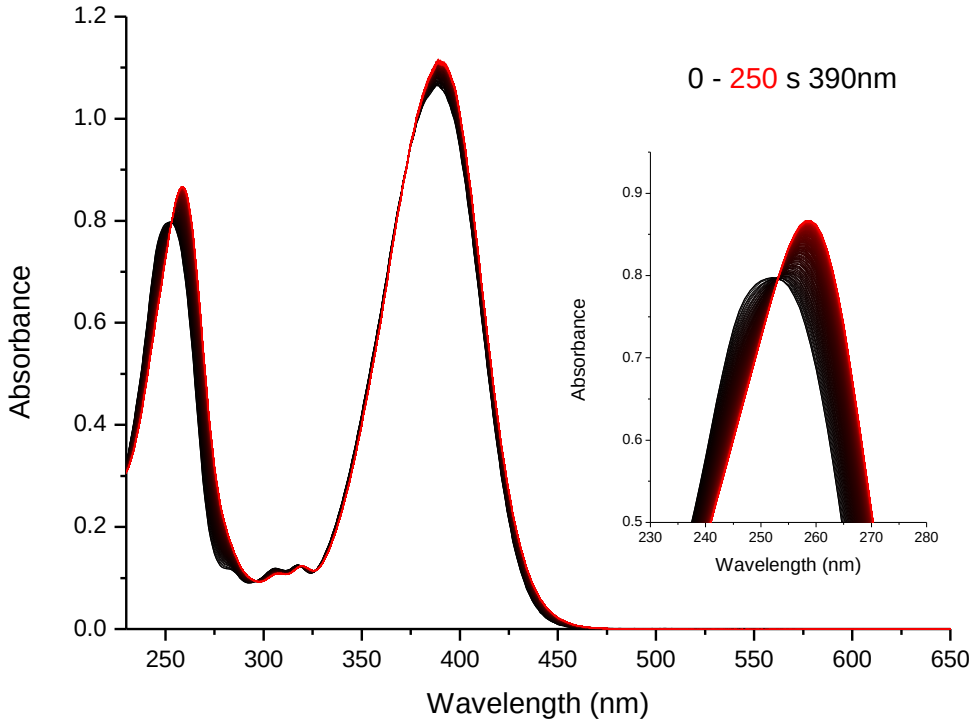

Figure S 62. UV-vis absorption spectra of compound **6** solution (50 µM, water/PrOH 1:1). A freshly prepared solution (black) and solution after irradiation (λ = 390 nm, red line). The insert highlights the isosbestic point.

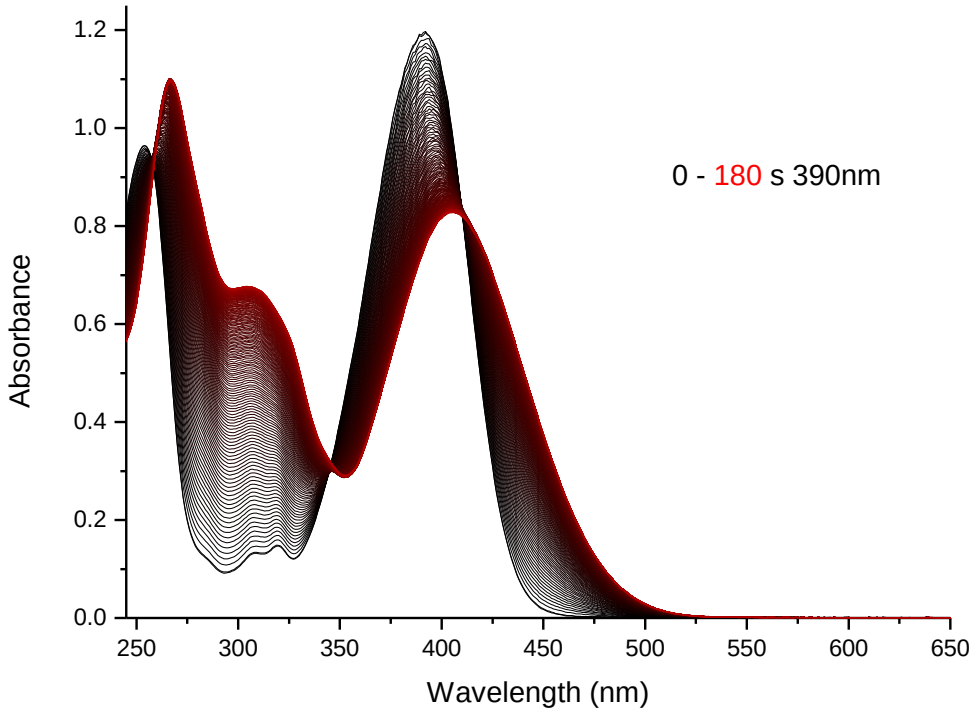

Figure S 63. UV-vis absorption spectra of compound **5** solution (50 µM, water/dioxane 1:1). A freshly prepared solution (black) and solution after irradiation (λ = 390 nm, red line).

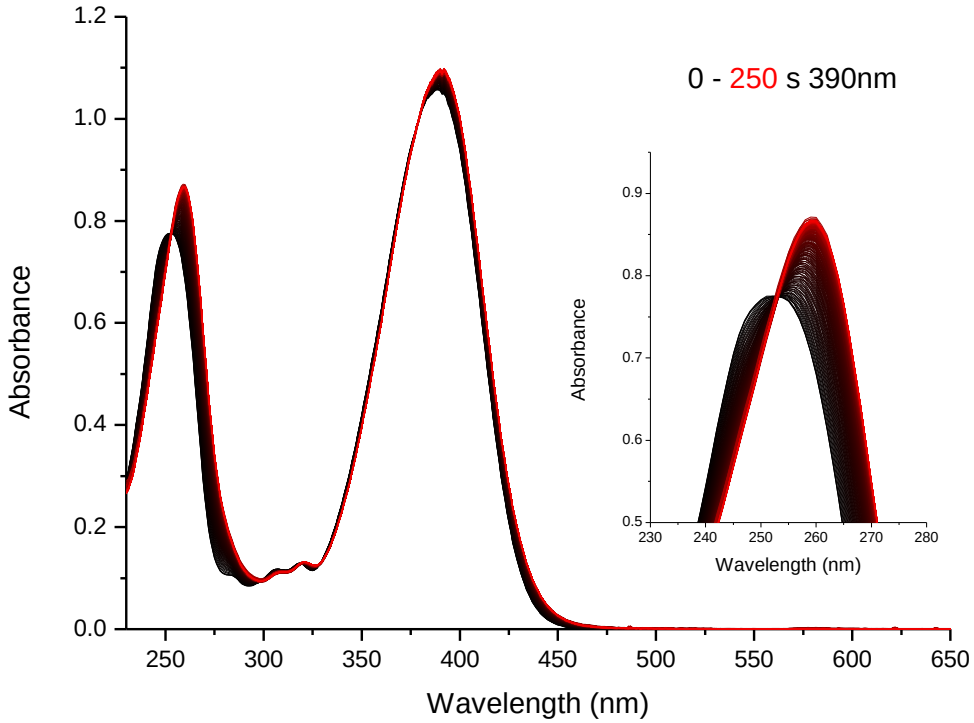

Figure S 64. UV-vis absorption spectra of compound **6** solution (50 µM, water/dioxane 1:1). A freshly prepared solution (black) and solution after irradiation (λ = 390 nm, red line). The insert highlights the isosbestic point.

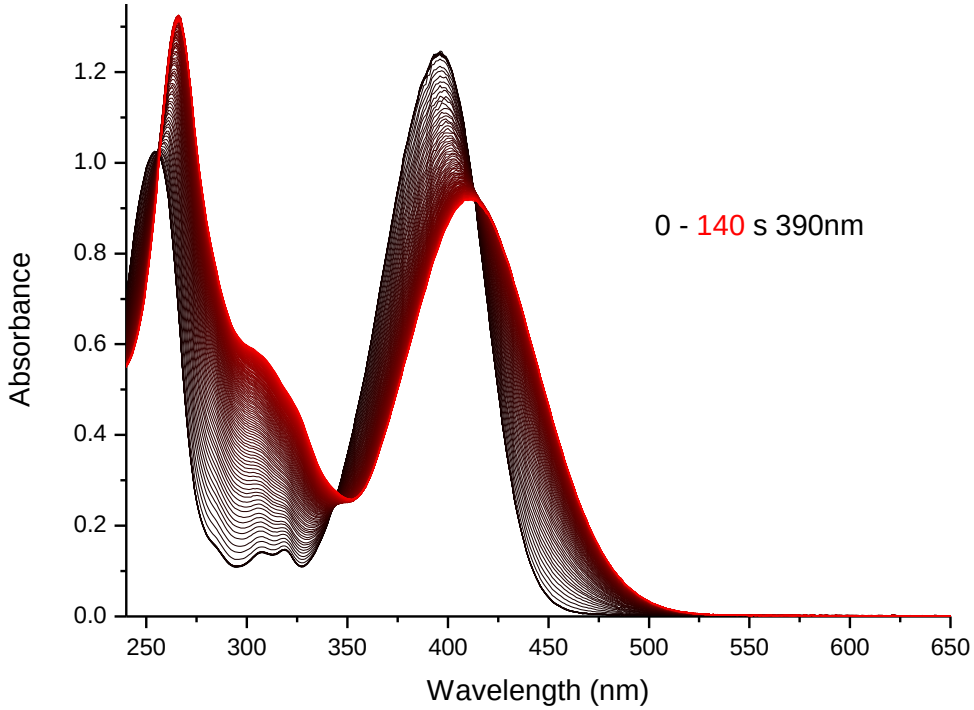

Figure S 65.UV-vis absorption spectra of compound **5** solution (50 µM, water/MeOH 1:1). A freshly prepared solution (black) and solution after irradiation (λ = 390 nm, red line).

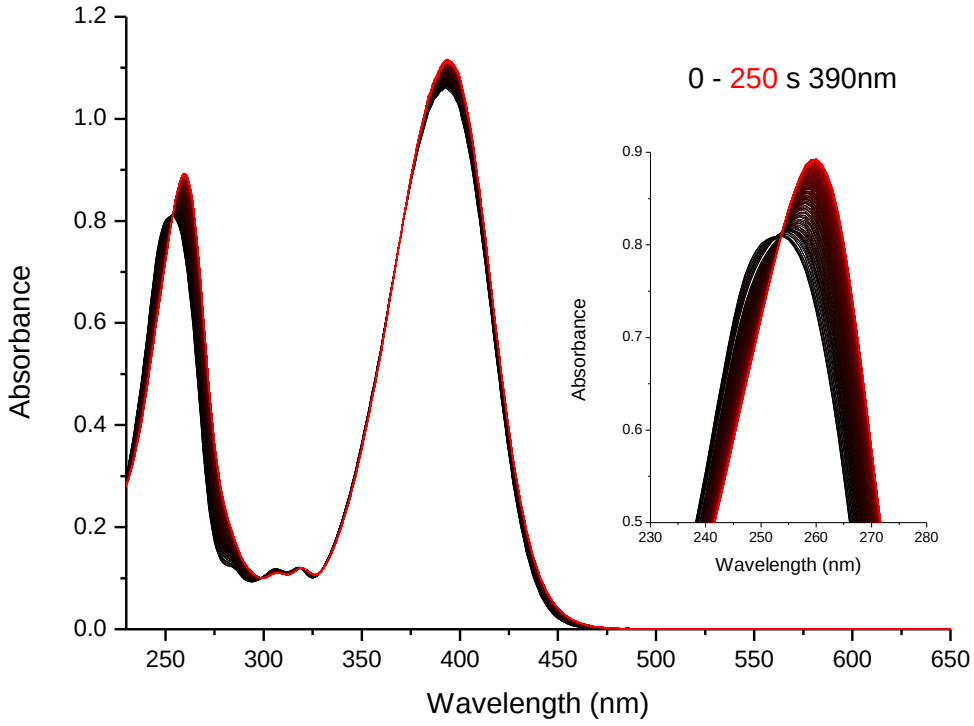

Figure S 66. UV-vis absorption spectra of compound **6** solution (50 µM, water/MeOH 1:1). A freshly prepared solution (black) and solution after irradiation (λ = 390 nm, red line). The insert highlights the isosbestic point.

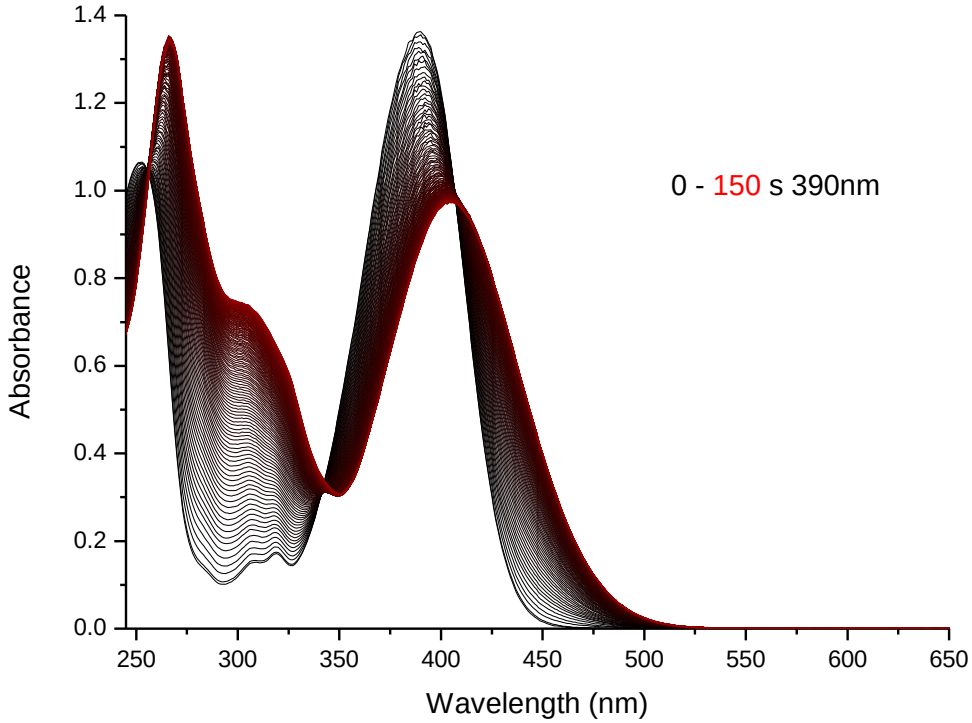

Figure S 67. UV-vis absorption spectra of compound **5** solution (60 µM, water/MeCN 1:1). A freshly prepared solution (black) and solution after irradiation (λ = 390 nm, red line).

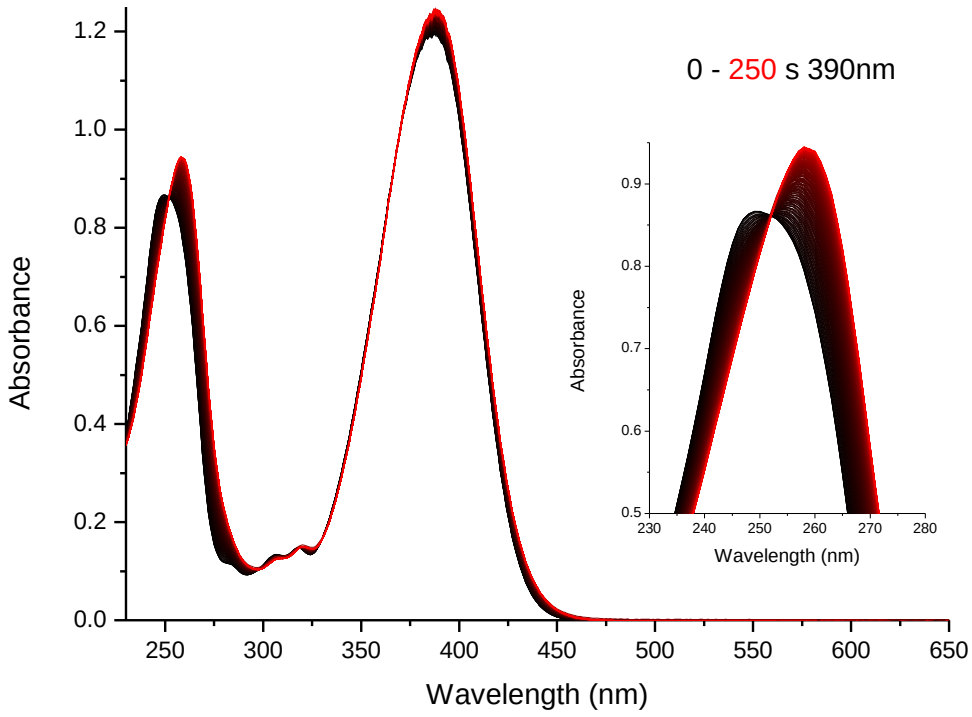

Figure S 68. UV-vis absorption spectra of compound **6** solution (60 µM, water/MeCN 1:1). A freshly prepared solution (black) and solution after irradiation (λ = 390 nm, red line). The insert highlights the isosbestic point.

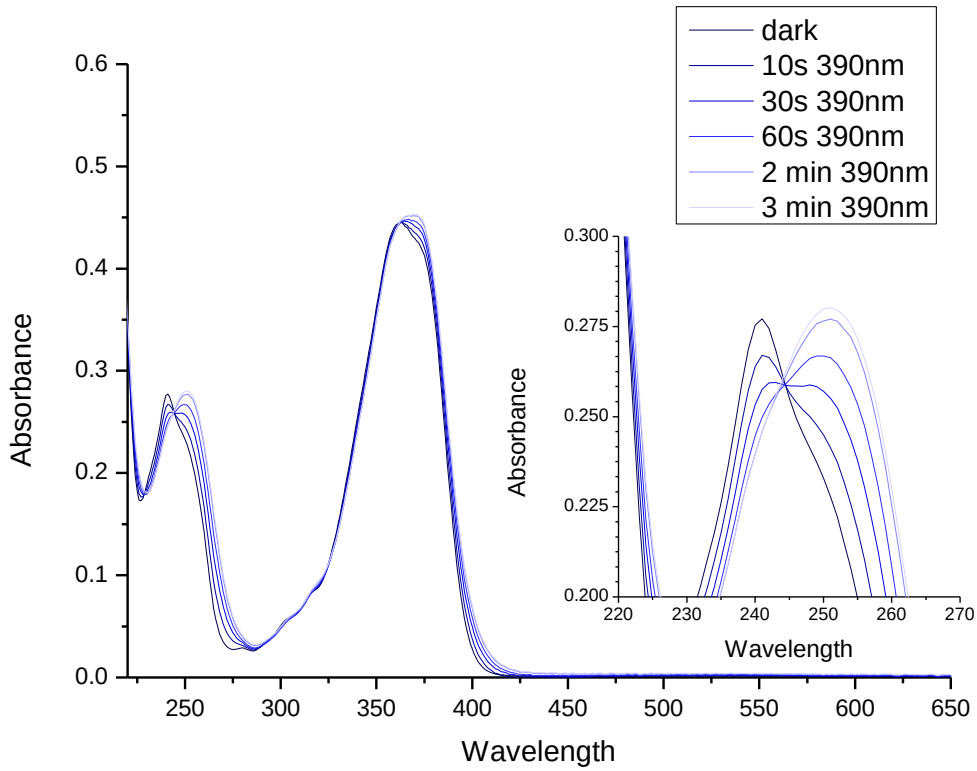

Figure S 69. UV-vis absorption spectra of compound **6** solution (20 µM, MTBE/MeCN 99:1). A freshly prepared solution (black) and solution after irradiation (λ = 390 nm, blue lines). The insert highlights the isosbestic point.

3.2.4 Quantum Yields of compounds 5 and 6 in various solvent mixtures

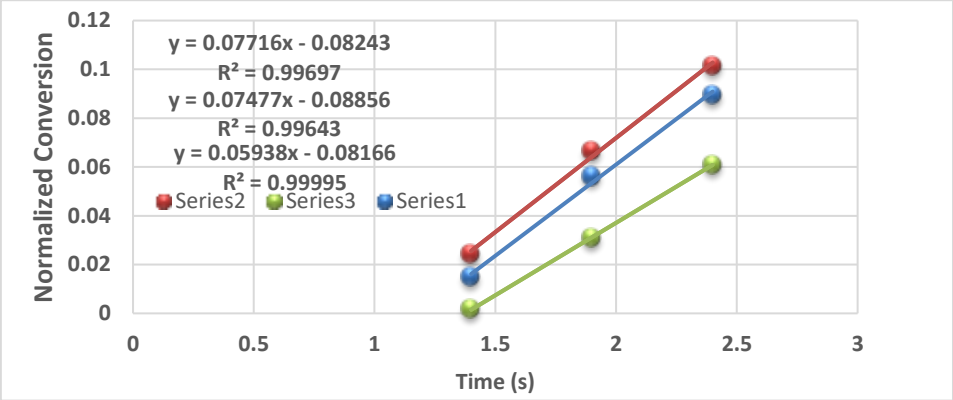

Water/DMSO 95:5	compound 5	rate	A_{390}	QY
	#1	0,07716	0,98	0,304
	#2	0,05938	0,98	0,234
	#3	0,07477	0,98	0,294
			Av. QY	**0,277**
			SD	0,031

Figure S 70. Normalized conversion of compound **5** (50 µM, 2mL water/DMSO 95:5, 25 °C) (y-axis) vs time (x-axis). Shown are the measurements taken after the start of irradiation (λ = 390 nm). A linear trendline allowed for the determination of the average rate over the first 10% of PPG consumption. Conversion followed at λ = 450 nm (photon flux 2,837*10^{-5} mmol/s). Normalization of the absorbance values was performed from data collection start (t=0) to the maximum achieved absorbance value at full deprotection.

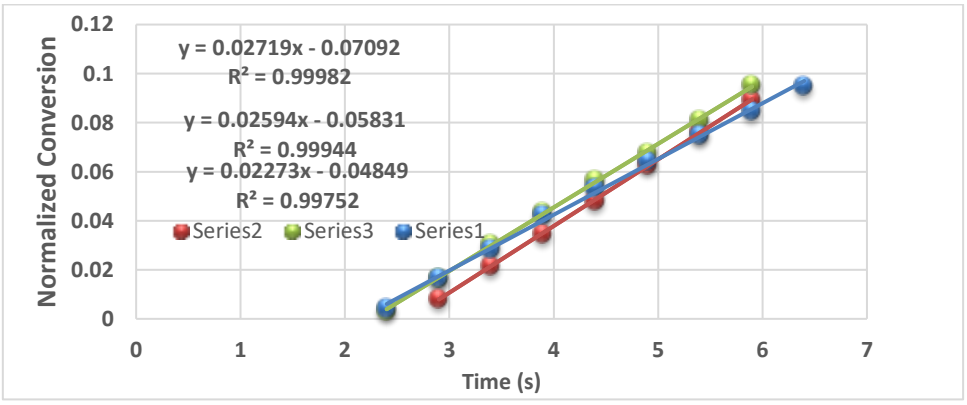

Water/DMSO 1:1	compound 5	rate	A_{390}	QY
	#1	0,02719	1,13	0,104
	#2	0,02594	1,12	0,099
	#3	0,02273	1,13	0,087
			Av. QY	**0,096**
			SD	0,007

Figure S 71. Normalized conversion of compound **5** (50 µM, 2mL water/DMSO 1:1, 25 °C) (y-axis) vs time (x-axis). Shown are the measurements taken after the start of irradiation (λ = 390 nm). A linear trendline allowed for the determination of the average rate over the first 10% of PPG consumption. Conversion followed at λ = 450 nm (photon flux 2,837*10^{-5} mmol/s). Normalization of the absorbance values was performed from data collection start (t=0) to the maximum achieved absorbance value at full deprotection.

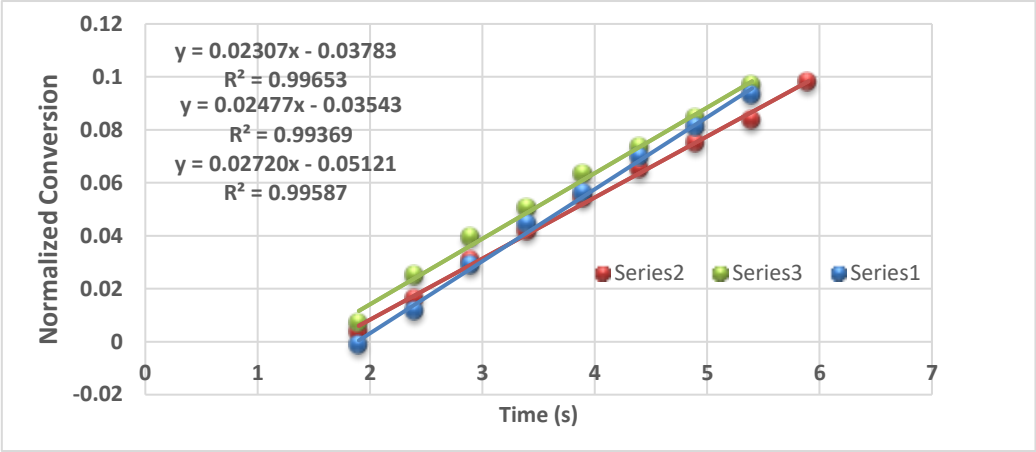

Water/DMSO 95:5	compound 6	rate	A_{390}	QY
	#1	0,02307	0,86	0,095
	#2	0,02477	0,85	0,102
	#3	0,02720	0,85	0,112
			Av. QY	**0,103**
			SD	0,007

Figure S 72**.** Normalized conversion of compound **6** (50 µM, 2mL water/DMSO 95:5, 25 °C) (y-axis) vs time (x-axis). Shown are the measurements taken after the start of irradiation (λ = 390 nm). A linear trendline allowed for the determination of the average rate over the first 10% of PPG consumption. Conversion followed at λ = 270 nm. (photon flux 2,837*10^{-5} mmol/s). Normalization of the absorbance values was performed from data collection start (t=0) to the maximum achieved absorbance value at full deprotection.

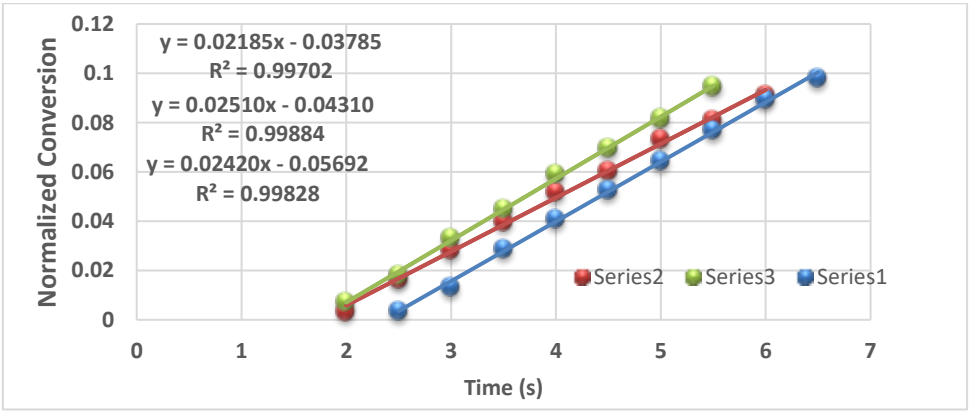

Water/DMSO 1:1	compound 6	rate	A_{390}	QY
	#1	0,02185	0,94	0,087
	#2	0,02510	0,94	0,100
	#3	0,02420	0,92	0,097
			Av. QY	**0,095**
			SD	0,005

Figure S 73**.** Normalized conversion of compound **6** (50 µM, 2mL water/DMSO 1:1, 25 °C) (y-axis) vs time (x-axis). Shown are the measurements taken after the start of irradiation (λ = 390 nm). A linear trendline allowed for the determination of the average rate over the first 10% of PPG consumption. Conversion followed at λ = 270 nm. (photon flux 2,837*10^{-5} mmol/s). Normalization of the absorbance values was performed from data collection start (t=0) to the maximum achieved absorbance value at full deprotection.

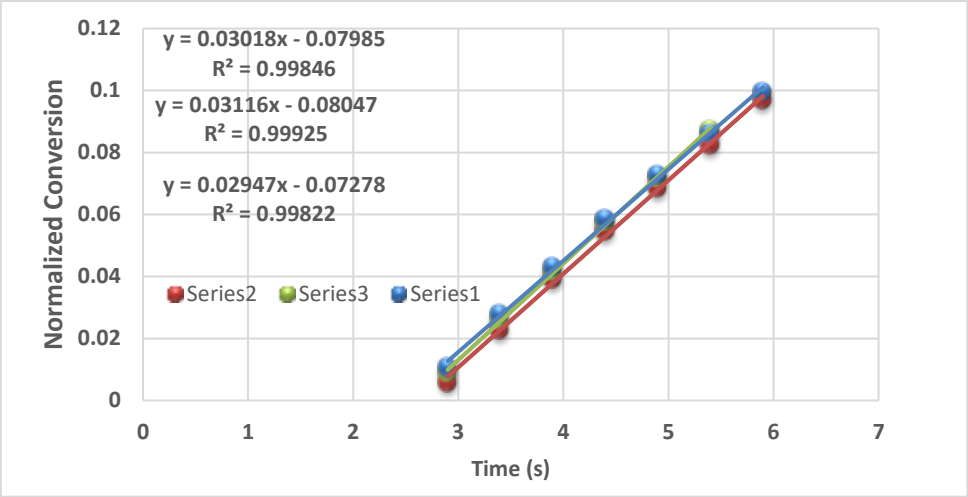

Water/EtOH 1:1	compound 5	rate	A_{390}	QY
	#1	0,03018	1,25	0,113
	#2	0,03116	1,20	0,117
	#3	0,02947	1,21	0,111
			Av. QY	**0,114**
			SD	0,003

Figure S 74. Normalized conversion of compound **5** (50 µM, 2mL water/EtOH 1:1, 25 °C) (y-axis) vs time (x-axis). Shown are the measurements taken after the start of irradiation (λ = 390 nm). A linear trendline allowed for the determination of the average rate over the first 10% of PPG consumption. Conversion followed at λ = 450 nm (photon flux 2,837*10^{-5} mmol/s). Normalization of the absorbance values was performed from data collection start (t=0) to the maximum achieved absorbance value at full deprotection.

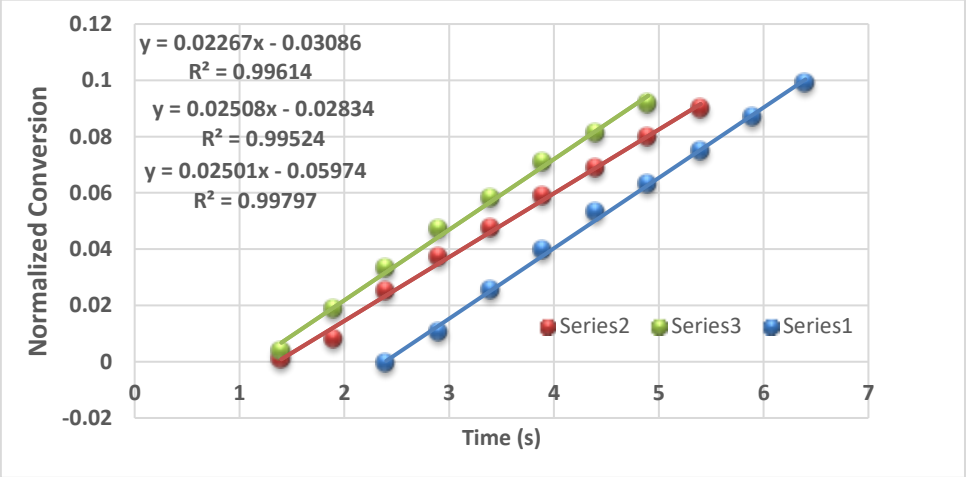

Water/EtOH 1:1	compound 6	rate	A_{390}	QY
	#1	0,02267	1,08	0,087
	#2	0,02508	1,10	0,096
	#3	0,02501	1,08	0,096
			Av. QY	**0,093**
			SD	0,004

Figure S 75**.** Normalized conversion of compound **6** (50 µM, 2mL water/EtOH 1:1, 25 °C) (y-axis) vs time (x-axis). Shown are the measurements taken after the start of irradiation (λ = 390 nm). A linear trendline allowed for the determination of the average rate over the first 10% of PPG consumption. Conversion followed at λ = 270 nm. (photon flux 2,837*10^{-5} mmol/s). Normalization of the absorbance values was performed from data collection start (t=0) to the maximum achieved absorbance value at full deprotection.

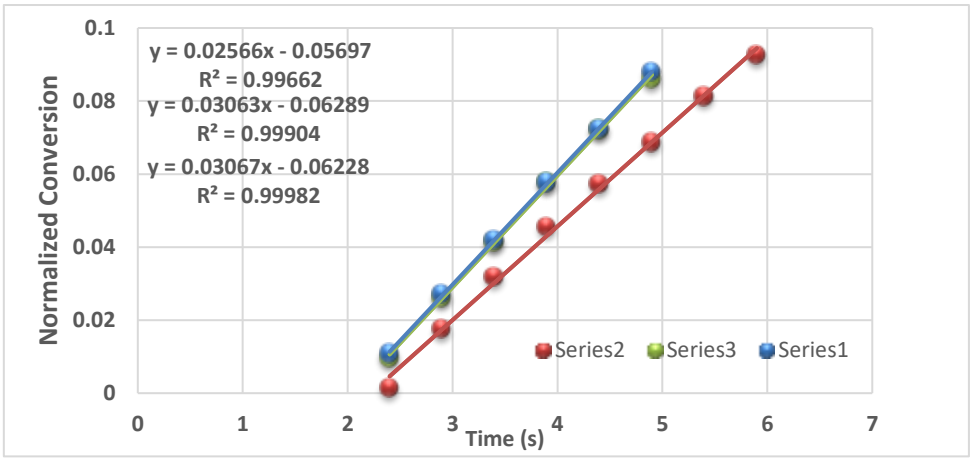

Water/PrOH 1:1	compound 5	rate	A_{390}	QY
	#1	0,02566	1,23	0,096
	#2	0,03063	1,21	0,115
	#3	0,03067	1,21	0,115
			Av. QY	**0,109**
			SD	0,009

Figure S 76. Normalized conversion of compound **5** (50 µM, 2mL water/PrOH 1:1, 25 °C) (y-axis) vs time (x-axis). Shown are the measurements taken after the start of irradiation (λ = 390 nm). A linear trendline allowed for the determination of the average rate over the first 10% of PPG consumption. Conversion followed at λ = 450 nm (photon flux 2,837*10^{-5} mmol/s). Normalization of the absorbance values was performed from data collection start (t=0) to the maximum achieved absorbance value at full deprotection.

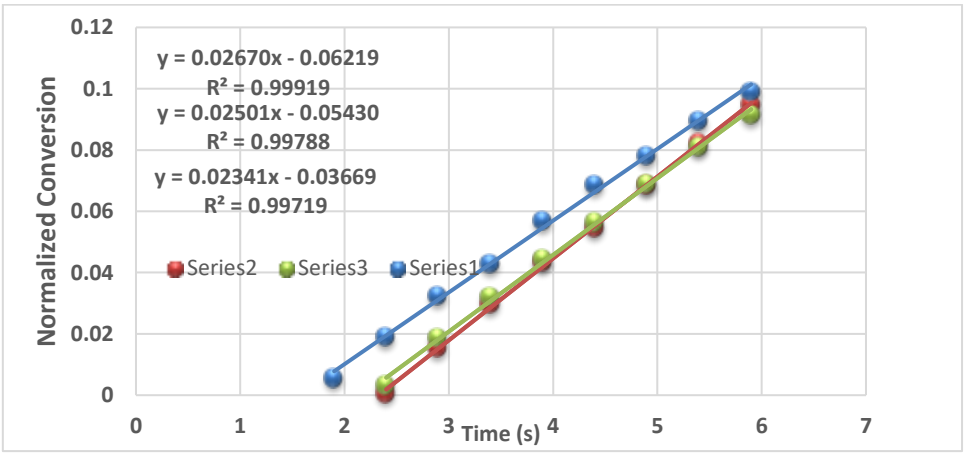

Water/PrOH 1:1	compound 6	rate	A_{390}	QY
	#1	0,02670	1,06	0,103
	#2	0,02501	1,05	0,097
	#3	0,02341	1,06	0,090
			Av. QY	**0,097**
			SD	0,005

Figure S 77. Normalized conversion of compound **6** (50 µM, 2mL water/PrOH 1:1, 25 °C) (y-axis) vs time (x-axis). Shown are the measurements taken after the start of irradiation (λ = 390 nm). A linear trendline allowed for the determination of the average rate over the first 10% of PPG consumption. Conversion followed at λ = 270 nm. (photon flux 2,837*10^{-5} mmol/s). Normalization of the absorbance values was performed from data collection start (t=0) to the maximum achieved absorbance value at full deprotection.

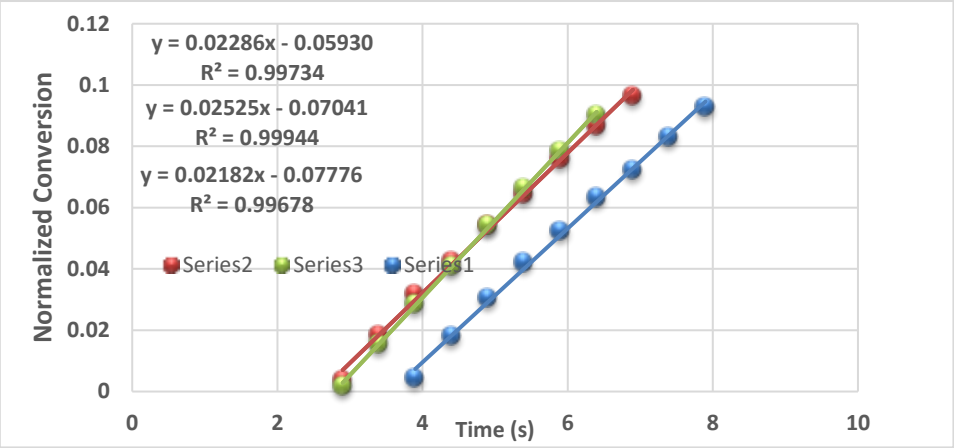

Water/dioxane 1:1	compound 5	rate	A_{390}	QY
	#1	0,02286	1,19	0,086
	#2	0,02525	1,22	0,095
	#3	0,02182	1,21	0,082
			Av. QY	**0,088**
			SD	0,005

Figure S 78**.** Normalized conversion of compound **5** (50 µM, 2mL water/dioxane 1:1, 25 °C) (y-axis) vs time (x-axis). Shown are the measurements taken after the start of irradiation (λ = 390 nm). A linear trendline allowed for the determination of the average rate over the first 10% of PPG consumption. Conversion followed at λ = 450 nm. (photon flux 2,837*10^{-5} mmol/s). Normalization of the absorbance values was performed from data collection start (t=0) to the maximum achieved absorbance value at full deprotection.

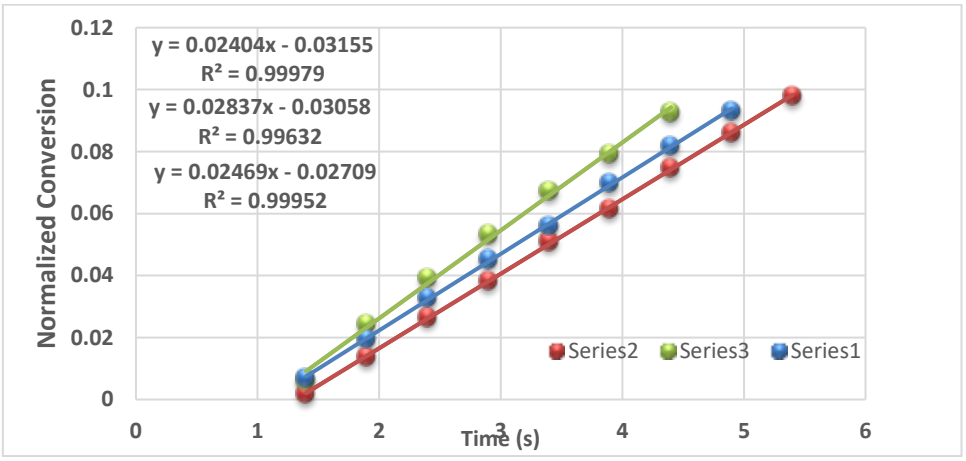

Water/dioxane 1:1	compound 6	rate	A_{390}	QY
	#1	0,02404	1,06	0,093
	#2	0,02837	1,06	0,110
	#3	0,02469	1,05	0,096
			Av. QY	**0,099**
			SD	0,007

Figure S 79**.** Normalized conversion of compound **6** (50 µM, 2mL water/dioxane 1:1, 25 °C) (y-axis) vs time (x-axis). Shown are the measurements taken after the start of irradiation (λ = 390 nm). A linear trendline allowed for the determination of the average rate over the first 10% of PPG consumption. Conversion followed at λ = 270 nm. (photon flux 2,837*10^{-5} mmol/s). Normalization of the absorbance values was performed from data collection start (t=0) to the maximum achieved absorbance value at full deprotection.

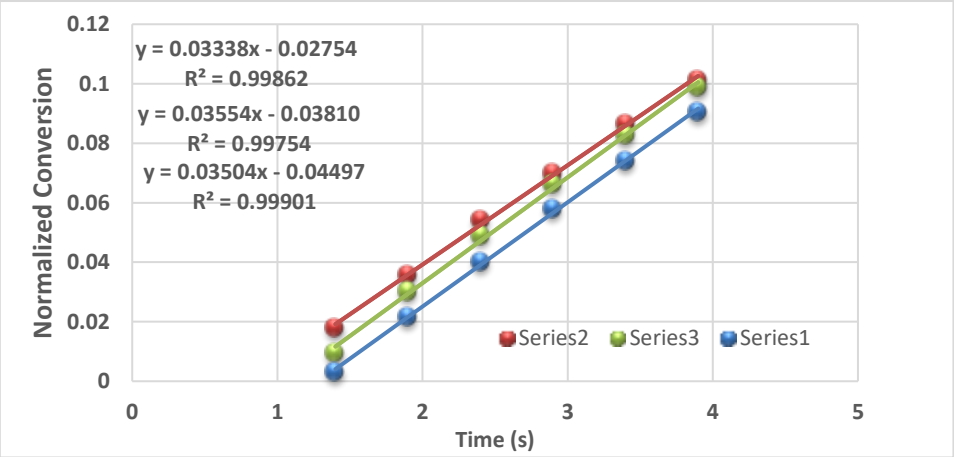

Water/MeOH 1:1	compound 5	rate	A_{390}	QY
	#1	0,03338	1,20	0,126
	#2	0,03554	1,21	0,133
	#3	0,03504	1,25	0,131
			Av. QY	**0,130**
			SD	0,003

Figure S 80**.** Normalized conversion of compound **5** (50 µM, 2mL water/MeOH 1:1, 25 °C) (y-axis) vs time (x-axis). Shown are the measurements taken after the start of irradiation (λ = 390 nm). A linear trendline allowed for the determination of the average rate over the first 10% of PPG consumption. Conversion followed at λ = 450 nm. (photon flux 2,837*10^{-5} mmol/s). Normalization of the absorbance values was performed from data collection start (t=0) to the maximum achieved absorbance value at full deprotection.

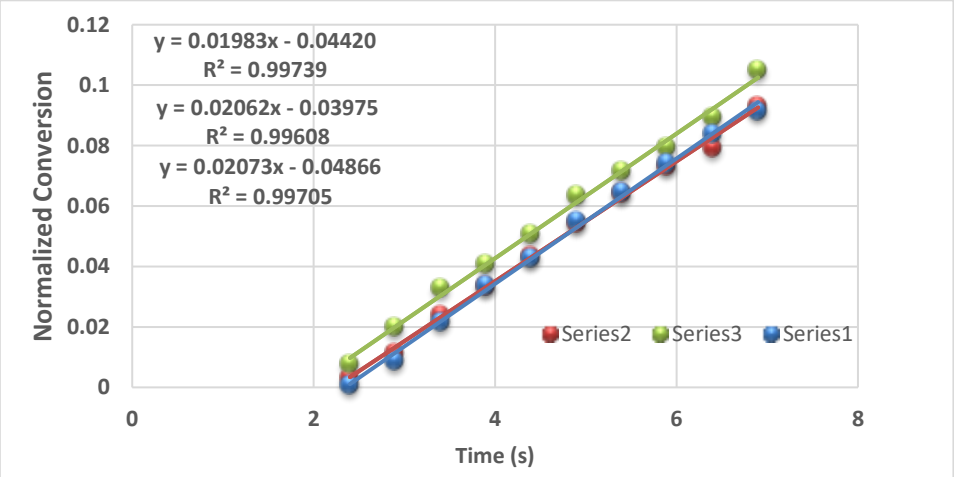

Water/MeOH 1:1	compound 6	rate	A_{390}	QY
	#1	0,01983	1,05	0,077
	#2	0,02062	1,05	0,080
	#3	0,02073	1,05	0,080
			Av. QY	**0,079**
			SD	0,002

Figure S 81**.** Normalized conversion of compound **6** (50 µM, 2mL water/MeOH 1:1, 25 °C) (y-axis) vs time (x-axis). Shown are the measurements taken after the start of irradiation (λ = 390 nm). A linear trendline allowed for the determination of the average rate over the first 10% of PPG consumption. Conversion followed at λ = 270 nm. (photon flux 2,837*10^{-5} mmol/s). Normalization of the absorbance values was performed from data collection start (t=0) to the maximum achieved absorbance value at full deprotection.

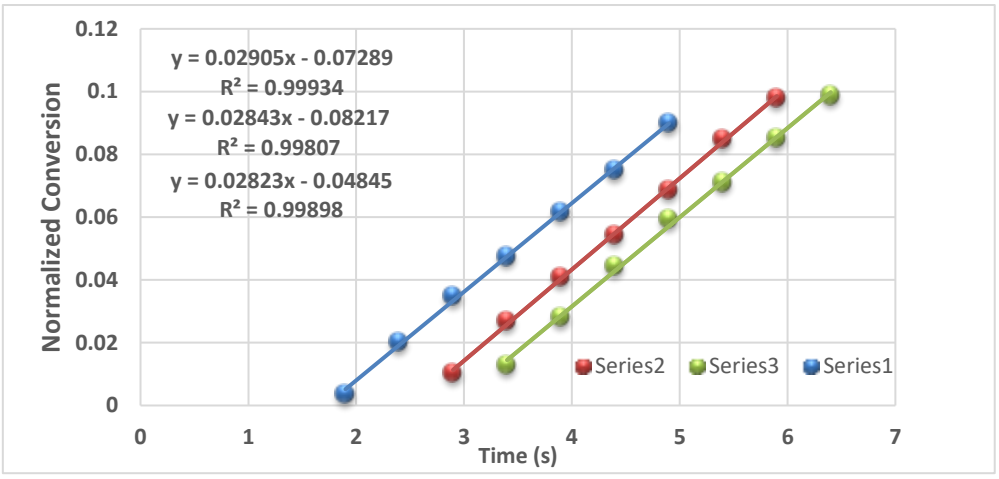

Water/MeCN 1:1	compound 5	rate	A_{390}	QY
	#1	0,02905	1,36	0,128
	#2	0,02843	1,39	0,125
	#3	0,02823	1,40	0,124
			Av. QY	**0,126**
			SD	0,002

Figure S 82. Normalized conversion of compound **5** (60 µM, 2mL water/MeCN 1:1, 25 °C) (y-axis) vs time (x-axis). Shown are the measurements taken after the start of irradiation (λ = 390 nm). A linear trendline allowed for the determination of the average rate over the first 10% of PPG consumption. Conversion followed at λ = 450 nm. (photon flux 2,837*10^{-5} mmol/s). Normalization of the absorbance values was performed from data collection start (t=0) to the maximum achieved absorbance value at full deprotection.

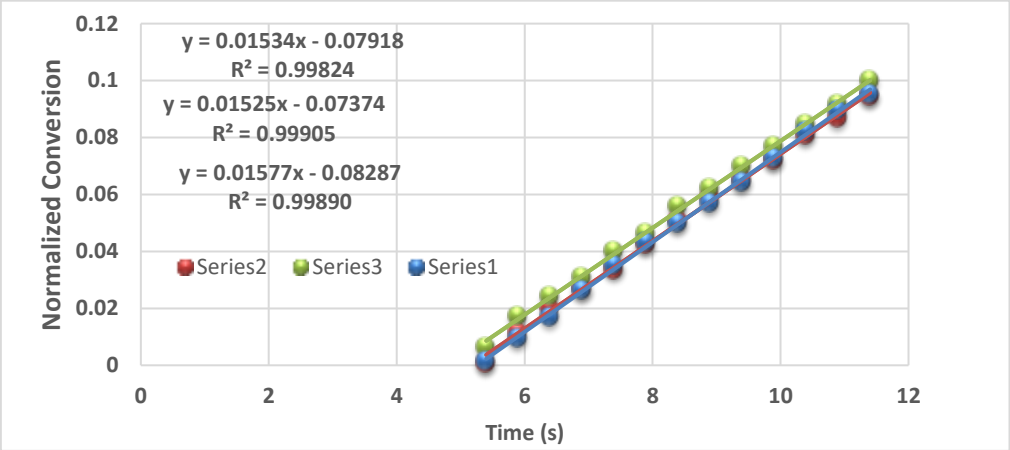

Water/MeCN 1:1	compound 6	rate	A_{390}	QY
	#1	0,01534	1,19	0,069
	#2	0,01525	1,19	0,069
	#3	0,01577	1,22	0,071
			Av. QY	**0,070**
			SD	0,001

Figure S 83. Normalized conversion of compound **6** (60 µM, 2mL water/MeCN 1:1, 25 °C) (y-axis) vs time (x-axis). Shown are the measurements taken after the start of irradiation (λ = 390 nm). A linear trendline allowed for the determination of the average rate over the first 10% of PPG consumption. Conversion followed at λ = 270 nm. (photon flux 2,837*10^{-5} mmol/s). Normalization of the absorbance values was performed from data collection start (t=0) to the maximum achieved absorbance value at full deprotection.

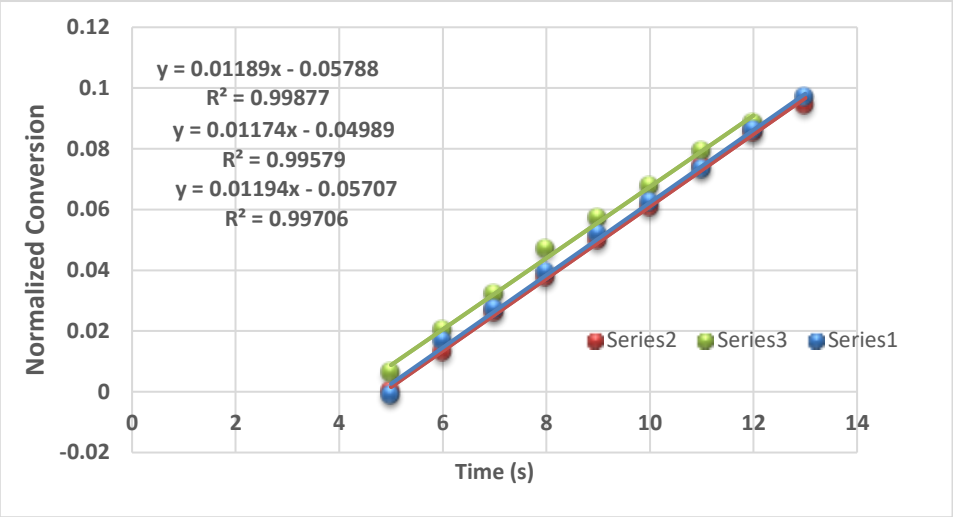

MTBE	compound 6	rate	A_{390}	QY
	#1	0,01189	0,94	0,095
	#2	0,01174	0,94	0,094
	#3	0,01194	0,95	0,095
			Av. QY	**0,094**
			SD	0,001

Figure S 84**.** Normalized conversion of compound **6** (96 µM, MTBE with 4.8 % MeCN, 2.08 mL, 25 °C) (y-axis) vs time (x-axis). Shown are the measurements taken after the start of irradiation (λ = 390 nm). A linear trendline allowed for the determination of the average rate over the first 10% of PPG consumption. Conversion followed at λ = 270 nm. (photon flux $2{,}837*10^{-5}$ mmol/s). Normalization of the absorbance values was performed from data collection start (t=0) to the maximum achieved absorbance value at full deprotection.

3.3 Payload effect

3.3.1 Irradiation-dependent absorption spectra of compounds **5** – **12**

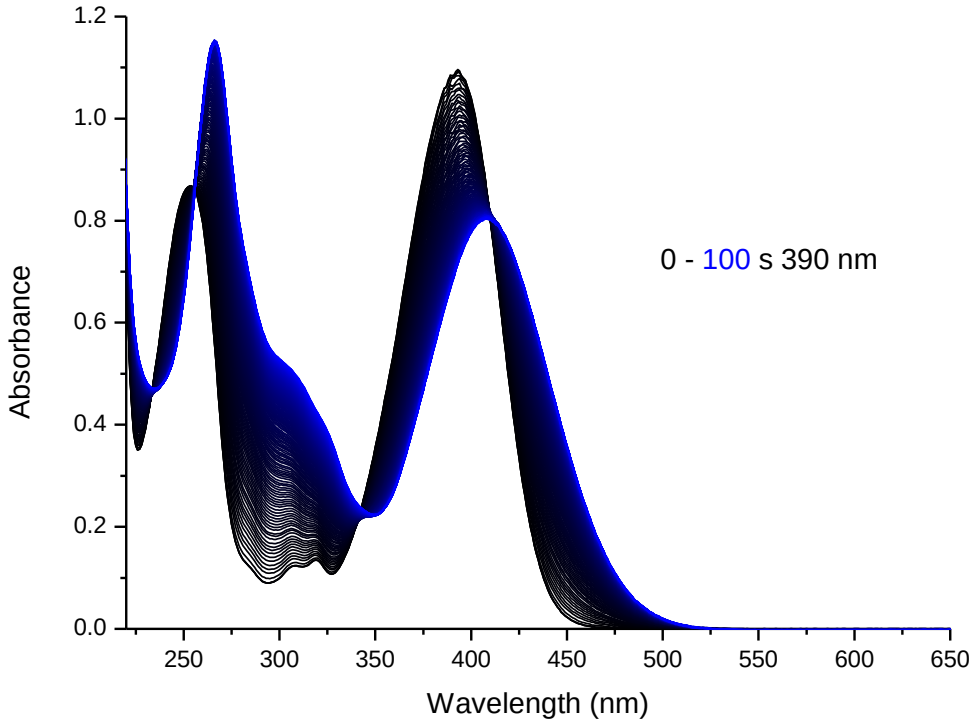

Figure S 85. UV-vis absorption spectra of compound **5** solution (50 µM, water/MeCN 65:35). A freshly prepared solution (black) and solution after irradiation (λ = 390 nm, blue line).

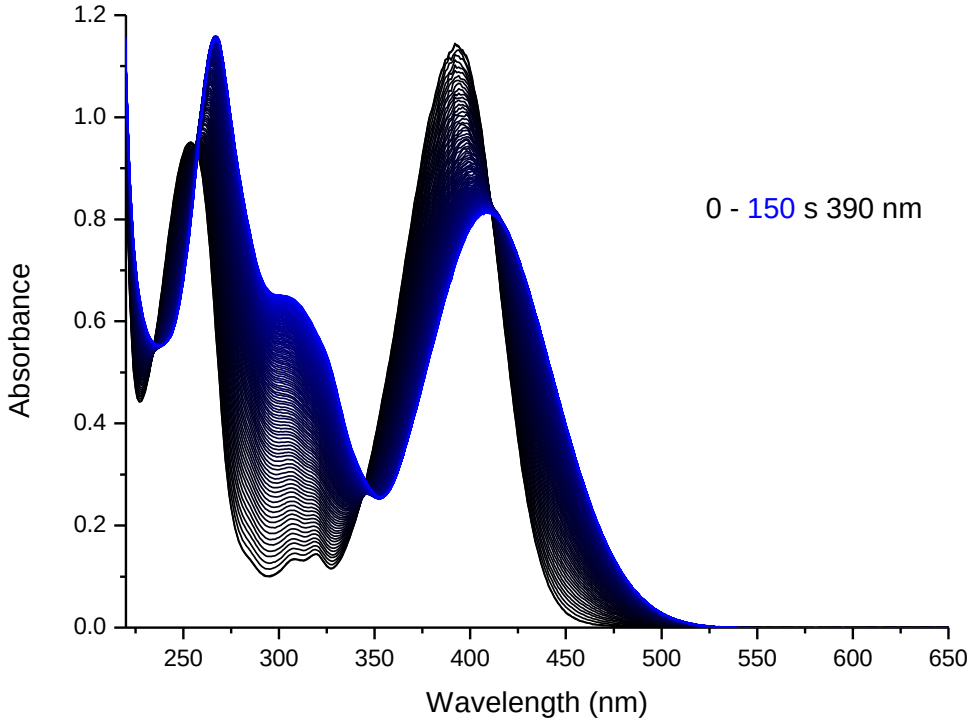

Figure S 86. UV-vis absorption spectra of compound **7** solution (50 µM, water/MeCN 65:35). A freshly prepared solution (black) and solution after irradiation (λ = 390 nm, blue line).

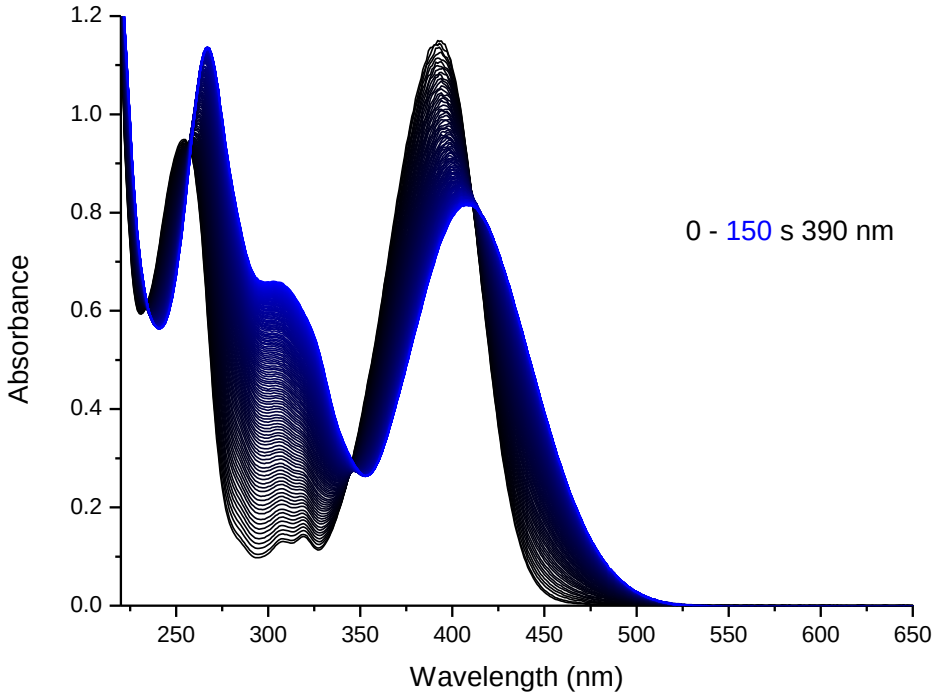

Figure S 87. UV-vis absorption spectra of compound **9** solution (50 µM, water/MeCN 65:35). A freshly prepared solution (black) and solution after irradiation (λ = 390 nm, blue line).

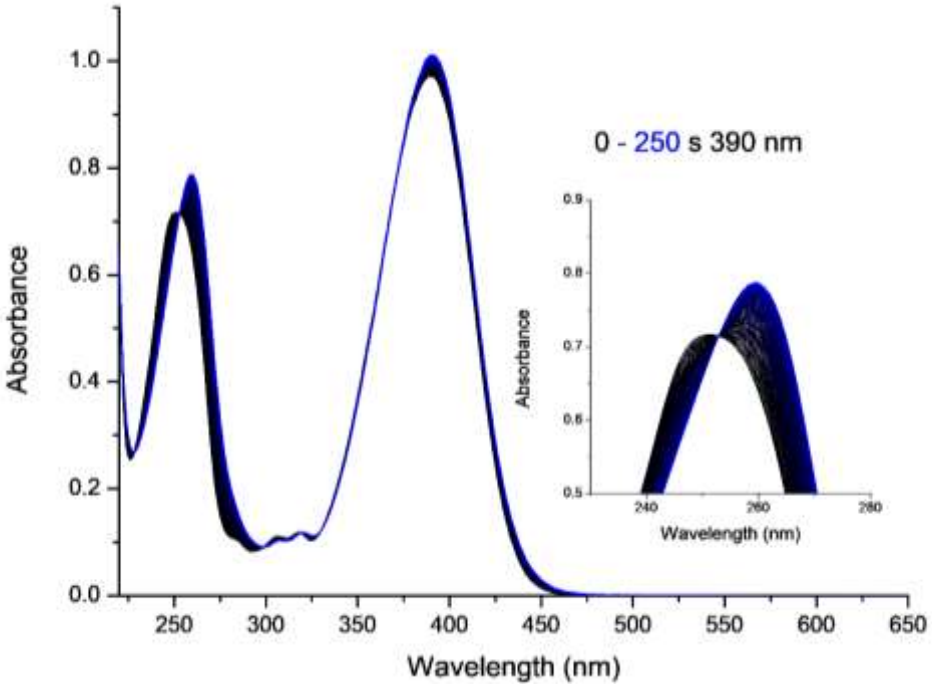

Figure S 88. UV-vis absorption spectra of compound **6** solution (50 µM, water/MeCN 65:35). A freshly prepared solution (black) and solution after irradiation (λ = 390 nm, blue line). The insert highlights the isosbestic point.

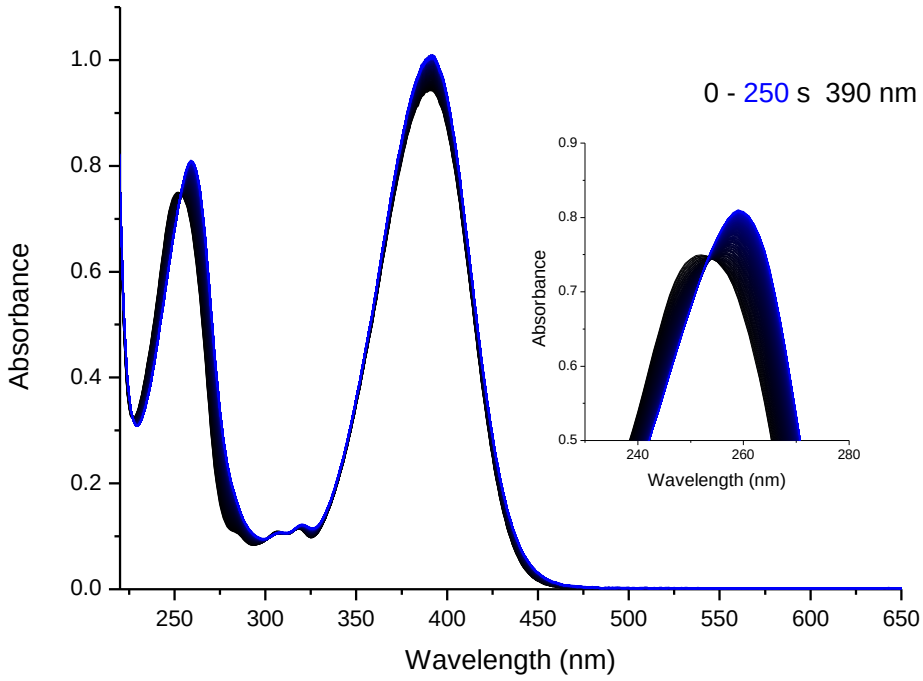

Figure S 89. UV-vis absorption spectra of compound **8** solution (50 µM, water/MeCN 65:35). A freshly prepared solution (black) and solution after irradiation (λ = 390 nm, blue line). The insert highlights the isosbestic point.

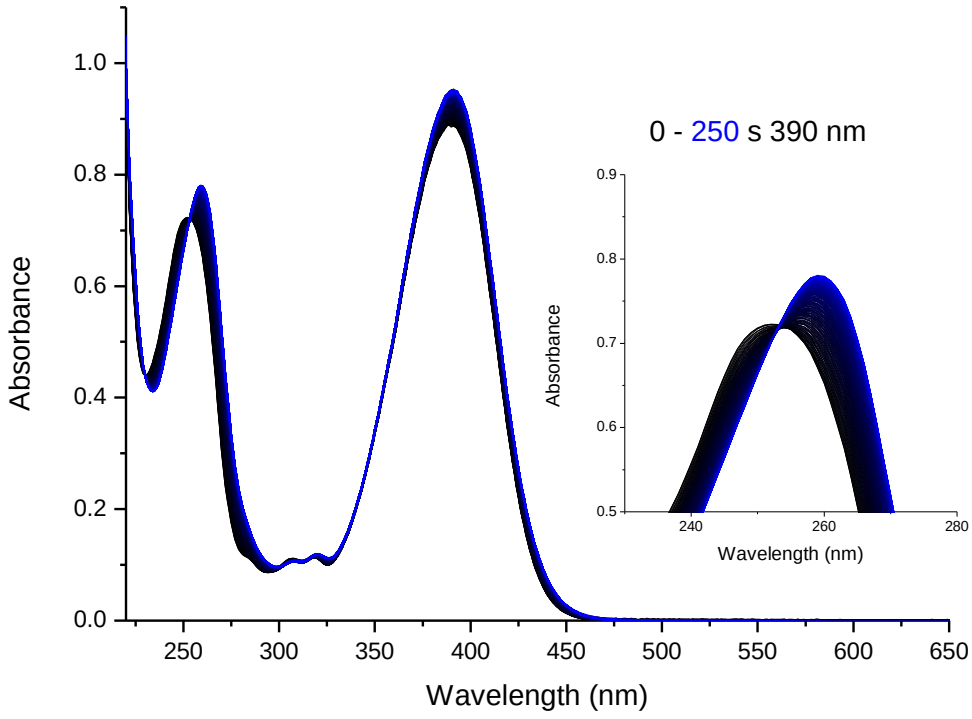

Figure S 90. UV-vis absorption spectra of compound **10** solution (50 µM, water/MeCN 65:35). A freshly prepared solution (black) and solution after irradiation (λ = 390 nm, blue line). The insert highlights the isosbestic point.

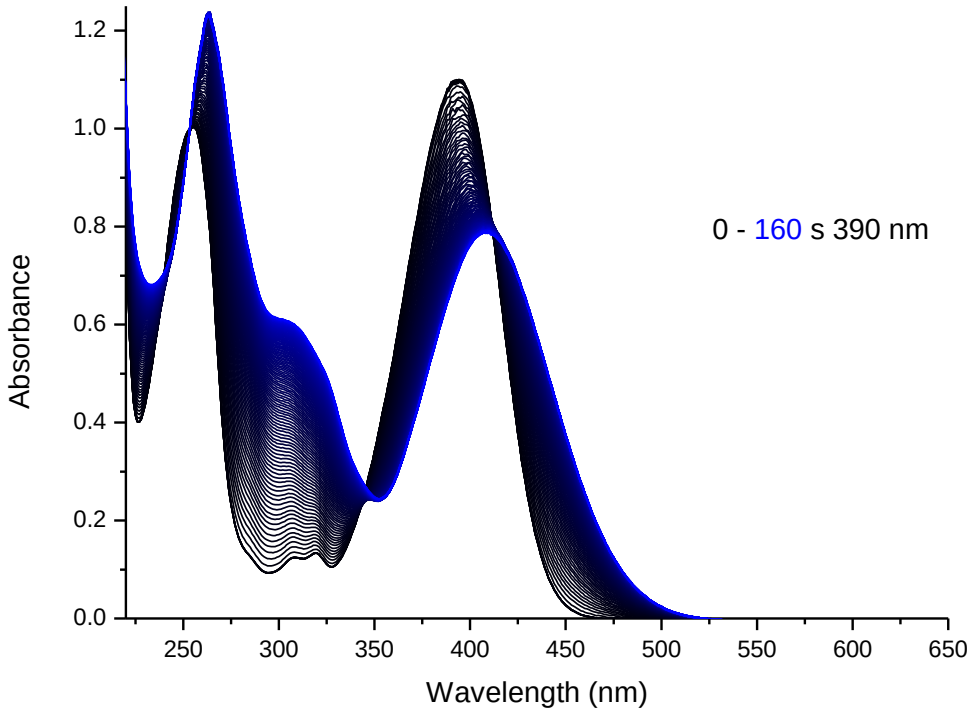

Figure S 91. UV-vis absorption spectra of compound **11** solution (50 µM, water/MeCN 65:35). A freshly prepared solution (black) and solution after irradiation (λ = 390 nm, blue line).

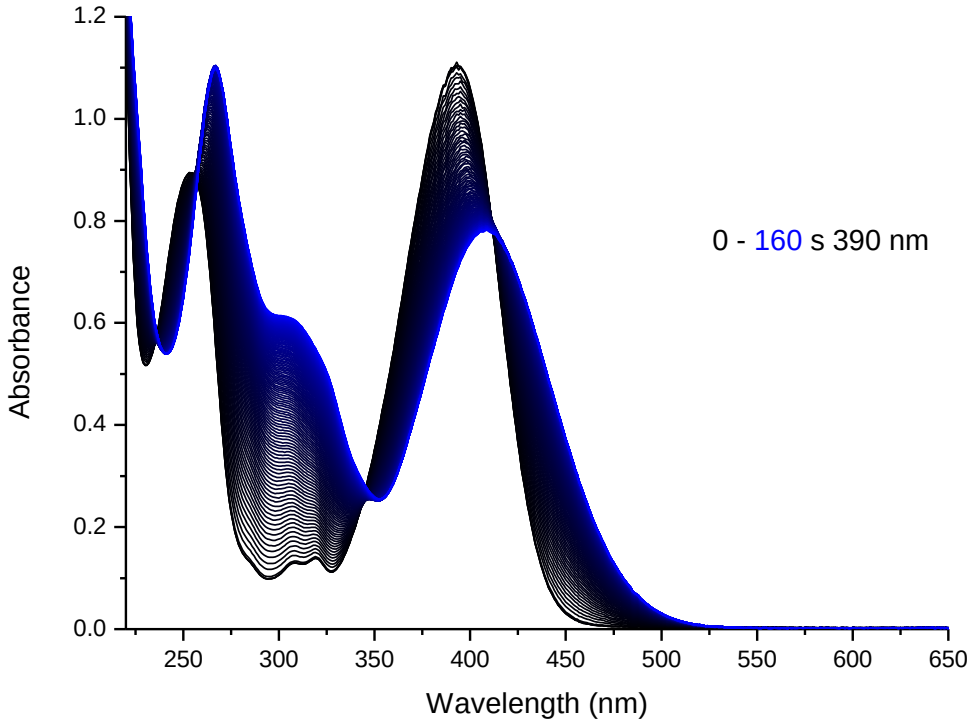

Figure S 92. UV-vis absorption spectra of compound **12** solution (50 µM, water/MeCN 65:35). A freshly prepared solution (black) and solution after irradiation (λ = 390 nm, blue line).

3.3.2 Quantum Yields of compounds 5 – 12

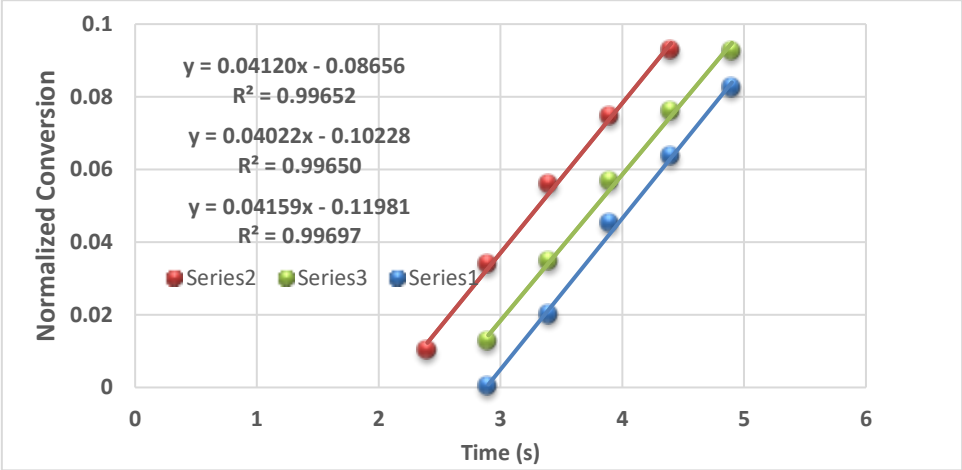

Water/MeCN 65:35	compound 5	rate	A_{390}	QY
	#1	0.04120	1.11	0.157
	#2	0.04022	1.11	0.154
	#3	0.04159	1.09	0.160
			Av. QY	**0.157**
			SD	0.002

Figure S 93. Normalized conversion of compound **5** (50 µM, 2mL water/MeCN 65:35, 25 °C) (y-axis) vs time (x-axis). Shown are the measurements taken after the start of irradiation (λ = 390 nm). A linear trendline allowed for the determination of the average rate over the first 10% of PPG consumption. Conversion followed at λ = 450 nm. (photon flux 2,837*10^{-5} mmol/s). Normalization of the absorbance values was performed from data collection start (t=0) to the maximum achieved absorbance value at full deprotection.

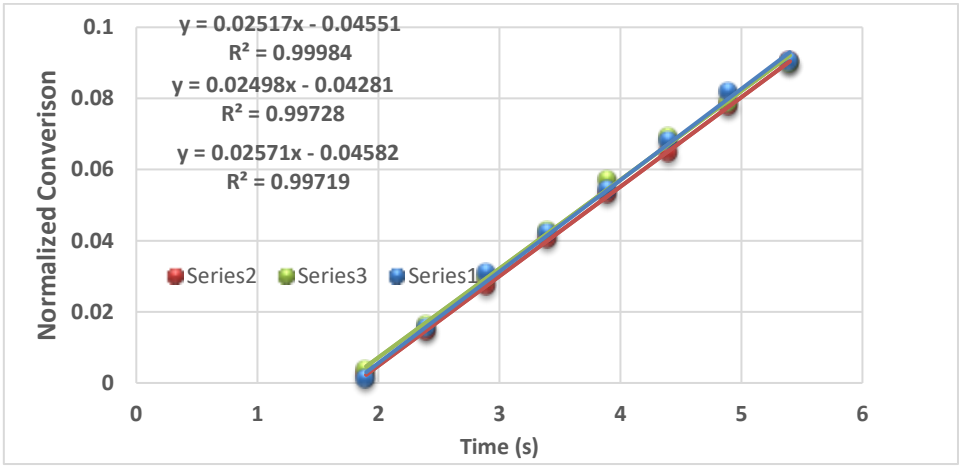

Water/MeCN 65:35	compound 7	rate	A_{390}	QY
	#1	0.02517	1.15	0.096
	#2	0.02498	1.19	0.094
	#3	0.02751	1.13	0.098
			Av. QY	**0.096**
			SD	0.002

Figure S 94**.** Normalized conversion of compound **7** (50 µM, 2mL water/MeCN 65:35, 25 °C) (y-axis) vs time (x-axis). Shown are the measurements taken after the start of irradiation (λ = 390 nm). A linear trendline allowed for the determination of the average rate over the first 10% of PPG consumption. Conversion followed at λ = 450 nm. (photon flux 2,837*10^{-5} mmol/s). Normalization of the absorbance values was performed from data collection start (t=0) to the maximum achieved absorbance value at full deprotection.

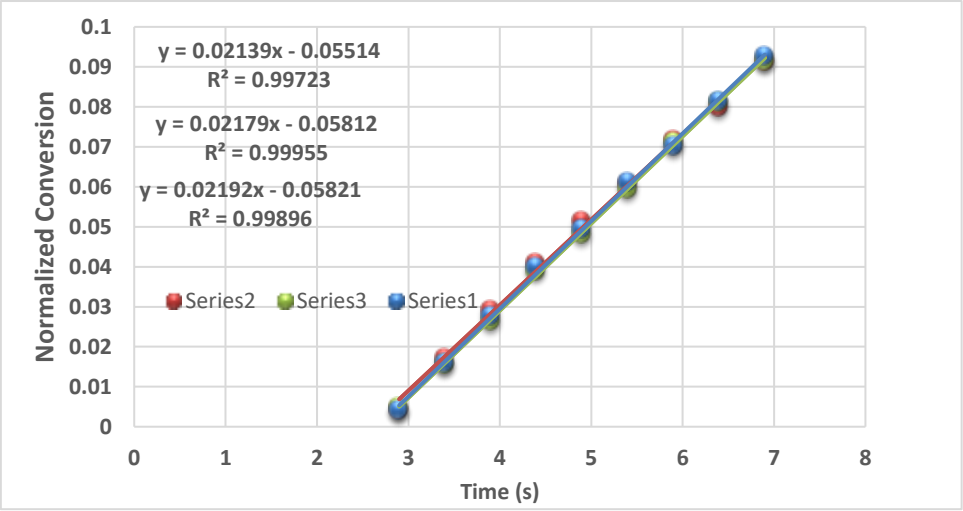

Water/MeCN 65:35	compound 9	rate	A_{390}	QY
	#1	0.02139	1.15	0.081
	#2	0.02179	1.14	0.083
	#3	0.02192	1.15	0.083
			Av. QY	**0.082**
			SD	0.001

Figure S 95**.** Normalized conversion of compound **9** (50 µM, 2mL water/MeCN 65:35, 25 °C) (y-axis) vs time (x-axis). Shown are the measurements taken after the start of irradiation (λ = 390 nm). A linear trendline allowed for the determination of the average rate over the first 10% of PPG consumption. Conversion followed at λ = 450 nm. (photon flux 2,837*10^{-5} mmol/s). Normalization of the absorbance values was performed from data collection start (t=0) to the maximum achieved absorbance value at full deprotection.

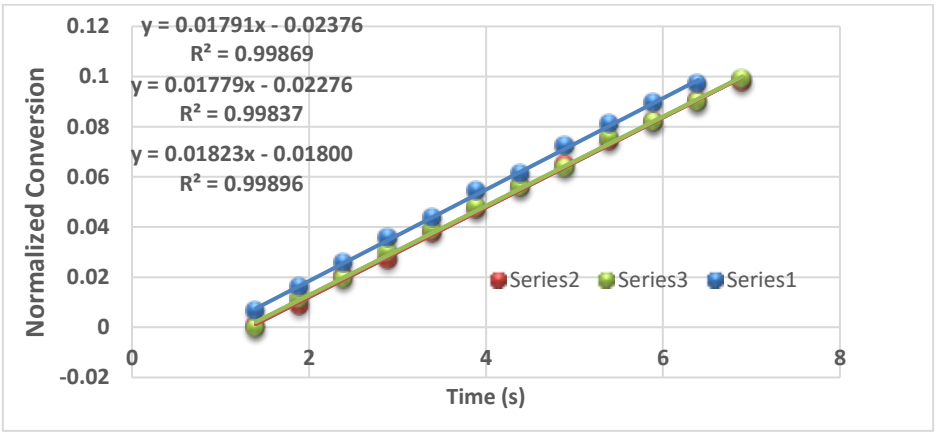

Water/MeCN 65:35	compound 6	rate	A_{390}	QY
	#1	0.01791	0.95	0.071
	#2	0.01779	0.95	0.071
	#3	0.01823	0.97	0.072
			Av. QY	**0.071**
			SD	0.001

Figure S 96**.** Normalized conversion of compound **6** (50 µM, 2mL water/MeCN 65:35, 25 °C) (y-axis) vs time (x-axis). Shown are the measurements taken after the start of irradiation (λ = 390 nm). A linear trendline allowed for the determination of the average rate over the first 10% of PPG consumption. Conversion followed at λ = 270 nm. (photon flux 2,837*10^{-5} mmol/s). Normalization of the absorbance values was performed from data collection start (t=0) to the maximum achieved absorbance value at full deprotection.

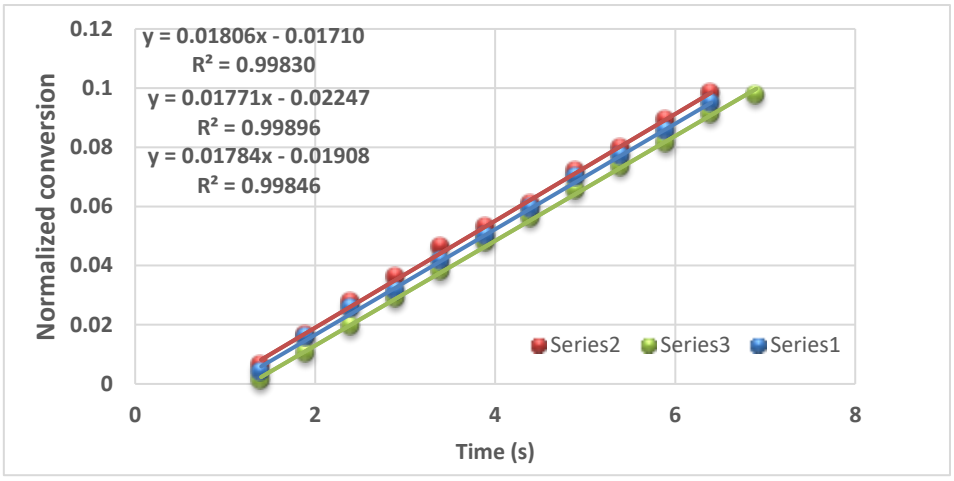

Water/MeCN 65:35	compound 8	rate	A_{390}	QY
	#1	0.01806	0.94	0.072
	#2	0.01771	0.95	0.070
	#3	0.01784	0.94	0.071
			Av. QY	**0.071**
			SD	0.001

Figure S 97**.** Normalized conversion of compound **8** (50 µM, 2mL water/MeCN 65:35, 25 °C) (y-axis) vs time (x-axis). Shown are the measurements taken after the start of irradiation (λ = 390 nm). A linear trendline allowed for the determination of the average rate over the first 10% of PPG consumption. Conversion followed at λ = 270 nm. (photon flux 2,837*10^{-5} mmol/s). Normalization of the absorbance values was performed from data collection start (t=0) to the maximum achieved absorbance value at full deprotection.

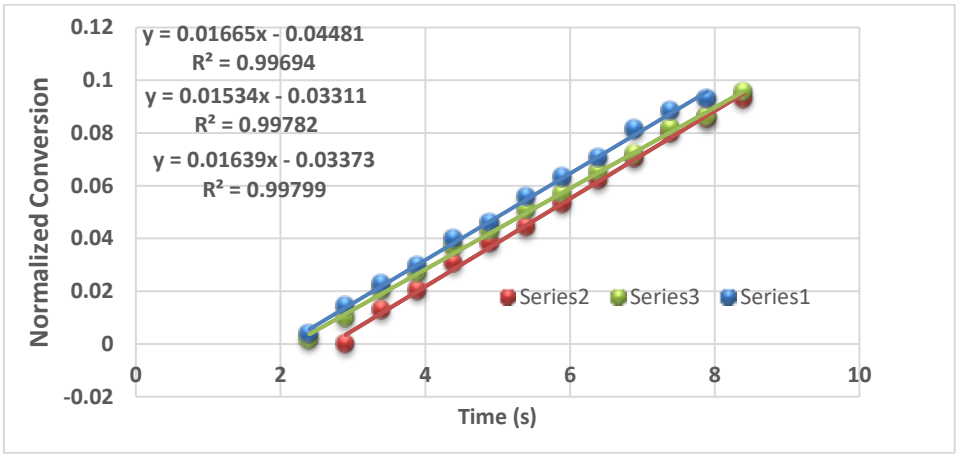

Water/MeCN 65:35	compound 10	rate	A_{390}	QY
	#1	0.01665	0.92	0.067
	#2	0.01534	0.92	0.062
	#3	0.01639	0.89	0.066
			Av. QY	**0.065**
			SD	0.002

Figure S 98**.** Normalized conversion of compound **10** (50 µM, 2mL water/MeCN 65:35, 25 °C) (y-axis) vs time (x-axis). Shown are the measurements taken after the start of irradiation (λ = 390 nm). A linear trendline allowed for the determination of the average rate over the first 10% of PPG consumption. Conversion followed at λ = 270 nm. (photon flux 2,837*10^{-5} mmol/s). Normalization of the absorbance values was performed from data collection start (t=0) to the maximum achieved absorbance value at full deprotection.

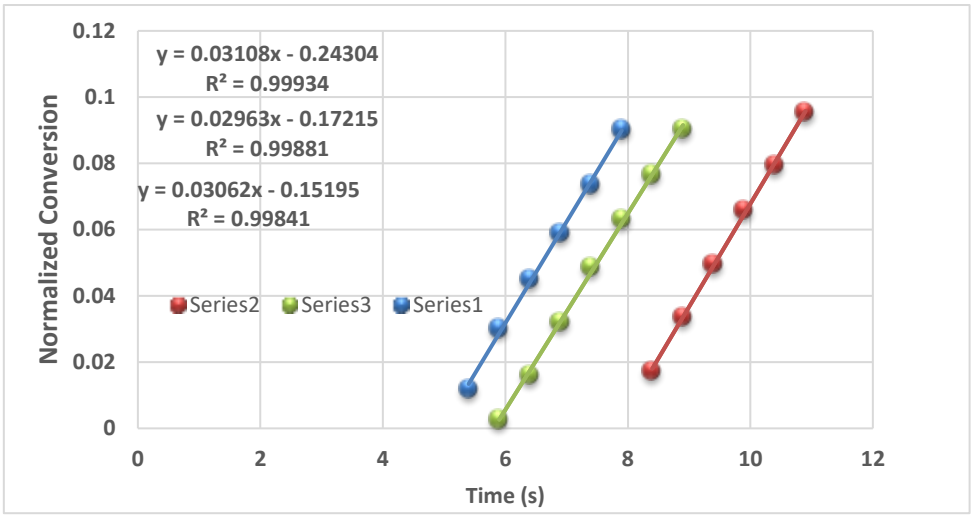

Water/MeCN 65:35	compound 11	rate	A_{390}	QY
	#1	0.03108	1.11	0.119
	#2	0.02963	1.05	0.115
	#3	0.03062	1.06	0.118
			Av. QY	**0.117**
			SD	0.002

Figure S 99**.** Normalized conversion of compound **11** (50 µM, 2mL water/MeCN 65:35, 25 °C) (y-axis) vs time (x-axis). Shown are the measurements taken after the start of irradiation (λ = 390 nm). A linear trendline allowed for the determination of the average rate over the first 10% of PPG consumption. Conversion followed at λ = 450 nm. (photon flux 2,837*10^{-5} mmol/s). Normalization of the absorbance values was performed from data collection start (t=0) to the maximum achieved absorbance value at full deprotection.

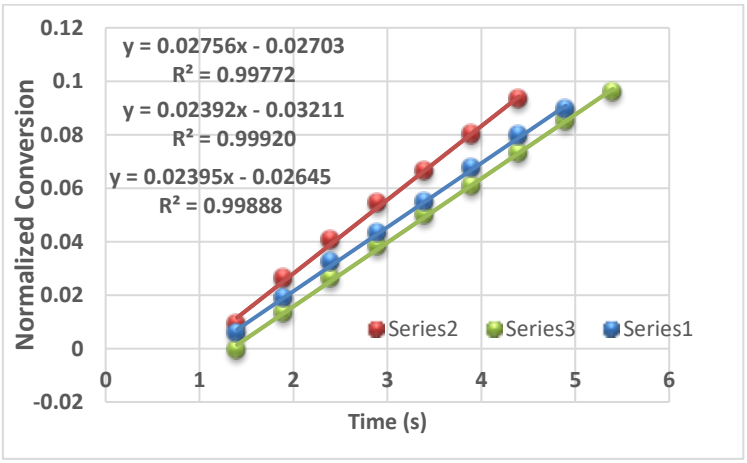

Water/MeCN 65:35	compound 12	rate	A_{390}	QY
	#1	0.02756	1.09	0.106
	#2	0.02392	1.13	0.091
	#3	0.02395	1.14	0.091
			Av. QY	**0.096**
			SD	0.007

Figure S 100**.** Normalized conversion of compound **12** (50 µM, 2mL water/MeCN 65:35, 25 °C) (y-axis) vs time (x-axis). Shown are the measurements taken after the start of irradiation (λ = 390 nm). A linear trendline allowed for the determination of the average rate over the first 10% of PPG consumption. Conversion followed at λ = 450 nm. (photon flux 2,837*10^{-5} mmol/s). Normalization of the absorbance values was performed from data collection start (t=0) to the maximum achieved absorbance value at full deprotection.

3.4 Quantum Yields of **5** and **11** at different buffer pH

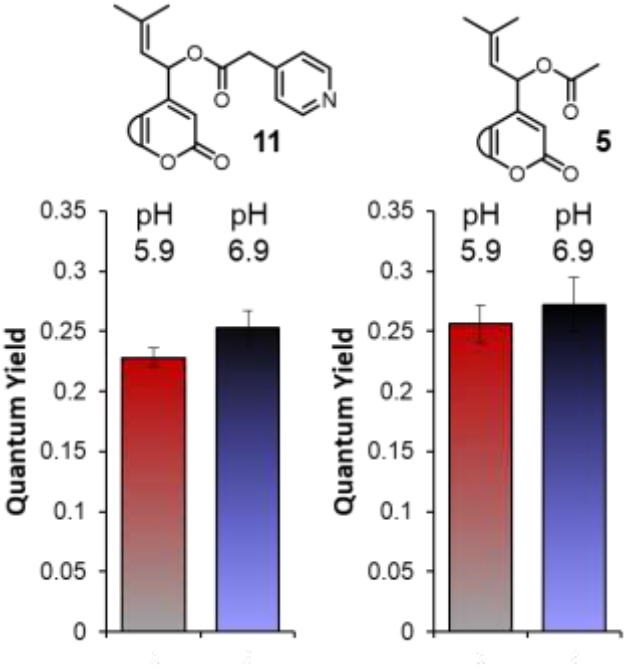

Figure S 101. The effect of buffer pH on the QYs of compound **11** and reference compound **5** (both 50 µM, bistris-buffer (500 mM, pH 5.9 or 6.9, water, 2.5 % DMSO, 25 °C). Shown are the averages and standard deviations of triplicate measurements. Both compounds showed a slightly lower QY at lower pH, although this effect was not statistically significant (p-value > 0.09 and > 0.45 for **11** and **5** respectively).

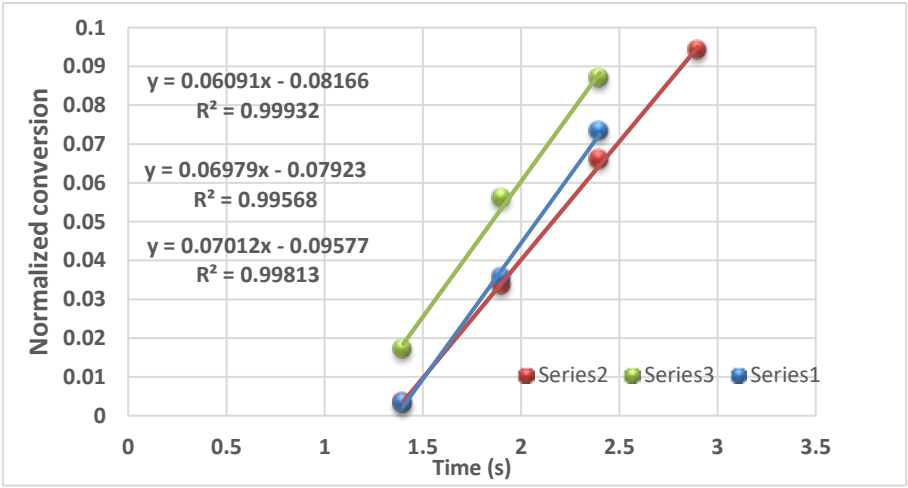

pH 5.9	**compound 5**	**rate**	**A_{390}**	**QY**
	#1	0.06091	0.90	0.234
	#2	0.06979	0.92	0.266
	#3	0.07012	0.91	0.268
			Av. QY	**0.256**
			SD	0.016

Figure S 102. Normalized conversion of compound **5** (50 µM, 2 mL, bistris-buffer 500 mM, pH 5.9, 2.5 % DMSO, 25 °C) (y-axis) vs time (x-axis). Shown are the measurements taken after the start of irradiation (λ = 390 nm). A linear trendline allowed for the determination of the average rate over the first 10% of PPG consumption. Conversion followed at λ = 450 nm. (photon flux $2.98*10^{-5}$ mmol/s). Normalization of the absorbance values was performed from data collection start (t=0) to the maximum achieved absorbance value at full deprotection.

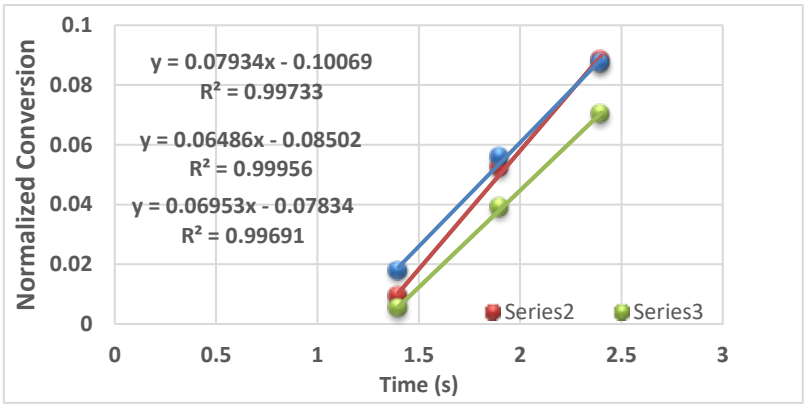

pH 6.9	compound 5	rate	A_{390}	QY
	#1	0.07934	0.92	0.302
	#2	0.06486	0.91	0.248
	#3	0.06953	0.91	0.266
			Av. QY	**0.272**
			SD	0.023

Figure S 103. Normalized conversion of compound **5** (50 µM, 2 mL, bistris-buffer 500 mM, pH 6.9, 2.5 % DMSO, 25 °C) (y-axis) vs time (x-axis). Shown are the measurements taken after the start of irradiation (λ = 390 nm). A linear trendline allowed for the determination of the average rate over the first 10% of PPG consumption. Conversion followed at λ = 450 nm. (photon flux 2.98*10^{-5} mmol/s). Normalization of the absorbance values was performed from data collection start (t=0) to the maximum achieved absorbance value at full deprotection.

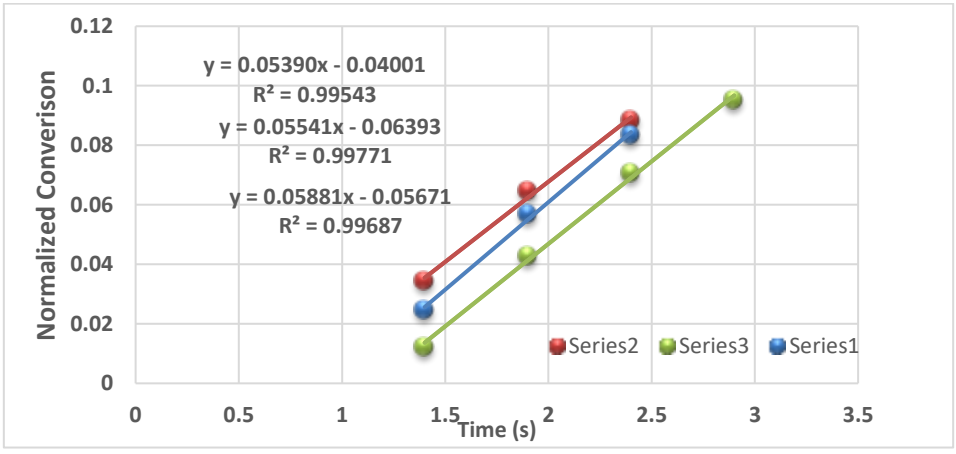

pH 5.9	compound 11	rate	A_{390}	QY
	#1	0.05390	0.73	0.222
	#2	0.05541	0.78	0.223
	#3	0.05881	0.76	0.239
			Av. QY	**0.228**
			SD	0.008

Figure S 104. Normalized conversion of compound **11** (50 µM, 2 mL, bistris-buffer 500 mM, pH 5.9, 2.5 % DMSO, 25 °C) (y-axis) vs time (x-axis). Shown are the measurements taken after the start of irradiation (λ = 390 nm). A linear trendline allowed for the determination of the average rate over the first 10% of PPG consumption. Conversion followed at λ = 450 nm. (photon flux 2.98*10^{-5} mmol/s). Normalization of the absorbance values was performed from data collection start (t=0) to the maximum achieved absorbance value at full deprotection.

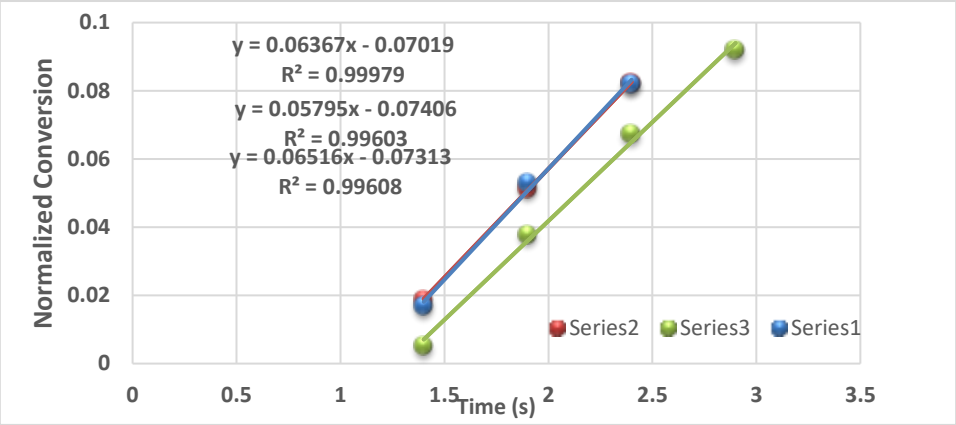

pH 6.9	compound 11	rate	A_{390}	QY
	#1	0.06367	0.73	0.263
	#2	0.05795	0.78	0.233
	#3	0.06516	0.76	0.265
			Av. QY	**0.253**
			SD	0.015

Figure S 105. Normalized conversion of compound **11** (50 µM, 2 mL, bistris-buffer 500 mM, pH 6.9, 2.5 % DMSO, 25 °C) (y-axis) vs time (x-axis). Shown are the measurements taken after the start of irradiation (λ = 390 nm). A linear trendline allowed for the determination of the average rate over the first 10% of PPG consumption. Conversion followed at λ = 450 nm. (photon flux $2.98*10^{-5}$ mmol/s). Normalization of the absorbance values was performed from data collection start (t=0) to the maximum achieved absorbance value at full deprotection.

3.5 Quantum Yields of **5** and **6** in the presence of $LiClO_4$

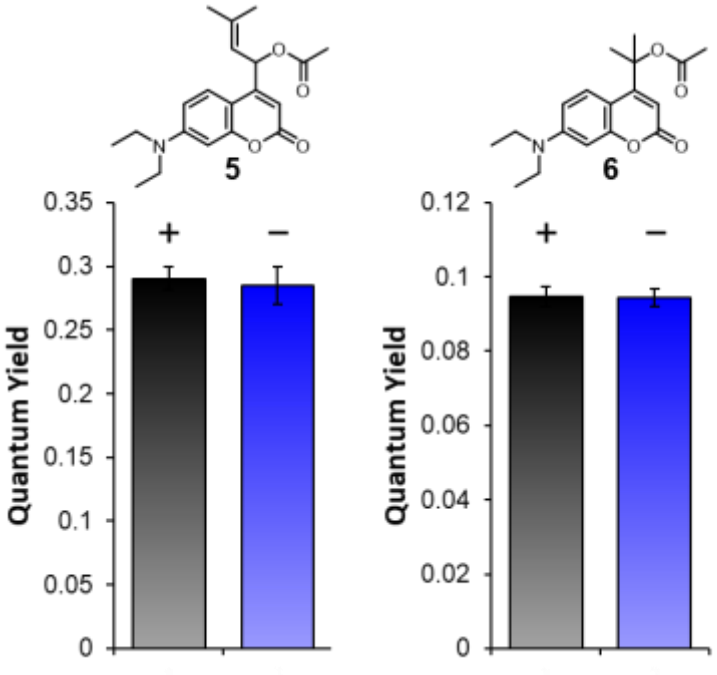

Figure S 106. QYs of compound **5** and **6** (50 µM, water/DMSO 95:5, 25 °C) with (+) and without (−) $LiClO_4$ (50 mM). Shown are averages and standard deviations of triplicate measurements.

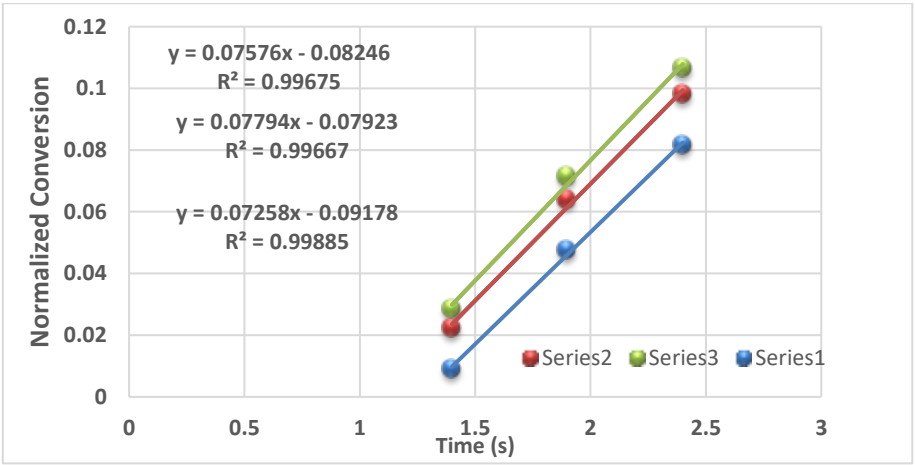

With $LiClO_4$	**compound 5**	**rate**	**A_{390}**	**QY**
	#1	0.07576	0.90	0.291
	#2	0.07794	0.88	0.301
	#3	0.07258	0.90	0.279
			Av. QY	**0.290**
			SD	0.009

Figure S 107. Normalized conversion of compound **5** (50 µM, 2 mL, water/DMSO 95:5, 25 °C, 50 mM $LiClO_4$) (y-axis) vs time (x-axis). Shown are the measurements taken after the start of irradiation (λ = 390 nm). A linear trendline allowed for the determination of the average rate over the first 10% of PPG consumption. Conversion followed at λ = 450 nm. (photon flux $2.98*10^{-5}$ mmol/s). Normalization of the absorbance values was performed from data collection start (t=0) to the maximum achieved absorbance value at full deprotection.

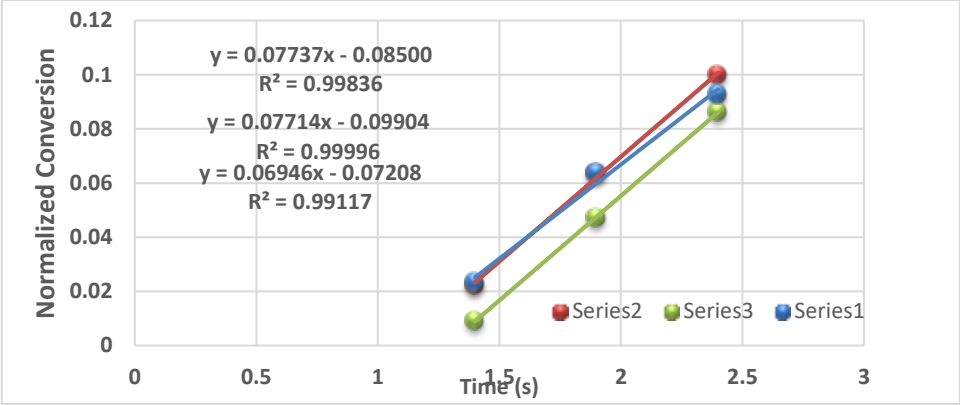

Without $LiClO_4$	compound 5	rate	A_{390}	QY
	#1	0.07737	0.91	0.296
	#2	0.07714	0.92	0.294
	#3	0.06946	0.93	0.264
			Av. QY	**0.285**
			SD	0.015

Figure S 108. Normalized conversion of compound **5** (50 µM, 2 mL, water/DMSO 95:5, 25 °C) (y-axis) vs time (x-axis). Shown are the measurements taken after the start of irradiation (λ = 390 nm). A linear trendline allowed for the determination of the average rate over the first 10% of PPG consumption. Conversion followed at λ = 450 nm. (photon flux $2.98*10^{-5}$ mmol/s). Normalization of the absorbance values was performed from data collection start (t=0) to the maximum achieved absorbance value at full deprotection.

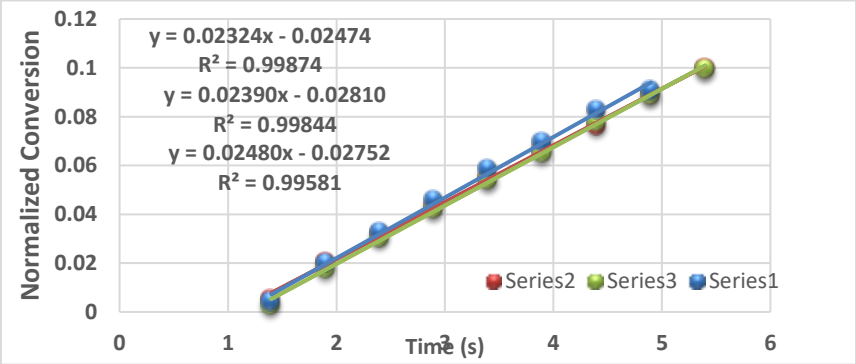

With $LiClO_4$	compound 6	rate	A_{390}	QY
	#1	0.02324	0.83	0.092
	#2	0.02390	0.82	0.095
	#3	0.02480	0.82	0.098
			Av. QY	**0.095**
			SD	0.003

Figure S 109. Normalized conversion of compound **6** (50 µM, 2 mL, water/DMSO 95:5, 25 °C, 50 mM $LiClO_4$) (y-axis) vs time (x-axis). Shown are the measurements taken after the start of irradiation (λ = 390 nm). A linear trendline allowed for the determination of the average rate over the first 10% of PPG consumption. Conversion followed at λ = 270 nm. (photon flux

2.98*10^{-5} mmol/s). Normalization of the absorbance values was performed from data collection start (t=0) to the maximum achieved absorbance value at full deprotection.

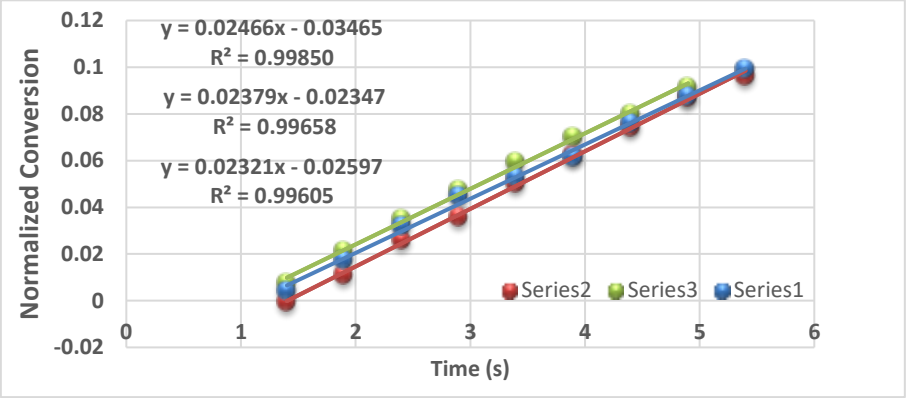

Without $LiClO_4$	compound 6	rate	A_{390}	QY
	#1	0.02466	0.82	0.098
	#2	0.02379	0.82	0.094
	#3	0.02321	0.82	0.092
			Av. QY	**0.094**
			SD	0.002

Figure S 110. Normalized conversion of compound **6** (50 µM, 2 mL, water/DMSO 95:5, 25 °C) (y-axis) vs time (x-axis). Shown are the measurements taken after the start of irradiation (λ = 390 nm). A linear trendline allowed for the determination of the average rate over the first 10% of PPG consumption. Conversion followed at λ = 270 nm. (photon flux 2.98*10^{-5} mmol/s). Normalization of the absorbance values was performed from data collection start (t=0) to the maximum achieved absorbance value at full deprotection.

3.6 Irradiation dependent absorption spectra and Quantum Yield of **6-D$_6$**

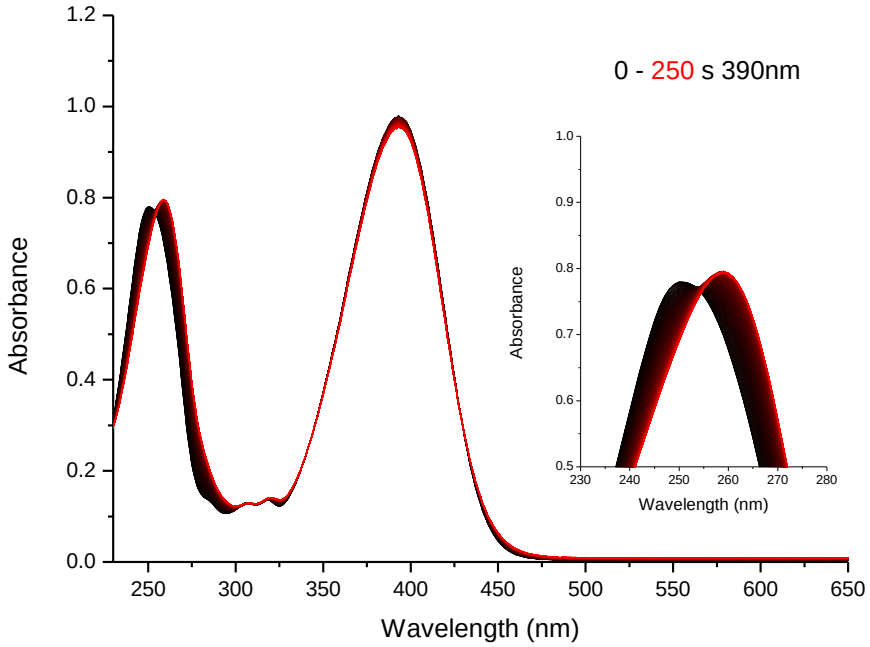

Figure S 111. UV-vis absorption spectra of compound **6-D$_6$** solution (54 µM, water 2.7 % MeCN, 25 °C). A freshly prepared solution (black) and solution after irradiation (λ = 390 nm, red line). The insert highlights the isosbestic point.

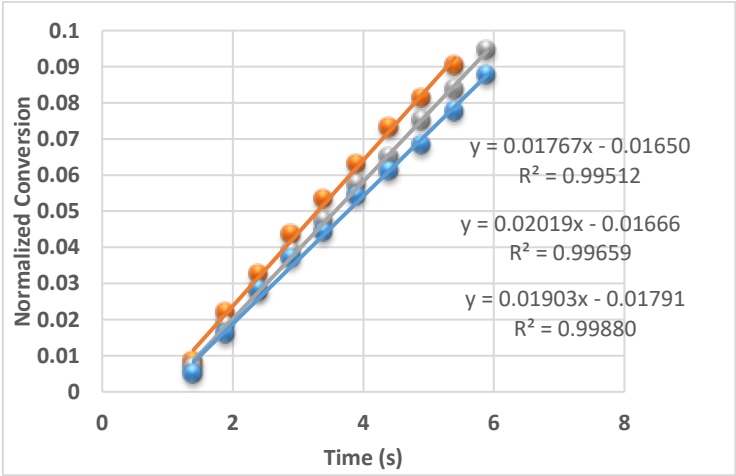

6-D$_6$	**rate**	**A$_{390}$**	**QY**
#1	0.01767	0.96	0.0652
#2	0.02019	0.94	0.0749
#3	0.01903	0.96	0.0702
		Av. QY	0.0701
		SD	**0.0040**

Figure S 112**.** Normalized conversion of compound **6-D$_6$** (y-axis) vs time (x-axis). Shown are the measurements taken after the start of irradiation (λ = 390 nm). A linear trendline allowed for the determination of the average rate over the first 10% of PPG consumption. 55 µL compound **6-D$_6$** (2 mM, MeCN) added to 1980 µL water (for the final concentration of 54 µM, in 2.7 % MeCN in water). Conversion followed at λ = 270 nm (photon flux $3.350*10^{-5}$ mmol/s). Normalization of the absorbance values was performed from data collection start (t=0) to the maximum achieved absorbance value at full deprotection.

3.7 Quantum Yields of compounds 1 and S9

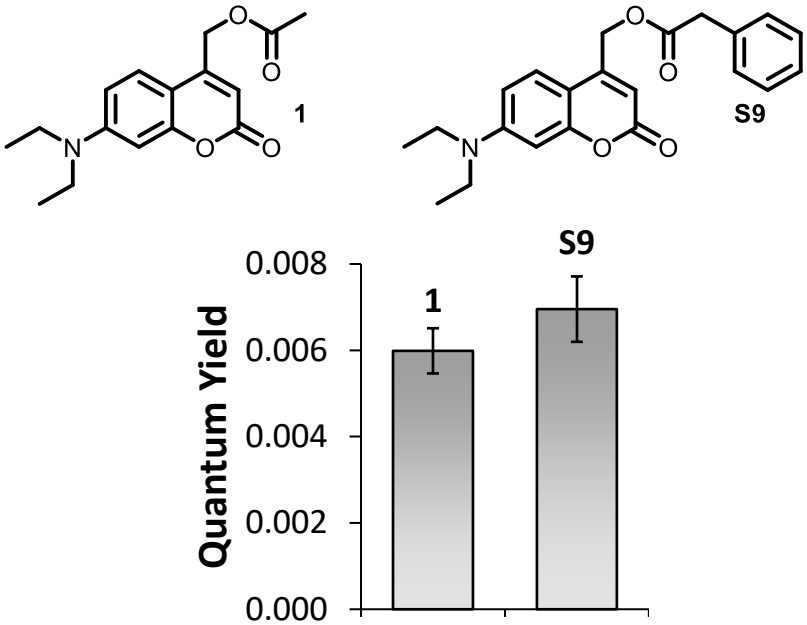

Figure S 113. Structures of primary coumarins **1** and **S9**, and their photolysis QY (determined at 50 µM, 7:3 Water/MeCN, 25 °C) (See figures S104-107). Note that the determined QYs in the solvent mixture are slightly lower than usual for primary coumarins, due to the requirement of the addition of MeCN to solubilize **S9**.

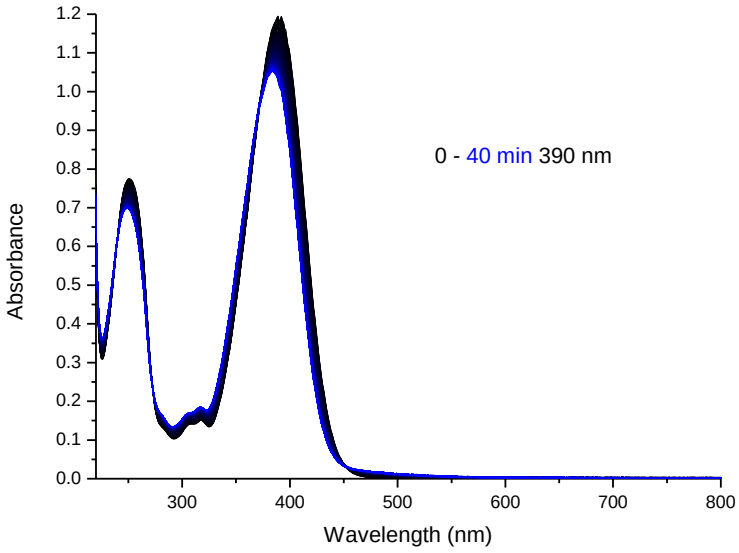

Figure S 114. UV-vis absorption spectra of compound **1** solution (50 µM, water/MeCN 7:3, 25 °C). A freshly prepared solution (black) and solution after irradiation (λ = 390 nm, blue line).

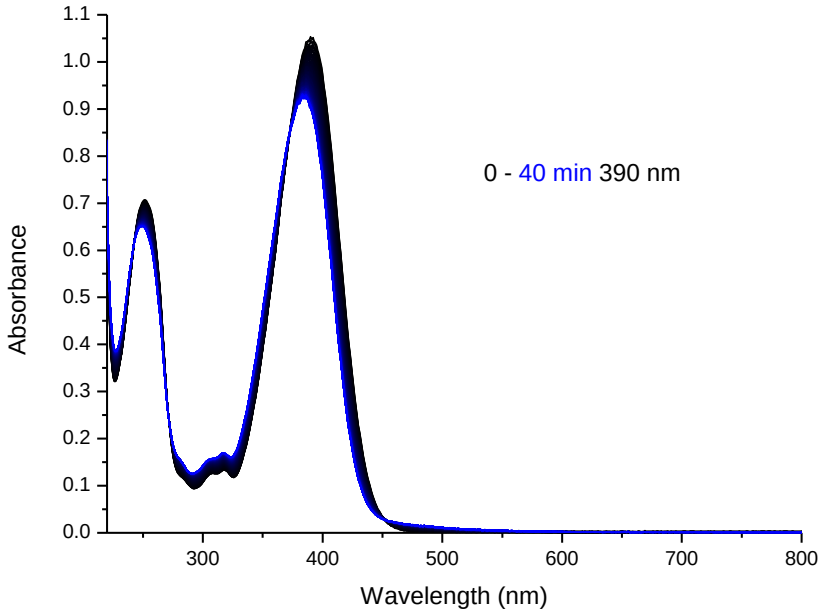

Figure S 115. UV-vis absorption spectra of compound **S9** solution (50 µM, water/MeCN 7:3, 25 °C). A freshly prepared solution (black) and solution after irradiation (λ = 390 nm, blue line).

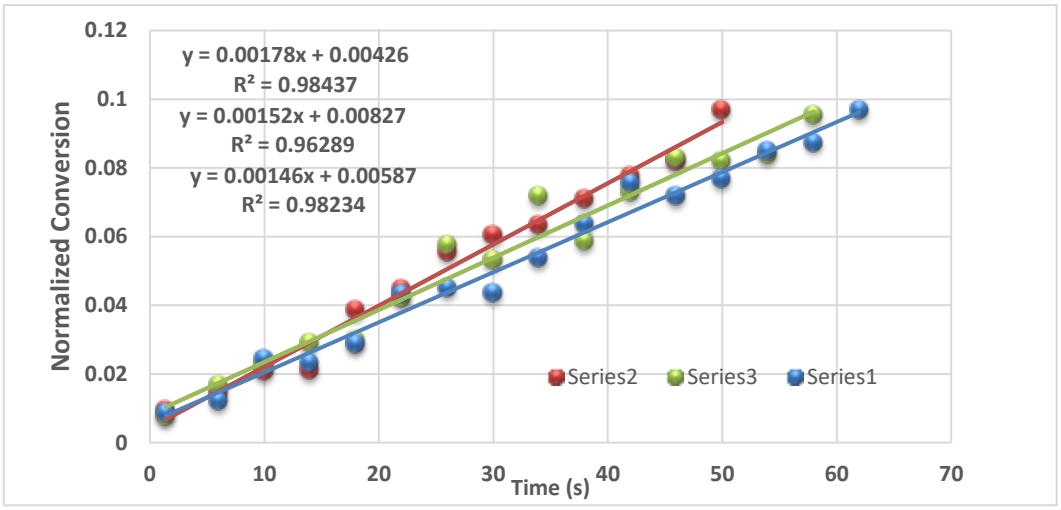

Water/MeCN 70:30	compound 1	rate	A_{390}	QY
	#1	0.00178	1.18	0.0067
	#2	0.00152	1.18	0.0057
	#3	0.00146	1.18	0.0055
			Av. QY	**0.0060**
			SD	0.0005

Figure S 116. Normalized conversion of compound **1** (50 µM, 2mL water/MeCN 70:30, 25 °C) (y-axis) vs time (x-axis). Shown are the measurements taken after the start of irradiation (λ = 390 nm). A linear trendline allowed for the determination of the average rate over the first 10% of PPG consumption. Conversion followed at λ = 317 nm. (photon flux 2,837*10^{-5} mmol/s). Normalization of the absorbance values was performed from data collection start (t=0) to the maximum achieved absorbance value at full deprotection.

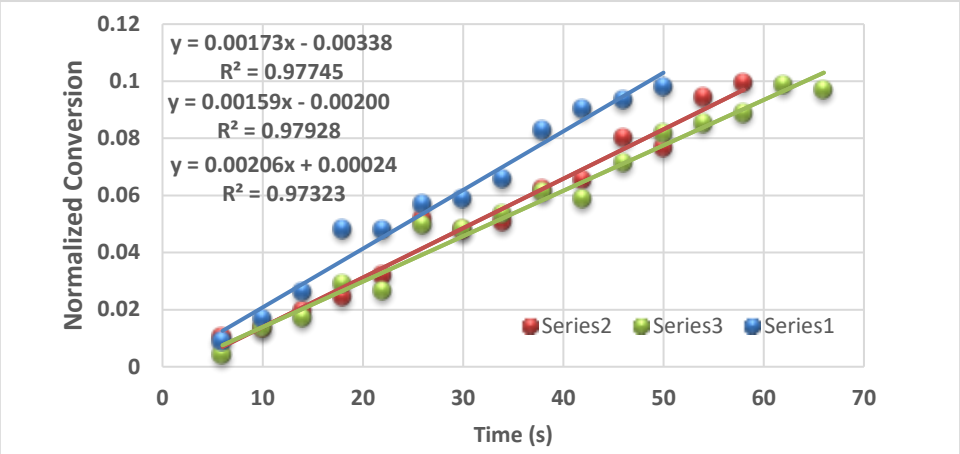

Water/MeCN 70:30	compound S9	rate	A_{390}	QY
	#1	0.00173	1.02	0.0067
	#2	0.00159	1.05	0.0062
	#3	0.00206	1.05	0.0080
			Av. QY	**0.0070**
			SD	0.0008

Figure S 117. Normalized conversion of compound **S9** (50 µM, 2mL water/MeCN 70:30, 25 °C) (y-axis) vs time (x-axis). Shown are the measurements taken after the start of irradiation (λ = 390 nm). A linear trendline allowed for the determination of the average rate over the first 10% of PPG consumption. Conversion followed at λ = 317 nm. (photon flux 2,837*10^{-5} mmol/s). Normalization of the absorbance values was performed from data collection start (t=0) to the maximum achieved absorbance value at full deprotection.

3.8 Fluorescent QYs of the parent alcohols of compounds 1-6

The synthesis of alcohols **3-OH**, **4-OH**, **5-OH**, **6-OH** was described by Schulte *et al.* in 2022.[1] The QYs for the parent alcohols of compounds **1**-**6** were determined using an Edinburgh Instruments FS5 fluorimeter equipped with an integrating sphere.

The following settings were used: excitation wavelength: 395 nm, emission bandwidth: 0.40 nm, excitation bandwidth: 4.00 nm, step size 0.40 nm, dwell time 0.15 s. For each measured QY, 5 emission spectra were recorded to increase the accuracy.

	1-OH	***2-OH***	***3-OH***	***4-OH***	***5-OH***	***6-OH***
QY 1	0.092	0.130	0.120	0.102	0.102	0.096
QY 2	0.091	0.106	0.119	0.099	0.101	0.091
QY 3	0.091	0.100	0.117	0.099	0.101	0.089
Average	0.091	0.112	0.119	0.100	0.101	0.092
SD	0.001	0.013	0.002	0.001	0.001	0.003

Table S 1. Fluorescence QYs of the parent alcohols of compounds **1**-**6** (95:5 water/DMSO, 13 µM coumarin-alcohol).

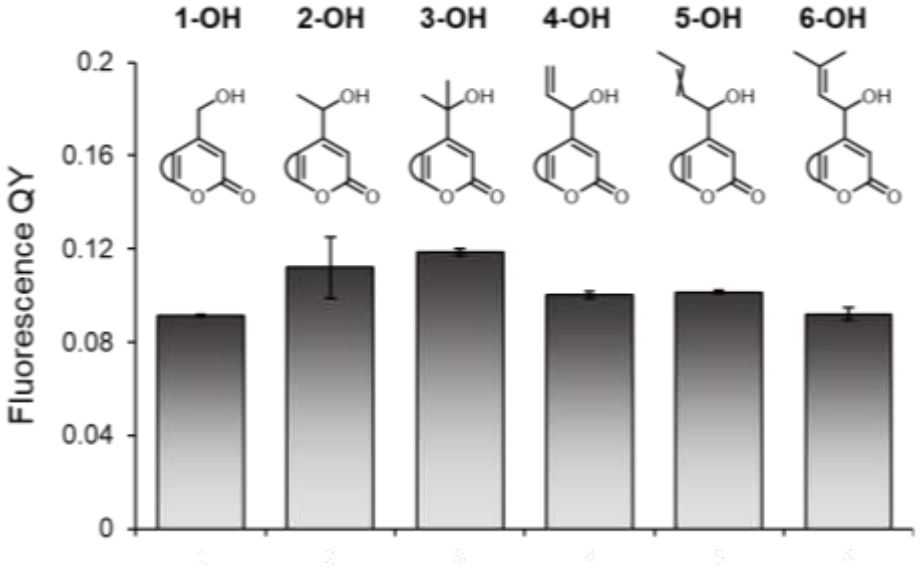

Figure S 118. Fluorescence QYs of the parent alcohols of compounds **1**-**6** (95:5 water/DMSO, 13 µM coumarin-alcohol). The diethylamino western ring of the coumarin is abbreviated as a semicircle.

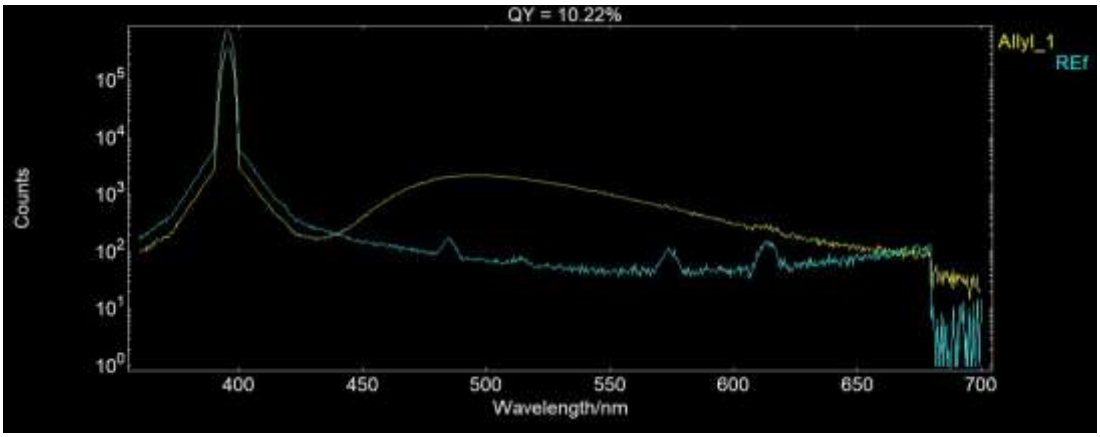

Figure S 119. Results of a typical QY measurement (**4-OH** #1**)** displaying counts (y-axis, logarithmic scale) vs wavelength (nm, x-axis).

3.9 Chemical yields of uncaging of 5, 6, 7 and 8.

The uncaging chemical yields were determined by qNMR. In an NMR tube, solutions of compounds **5** – **8** (1 mM, 0.6 mL) in DMSO-d_6/D_2O (1:1 for **5**, 3:1 for **6**-**8**) with $DMSO_2$ as an internal standard (1 mM) were irradiated for 10 min with violet light (λ = 400 nm), resulting in complete uncaging for all PPGs. The relative integrals of the substrate and product signals were determined as compared to that of $DMSO_2$ (at ~ 2.9 ppm, integrated to 60.00). The chemical yields (CYs) were determined through dividing the product integral by the substrate integral.

Compound **5**	**Relative integrals**		
	Acetate CH_3	AcOH CH_3	CY (%)
1	27.98	24.73	88.4
2	27.55	25.11	91.1
3	27.01	24.27	89.9
		Average CY	**89.8**
		SD	**1.1**

Compound **6**	**Relative integrals**		
	Acetate CH_3	AcOH CH_3	CY (%)
1	19.25	17.21	89.4
2	20.91	18.71	89.5
3	19.38	17.38	89.7
		Average CY	**89.5**
		SD	**0.1**

Compound **7**	**Relative integrals**		
	Phenylacetate CH_2	Phenylacetic acid CH_2	CY (%)
1	17.44	16.46	94.4
2	17.97	17.92	99.7
3	19.43	18.33	94.3
		Average CY	**96.1**
		SD	**2.5**

Compound **8**	**Relative integrals**		
	Phenylacetate CH_2	Phenylacetic acid CH_2	CY (%)
1	16.01	16.07	100.4
2	16.14	16.38	101.5
3	16.47	16.84	102.2
		Average CY	**101.4**
		SD	**0.8**

Table S 2. Integrals of the irradiation experiments of compounds **5**-**8**, displaying the chemical yields (CY).

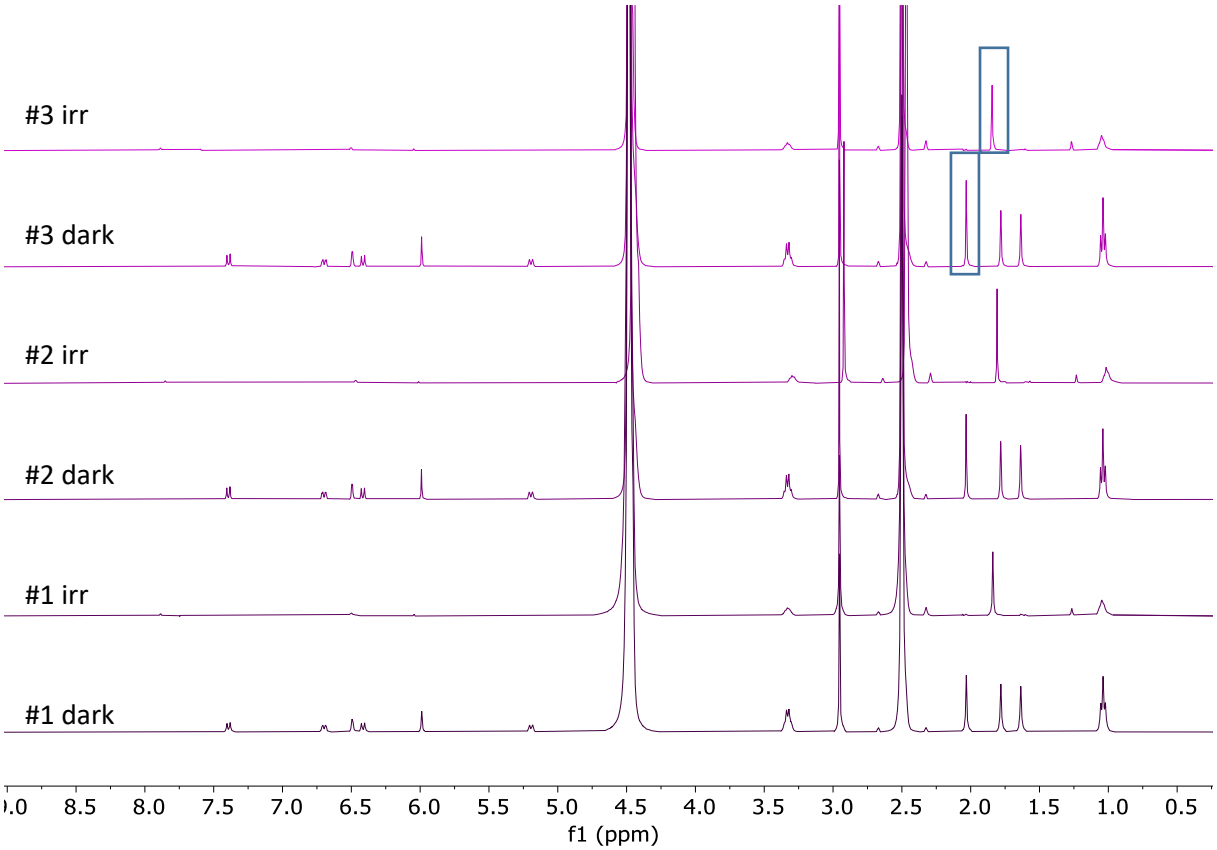

Figure S 120. ^{1}H-NMR spectra of compound **5** (1 mM, 1:1 DMSO-d_6/D_2O, 1 mM $DMSO_2$). The integrated acetate and acetic acid signals can be observed at 2.03 and 1.84 ppm respectively.

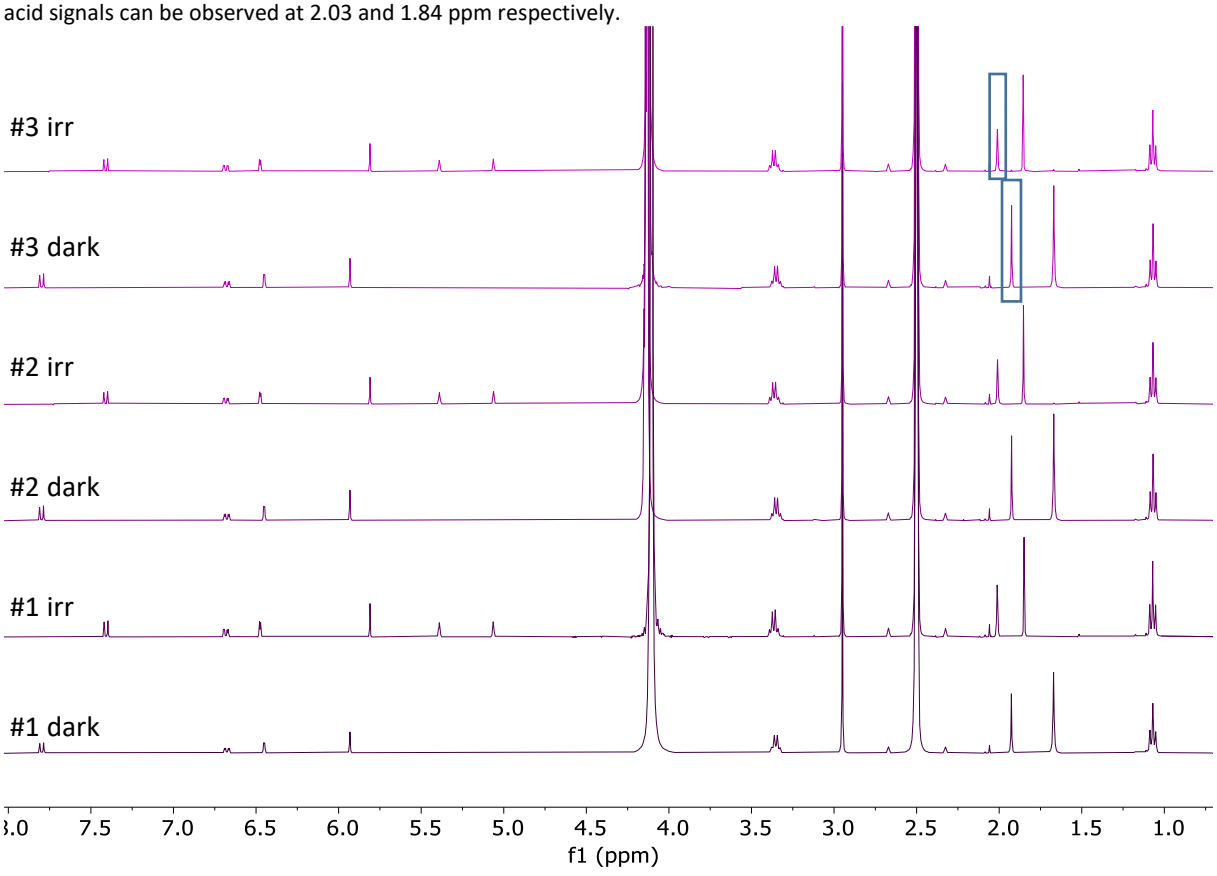

Figure S 121. ^{1}H-NMR spectra of compound **6** (1 mM, 3:1 DMSO-d_6/D_2O, 1 mM $DMSO_2$). The integrated acetate and acetic acid signals can be observed at 1.93 and 2.01 ppm respectively.

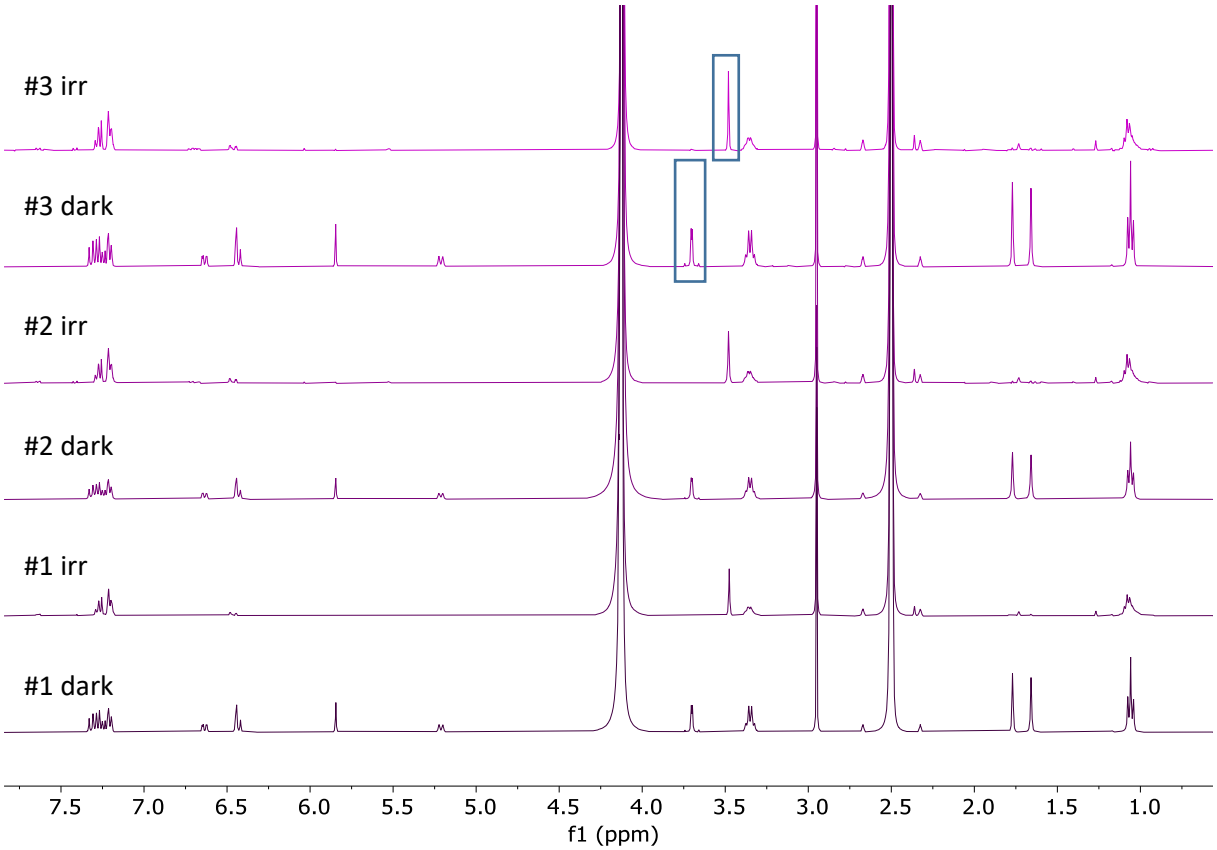

Figure S 122. ^{1}H-NMR spectra of compound **7** (1 mM, 3:1 DMSO-d_6/D_2O, 1 mM $DMSO_2$). The integrated phenylacetate and phenylacetic acid signals can be observed at 3.70 (dd) and 3.48 ppm (s) respectively.

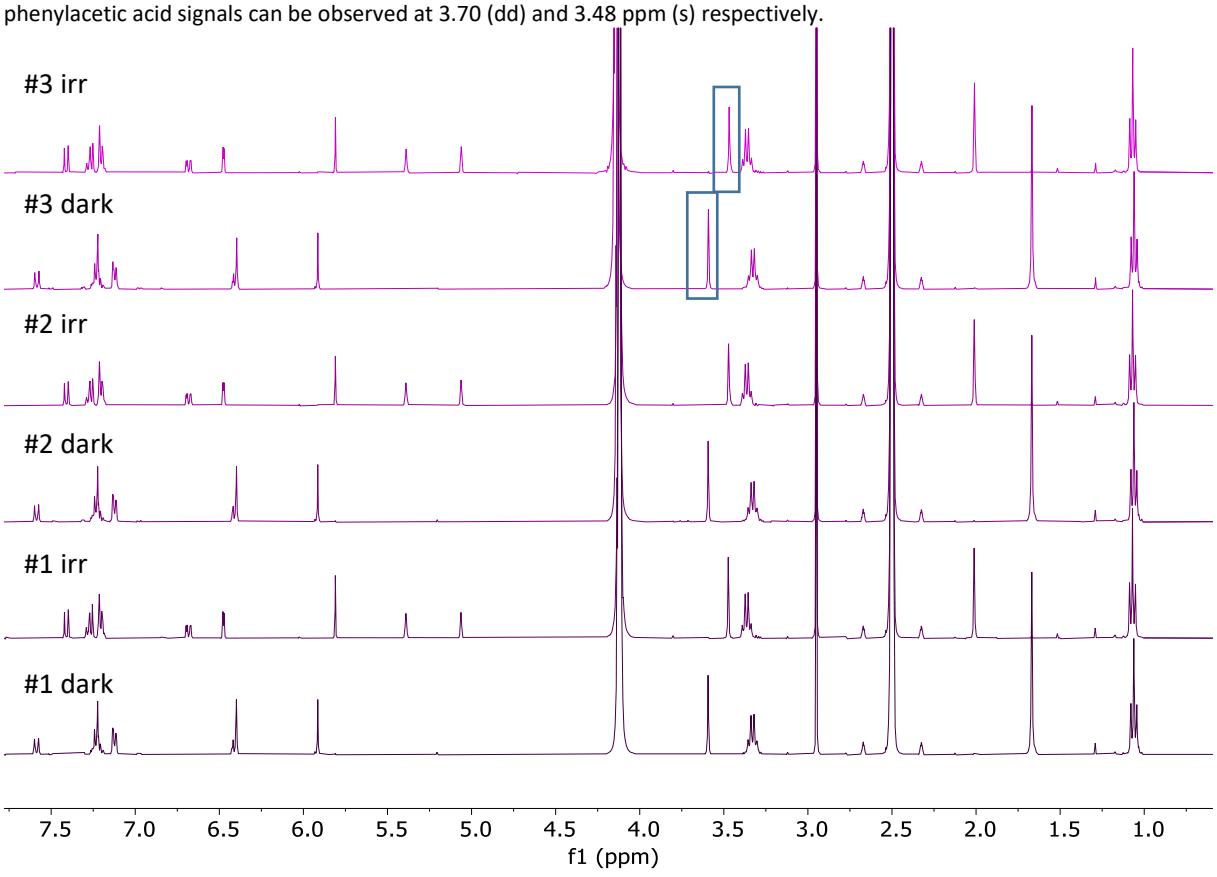

Figure S 123. ^{1}H-NMR spectra of compound **8** (1 mM, 3:1 DMSO-d_6/D_2O, 1 mM $DMSO_2$). The integrated phenylacetate and phenylacetic acid signals can be observed at 3.59 (s) and 3.48 ppm (s) respectively.

3.10 Hydrolytic stability of tertiary coumarins 6, 8 and 10.

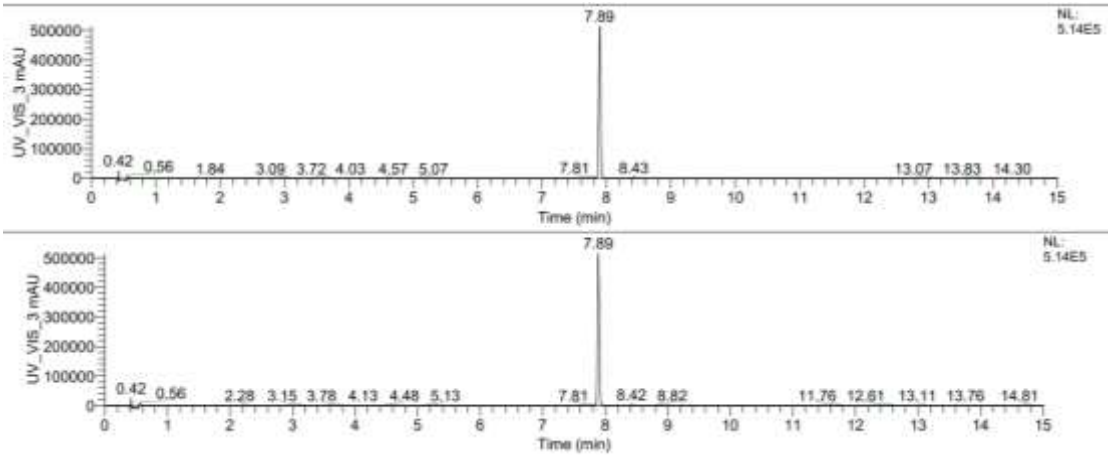

Figure S 124. UPLC-MS chromatograms (showing the λ = 390 nm trace) of a solution of compound **6** (20 µM, water, 20 % DMSO) before (top) and after (bottom) incubation at 21 °C for 17 h. The peak intensity (top right) remained the same and no other peaks were formed.

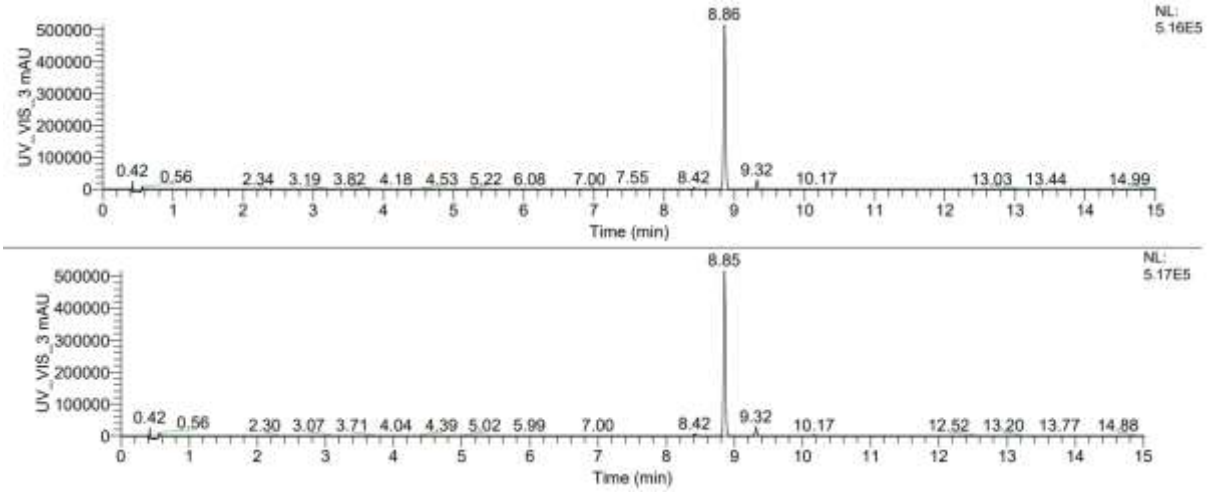

Figure S 125. UPLC-MS chromatograms (showing the λ = 390 nm trace) of a solution of compound **8** (20 µM, water, 20 % DMSO) before (top) and after (bottom) incubation at 21 °C for 17 h. The peak intensity (top right) remained the same and no other peaks were formed.

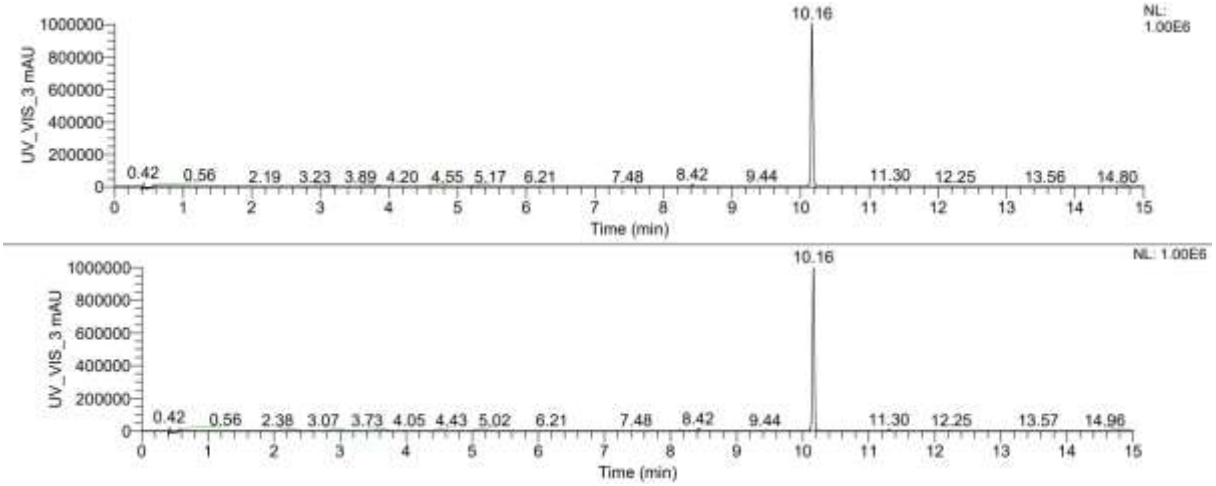

Figure S 126. UPLC-MS chromatograms (showing the λ = 390 nm trace) of a solution of compound **10** (20 µM, water, 33 % DMSO) before (top) and after (bottom) incubation at 21 °C for 17 h. The peak intensity (top right) remained the same and no other peaks were formed.

4. Computational data

4.1 Overview of Methods and Results

All computational input files were prepared in GaussView 6.0 on a local Windows 10 terminal. Input files were then transferred to the University of Groningen Peregrine HPC cluster where DFT or TD-DFT calculations were carried out using the Gaussian 16 (g16) suite of programs.

The DFT thermochemistry of heterolysis for coumarin PPG **6** was examined. Geometry optimization of structures were attempted to either ground state S_0 or excited state S_1 minima or transition states (TS) using the g16 *opt* command at the MN15 functional and Def2SVP basis set level of theory with implicit solvation using the Solvation Model based on Density (SMD = water).[4–6] Transition state geometry inputs were the result of rational guess based on bond-breaking atomic distances, or were the result of potential energy surface relaxed coordinate scans using the g16 *scan* command at the MN15/Def2SVP/SMD=water level. Intrinsic reaction coordinate (IRC)iv calculations were carried out on the transition state structures to verify that they connected to the associated reactant and product minima structures. The S_0 optimizations of solvent-encapsulated CIP structures arising from the heterolysis of **6** were all unsuccessful, despite various optimization attempts with modified input structures with varying lengths 3-6 Å between the leaving group acetate and the chromophore cation. Likewise, no heterolysis transition states were found for PPG **6** on the S_0 potential energy surface at the same level of theory. Instead, only a concerted heterolysis/elimination pathway TS was detected, and is shown as **S_0-[3.3]-TS**. Thus, only the S_1 thermochemistry arising from the reactant, TS, or CIP MN15/Def2SVP/SMD=water geometries are shown.

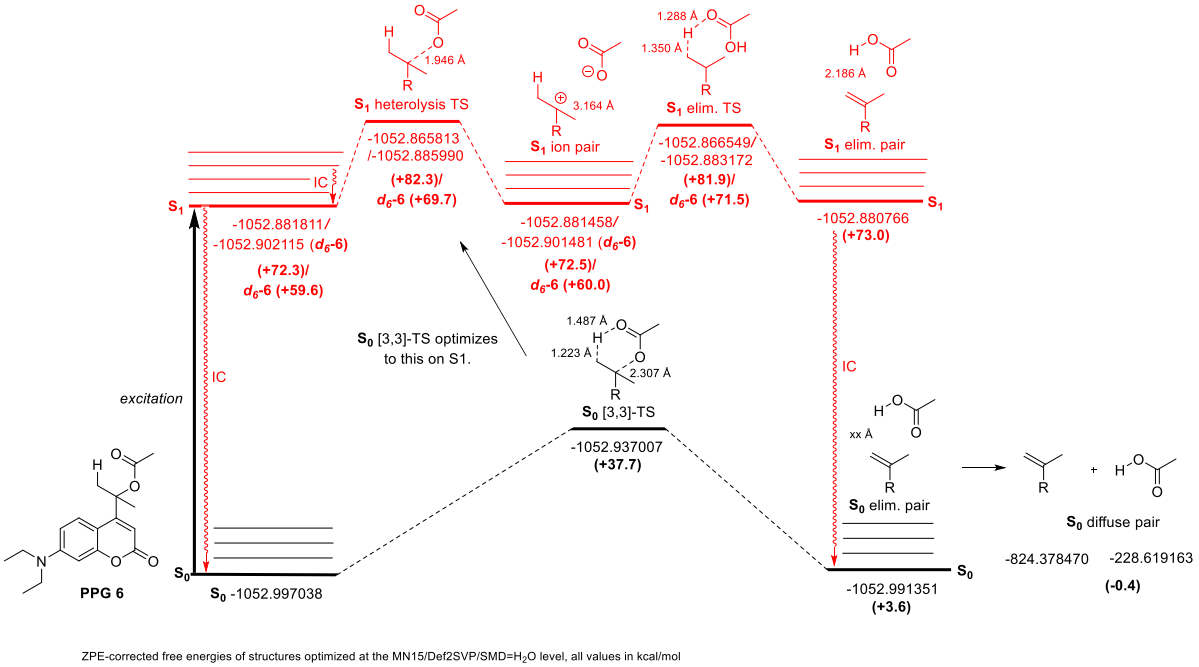

ZPE-corrected free energies of structures optimized at the MN15/Def2SVP/SMD=H_2O level, all values in kcal/mol

Figure S 127. The S_1 excited state barriers for the $\mathbf{k_1}$, $\mathbf{k_{-1}}$, and $\mathbf{k_2}$ steps for PPG **6** and **6-D$_6$** as calculated by DFT. (obtained at the MN15/Def2SVP/SMD=H_2O level of theory).

After optimization, frequency DFT calculations of the optimized structures were carried out using the g16 *freq* command at the MN15/Def2SVP/SMD=water level, to confirm that minima structures had zero imaginary frequencies and that transition states had a single imaginary frequency. ZPE-corrected energies of the hexadeuterated variant ***d$_6$*-6** was obtained from a separate *freq* calculation. All shown free energies (Figure S127) are ZPE and thermally corrected and were obtained from the frequency calculations. All shown free energies are reported in kcal/mol, at 298.15 K and 1 atm.

4.2 Optimized Geometries and XYZ Coordinates

PPG 6 (S_0) optimized geometry (# opt=calcfc freq scrf=(smd,solvent=water) def2svp mn15)

EE + Thermal Free Energy Correction: -1052.997038 Ha (+0.0 kcal/mol)

0 1

C	-1.83313900	0.96847600	0.07372100
C	-2.07439700	2.27815000	-0.21657500
C	-1.01361600	3.23508500	-0.43491300
O	0.26207000	2.76508000	-0.33836000
C	0.56230500	1.46301700	-0.05047900
C	-0.45640600	0.51331800	0.16155400
C	-0.00287000	-0.80047600	0.43809800
C	1.33661300	-1.12233600	0.51066200
C	2.35484000	-0.14148600	0.31744400
N	3.69023300	-0.44518200	0.42791700
C	4.11164300	-1.84268800	0.41032100
C	4.64910400	0.57650100	-0.00041300
C	1.91898800	1.16472800	0.01075600
H	-3.07917200	2.68855900	-0.29833700
H	-0.72542100	-1.60015200	0.59235400
H	1.60105200	-2.15742900	0.72041500
H	5.12615900	-1.89948900	0.82340300
H	3.48913500	-2.41480200	1.11130700
H	4.46439300	0.84329300	-1.05889100
H	4.45406600	1.49132000	0.58026500
H	2.60899800	1.98435500	-0.17929200
C	-3.00154100	0.02393200	0.36320400
O	-2.72407600	-1.12439800	-0.47554200
C	-3.38844000	-2.28181600	-0.38231900
O	-4.33372700	-2.46687600	0.35812100
C	-2.80277900	-3.30916800	-1.29958200
H	-2.72837000	-2.90281900	-2.31720400
H	-1.78211200	-3.54620200	-0.96314500
H	-3.41842600	-4.21460500	-1.28953100
C	-4.35177300	0.59968000	-0.04004100
H	-4.35111100	0.90872900	-1.09455900
H	-5.12191100	-0.16695700	0.11052700
H	-4.60575700	1.46418400	0.58784800
C	4.07252700	-2.46167900	-0.97868900
H	4.40716500	-3.50891200	-0.94964900

H	3.05204600	-2.43995800	-1.39221300
H	4.73099800	-1.91075300	-1.66881400
C	6.10744200	0.20405900	0.18224700
H	6.33343300	-0.05321700	1.22771600
H	6.41334200	-0.63545600	-0.45880400
H	6.72490400	1.07122400	-0.09085900
O	-1.16039100	4.41662000	-0.69685200
C	-2.99000700	-0.31252600	1.85759500
H	-2.10126000	-0.89282900	2.13899300
H	-2.97798700	0.63166500	2.42094200
H	-3.88775500	-0.87552200	2.13762900

PPG 6 (S_0 [3,3]-TS) optimized geometry # opt=(calcfc,ts,noeigentest) freq scrf=(smd,solvent=water) def2svp mn15)

EE + Thermal Free Energy Correction: -1052.937007 Ha (+37.7 kcal/mol)

0 1

C	-2.11668200	0.87352500	0.26123700
C	-2.49403300	2.11452200	-0.16696400
C	-1.52473700	3.15168000	-0.46396900
O	-0.21318500	2.81276700	-0.33656100
C	0.21431200	1.57078300	0.04708100
C	-0.70698200	0.56175600	0.38521400
C	-0.14106800	-0.68272500	0.74448700
C	1.22148600	-0.89279200	0.77105200
C	2.14494000	0.14313800	0.43808400
N	3.50212400	-0.05599700	0.47725800
C	4.02191700	-1.41907400	0.54515500
C	4.35137800	0.98923100	-0.10132300
C	1.59121700	1.38645600	0.06205100
H	-3.53677200	2.40948800	-0.27708000
H	-0.78242600	-1.52219200	1.00659500
H	1.57847600	-1.88317200	1.04840000
H	5.06710400	-1.37049400	0.87355500
H	3.50011700	-1.96297700	1.34411200
H	4.06643200	1.15784400	-1.15751600
H	4.13666200	1.93257300	0.42422000
H	2.20332700	2.23754000	-0.22966600
C	-3.20585900	-0.05681200	0.65435900
O	-2.59505200	-1.44117600	-1.08690500
C	-2.18995400	-2.57401400	-0.72067100
O	-2.55783500	-3.11884600	0.37204600
C	-1.17459700	-3.29887400	-1.56572800
H	-1.24125900	-4.38334100	-1.41284100
H	-1.30051200	-3.04504900	-2.62586400
H	-0.17146200	-2.96522300	-1.25069200
C	-4.54175500	0.09590000	0.02543000
H	-4.48060500	0.37792500	-1.03127000
H	-5.11991800	-0.82873000	0.15020000
H	-5.07343800	0.89040600	0.57849000
C	3.91793200	-2.16570300	-0.77629100
H	4.33429800	-3.17948300	-0.68519600

H	2.86850400	-2.25568100	-1.09980900
H	4.47321300	-1.63649900	-1.56676500
C	5.84198400	0.72714500	-0.01408500
H	6.16832600	0.57168900	1.02490300
H	6.15412800	-0.14075100	-0.61293700
H	6.37270700	1.60681000	-0.40430000
O	-1.78989100	4.28523300	-0.81744000
C	-3.09175600	-0.88481400	1.79781100
H	-2.25446300	-0.70173800	2.47803800
H	-4.05127200	-1.11531500	2.27860300
H	-2.88477800	-1.94143600	1.21931600

PPG 6 (elim. pair) optimized geometry (# opt=calcfc freq scrf=(smd,solvent=water) def2svp mn15)

EE + Thermal Free Energy Correction: -1052.991351 Ha (+3.6) kcal/mol)

0 1

C	-2.31695700	0.80030300	0.44638900
C	-2.77690600	1.94519100	-0.14720200
C	-1.89400100	2.98379500	-0.61753100
O	-0.55261900	2.75902300	-0.47546200
C	-0.03681700	1.60490600	0.04268600
C	-0.88356500	0.59192900	0.53051100
C	-0.23302500	-0.57900800	0.98234600
C	1.14005400	-0.71123200	0.97785500
C	1.98837900	0.34095100	0.51922100
N	3.35800400	0.23060900	0.53922700
C	3.96451700	-1.08370400	0.72827300
C	4.12481500	1.25683200	-0.17233500
C	1.34961300	1.50130500	0.03011700
H	-3.84130200	2.15387100	-0.25522400
H	-0.83306400	-1.42430900	1.32121400
H	1.56444600	-1.65331000	1.32204700
H	5.01074000	-0.93883600	1.02390500
H	3.49337800	-1.57500300	1.59032200
H	3.80814600	1.29227600	-1.23251600
H	3.86129500	2.23675500	0.25482700
H	1.90114100	2.34598000	-0.37798600
C	-3.29904900	-0.19119700	0.96568200
O	-1.84457500	-1.73685600	-1.69600000
C	-1.42078100	-2.69343600	-1.07443900
O	-2.15634300	-3.32661700	-0.15402500
C	-0.06572300	-3.29910700	-1.25175700
H	0.38791500	-3.51368800	-0.27471800
H	-0.17681500	-4.25534200	-1.78536000
H	0.56839700	-2.62410900	-1.83710400
C	-4.51559400	-0.45196700	0.11878700
H	-4.22469500	-0.71055900	-0.91073800
H	-5.11083000	-1.27347400	0.54142800
H	-5.16218100	0.43784000	0.06032100
C	3.88434800	-1.96569000	-0.50902000
H	4.36555800	-2.93779700	-0.32719800

H	2.83744700	-2.15192400	-0.79765700
H	4.39155100	-1.48660500	-1.36141700
C	5.63100100	1.09979200	-0.09818100
H	5.98720900	1.07758300	0.94239100
H	5.98762700	0.19400000	-0.60975300
H	6.09559500	1.96403000	-0.59322500
O	-2.23196500	4.04467700	-1.11654000
C	-3.13150300	-0.77840700	2.16251500
H	-2.27651200	-0.55421100	2.80487400
H	-3.88123800	-1.47692800	2.54545000
H	-3.02864100	-2.88984800	-0.08576700

PPG 6 (eliminated) optimized geometry (# opt=calcfc freq scrf=(smd,solvent=water) def2svp mn15)

EE + Thermal Free Energy Correction: -824.378470 Ha

0 1

C	2.63412200	-0.25689900	-0.04749900
C	3.23989200	0.95993500	0.11543700
C	2.49782500	2.19579300	0.14095200
O	1.13946100	2.09873800	0.01125600
C	0.47886800	0.90759500	-0.09199200
C	1.18726400	-0.30895000	-0.11696000
C	0.39385200	-1.47847900	-0.15138200
C	-0.98386800	-1.43304300	-0.20737300
C	-1.68756300	-0.19113400	-0.24350000
N	-3.05583400	-0.13294900	-0.35362300
C	-3.84771400	-1.33498600	-0.11137100
C	-3.69319400	1.17147000	-0.15485700
C	-0.90751200	0.98303000	-0.15224400
H	4.32294200	1.06198000	0.18653800
H	0.88315700	-2.45233600	-0.11309900
H	-1.52844800	-2.37579900	-0.21579300
H	-4.83936300	-1.18705900	-0.55616400
H	-3.40962600	-2.17207300	-0.67113500
H	-3.43494900	1.56597700	0.84671800
H	-3.25820000	1.87692500	-0.87945200
H	-1.34684200	1.97819000	-0.12366000
C	3.47479300	-1.48226900	-0.14388500
C	4.61292000	-1.60380700	0.83111500
H	4.25387300	-1.51639700	1.86827500
H	5.12507600	-2.56799500	0.71154400
H	5.35394300	-0.80297200	0.68108300
C	-3.97793700	-1.67884900	1.36476500
H	-4.58790900	-2.58349000	1.50296900
H	-2.99041800	-1.85973800	1.81735900
H	-4.45844100	-0.85463000	1.91534100
C	-5.19909600	1.18357400	-0.33157900
H	-5.49530600	0.81413800	-1.32455700
H	-5.71993500	0.58903100	0.43293900
H	-5.55135800	2.22063700	-0.24088600
O	2.96852500	3.31623500	0.25055800

C	3.25356100	-2.39487200	-1.10379800
H	2.45010300	-2.28081900	-1.83598400
H	3.90136600	-3.27137100	-1.19615800

AcOH optimized geometry (# opt=calcfc freq scrf=(smd,solvent=water) def2svp mn15)

EE + Thermal Free Energy Correction: -228.619163 Ha

0 1

O	0.62449500	1.20494600	0.00000400
C	0.08661900	0.11477100	-0.00002500
O	0.79023000	-1.02395600	-0.00000400
C	-1.38856300	-0.12297700	-0.00001000
H	-1.66265600	-0.71398900	-0.88528200
H	-1.66277300	-0.71245000	0.88626100
H	-1.92272200	0.83250300	-0.00081800
H	1.74201500	-0.80475000	0.00005500

PPG 6 (S_1) optimized geometry (# opt=calcfc freq td=(root=1) scrf=(smd,solvent=water) def2svp mn15)

EE + Thermal Free Energy Correction: ***H_6*-6**: -1052.881811Ha (+72.3 kcal/mol) / ***d_6*-6**: -1052.902115 (+59.6 kcal/mol)

0 1

C	-1.82438900	0.95217500	0.08152400
C	-2.04797200	2.32203500	-0.21205000
C	-1.01955600	3.26760800	-0.41849300
O	0.29660800	2.80707000	-0.33217900
C	0.57964200	1.49611800	-0.06859800
C	-0.46210200	0.52446000	0.14291400
C	0.00335500	-0.81305900	0.39021100
C	1.33815000	-1.14229300	0.45097700
C	2.35520000	-0.15435600	0.26031200
N	3.68066300	-0.45137800	0.32899700
C	4.12080300	-1.83445500	0.47683100
C	4.66403700	0.58436300	-0.01276200
C	1.91530800	1.17971300	-0.01561400
H	-3.05544300	2.72966600	-0.29330500
H	-0.72671700	-1.60825800	0.52670800
H	1.60389300	-2.18156200	0.63793300
H	5.12317500	-1.82712900	0.91903100
H	3.47443400	-2.33743800	1.20780800
H	4.47643700	0.90975400	-1.05171200
H	4.46688200	1.46236500	0.62179100
H	2.61864500	1.99194300	-0.18926300
C	-2.98044800	0.02064100	0.39385400
O	-2.75280100	-1.13837300	-0.46915200
C	-3.45679800	-2.26968800	-0.40340900
O	-4.41501000	-2.44392100	0.32586400
C	-2.90337000	-3.30102600	-1.33861700
H	-3.55631400	-4.18002600	-1.35638300
H	-2.79898500	-2.87636300	-2.34605400
H	-1.89825100	-3.58981400	-0.99589100
C	-4.33375600	0.62014100	0.03463000
H	-4.35830900	0.93211200	-1.01916100
H	-5.11908200	-0.12579000	0.20792800
H	-4.54572600	1.49237800	0.66773500
C	4.13154100	-2.58538300	-0.84888100

H	4.47587500	-3.61732600	-0.69144000
H	3.12332000	-2.61767500	-1.28896200
H	4.80811500	-2.09958500	-1.56801500
C	6.11627100	0.18438400	0.14284900
H	6.36245500	-0.08121800	1.18076500
H	6.39670100	-0.65059400	-0.51479400
H	6.73386400	1.04941300	-0.13545700
O	-1.13539700	4.47337200	-0.66984700
C	-2.94649000	-0.36439500	1.87588000
H	-2.00701700	-0.86757400	2.14358800
H	-3.01837700	0.56114800	2.46542200
H	-3.78796500	-1.01585700	2.14190700

PPG 6 (S_1 het. TS) optimized geometry (# opt=calcfc freq td=(root=1) scrf=(smd,solvent=water) def2svp mn15)

EE + Thermal Free Energy Correction: ***H_6*-6**: -1052.865813 Ha (+82.3 kcal/mol) / ***d_6*-6**: 1052.885990 Ha (+69.7 kcal/mol)

0 1

C	-1.75968300	1.04283100	0.28727500
C	-1.96725200	2.30743200	-0.30038600
C	-0.91763300	3.21969900	-0.60426700
O	0.38225400	2.81117100	-0.32783900
C	0.65717700	1.51444400	-0.01927800
C	-0.38319200	0.58089700	0.26479900
C	0.02165800	-0.77788200	0.41931000
C	1.33899500	-1.15800000	0.42913900
C	2.38363500	-0.18514600	0.25475500
N	3.68825900	-0.52401100	0.30320500
C	4.09487700	-1.92117200	0.45067500
C	4.70829000	0.49058400	-0.01403800
C	1.98713700	1.16198200	-0.00899700
H	-2.97024100	2.69602500	-0.48004200
H	-0.75064400	-1.53964400	0.51276500
H	1.57743700	-2.21273100	0.55099100
H	5.08917700	-1.93454200	0.90959400
H	3.42588200	-2.41140500	1.16804800
H	4.53223300	0.83501600	-1.04703800
H	4.52942800	1.35822600	0.63813900
H	2.71047100	1.94550000	-0.22424300
C	-2.84725900	0.24328900	0.78850300
O	-2.85899900	-1.15090700	-0.56905900
C	-3.69980200	-2.12834900	-0.57573600
O	-4.59962600	-2.31767800	0.25527100
C	-3.48845000	-3.11322300	-1.70865900
H	-4.38345200	-3.73085500	-1.85368100
H	-3.22732100	-2.58826200	-2.63682100
H	-2.64440200	-3.77016600	-1.44815500
C	-4.23343900	0.78755700	0.60641500
H	-4.42984900	1.05834100	-0.43975100
H	-4.97107300	0.04207900	0.92536300
H	-4.35563800	1.69236000	1.22555700
C	4.11039600	-2.65799400	-0.88130900

H	4.43762100	-3.69559100	-0.72690100
H	3.10711000	-2.67161100	-1.33328000
H	4.80275400	-2.17699800	-1.58816200
C	6.14641600	0.04412400	0.14173200
H	6.38235400	-0.23906400	1.17714300
H	6.40470300	-0.79010300	-0.52544000
H	6.78829700	0.89480600	-0.12528100
O	-1.03363000	4.35793900	-1.05098600
C	-2.66233500	-0.54021600	2.05873200
H	-1.61663000	-0.76399900	2.29798800
H	-3.06833300	0.07196700	2.88200500
H	-3.24490600	-1.47060300	2.02766100

PPG 6 (S_1 ion pair) optimized geometry (# opt=calcfc freq td=(root=1) scrf=(smd,solvent=water) def2svp mn15)

EE + Thermal Free Energy Correction: **H_6-6**: -1052.881458 Ha (+72.5 kcal/mol) / ***d_6*-6**: 1052.901481 Ha (+60.0 kcal/mol)

0 1

C	-1.85666800	0.91497700	0.57373300
C	-2.20798100	2.09784900	-0.04168900
C	-1.23767900	3.04410000	-0.55192300
O	0.08832500	2.72493100	-0.40653200
C	0.48743500	1.49288500	0.01086000
C	-0.45625800	0.53370600	0.46683600
C	0.02699000	-0.78427300	0.70216100
C	1.35768200	-1.08968300	0.62782200
C	2.32481700	-0.07540700	0.28722200
N	3.64038800	-0.34211900	0.24844000
C	4.14008900	-1.70132500	0.46748600
C	4.57779600	0.69594300	-0.22418700
C	1.83262700	1.22306900	-0.05883200
H	-3.24450100	2.43614600	-0.08753400
H	-0.69558900	-1.57740400	0.89506200
H	1.66974200	-2.11648900	0.80400600
H	5.16592300	-1.62380600	0.84184000
H	3.55939600	-2.16806800	1.27097600
H	4.30618900	0.94146400	-1.26354200
H	4.39361500	1.60072000	0.37249900
H	2.48670300	2.01795500	-0.41046600
C	-2.82747400	0.11947600	1.26733000
O	-2.29813700	-1.19263100	-1.56237900
C	-3.04138200	-2.07681200	-1.06091900
O	-2.74670500	-2.81191500	-0.07826700
C	-4.41139700	-2.29897600	-1.69541100
H	-5.19225100	-2.26996900	-0.92104800
H	-4.62647000	-1.55043100	-2.46920100
H	-4.44274400	-3.30263700	-2.14668700
C	-4.26312400	0.21974000	0.88782200
H	-4.39115800	0.39212700	-0.19056400
H	-4.79137400	-0.70260700	1.17090900
H	-4.75354300	1.05190100	1.42540200
C	4.09292100	-2.53256600	-0.80614800

H	4.49678700	-3.53464100	-0.60676300
H	3.05903800	-2.63733600	-1.16792200
H	4.69401800	-2.06714300	-1.60121300
C	6.04625900	0.33869200	-0.14509600
H	6.37292000	0.15100600	0.88730200
H	6.30473900	-0.52922000	-0.76767300
H	6.61467500	1.19953700	-0.52281400
O	-1.50051800	4.12245900	-1.04653700
C	-2.49848200	-0.68066300	2.47677400
H	-1.48802200	-0.49898000	2.86437600
H	-3.22995900	-0.44654400	3.26776300
H	-2.61158800	-1.75788100	2.26289500

PPG 6 (elim. TS) optimized geometry (# opt=(calcfc,ts,noeigentest) freq td=(root=1) scrf=(smd,solvent=water) def2svp mn15)

EE + Thermal Free Energy Correction: ***H*$_6$-6**:-1052.866549 Ha (+81.9 kcal/mol) / ***d*$_6$-6**: 1052.883172 Ha (+71.5 kcal/mol)

0 1

C	-1.97753500	1.16320900	0.39556700
C	-2.21727800	2.35944500	-0.30391800
C	-1.19354200	3.26799300	-0.70830200
O	0.11431100	2.91739100	-0.41893600
C	0.42595900	1.65561700	-0.02029400
C	-0.58446400	0.72256400	0.36027700
C	-0.14365900	-0.61490900	0.57478600
C	1.18138900	-0.96593400	0.56079400
C	2.19906700	0.01869900	0.30872500
N	3.50947800	-0.28745300	0.34755000
C	3.95336600	-1.66489200	0.56400800
C	4.50057000	0.73356000	-0.03870800
C	1.76415700	1.33747900	-0.02355600
H	-3.23062000	2.71449100	-0.49339900
H	-0.87795800	-1.39804000	0.74878800
H	1.44634200	-2.00734600	0.73077700
H	4.95457700	-1.62857800	1.00596400
H	3.30764900	-2.13164100	1.31703900
H	4.30090300	1.01585600	-1.08566100
H	4.30676700	1.62922000	0.56932300
H	2.46071200	2.12190700	-0.31132600
C	-3.03722800	0.45751100	1.03560400
O	-2.81332300	-1.58092600	-1.30390400
C	-2.74508000	-2.68481900	-0.74965800
O	-2.78677600	-2.86198000	0.53458700
C	-2.57293000	-3.95262100	-1.55111100
H	-1.54115000	-4.31334600	-1.42243700
H	-3.24397300	-4.73582100	-1.17337700
H	-2.75873700	-3.76660100	-2.61562300
C	-4.44019600	0.85538200	0.68559000
H	-4.59775800	0.82373000	-0.40526000
H	-5.16617900	0.18669800	1.16537700
H	-4.66006200	1.88623100	1.01023100
C	3.96594600	-2.46874100	-0.72815700

H	4.32497700	-3.48733300	-0.52611800
H	2.95552400	-2.53302000	-1.15924900
H	4.63192400	-2.00641300	-1.47177000
C	5.95112100	0.33106500	0.11940600
H	6.20751400	0.10702000	1.16430000
H	6.22202800	-0.52909800	-0.50870000
H	6.56713100	1.18294900	-0.19948000
O	-1.35236100	4.35665700	-1.24644600
C	-2.86022700	-0.63064400	1.93502000
H	-1.90129500	-0.70925900	2.46323000
H	-3.72960700	-0.83369000	2.57365900
H	-2.85647400	-1.74465300	1.17202100

PPG 6 (elim. pair) optimized geometry (# opt=calcfc freq td=(root=1) scrf=(smd,solvent=water) def2svp mn15)

EE + Thermal Free Energy Correction: -1052.880766 Ha (+73.0 kcal/mol)

0 1

C	-1.97338400	1.13299100	0.52609000
C	-2.26364300	2.26123600	-0.29578000
C	-1.28614700	3.15105500	-0.79269400
O	0.04844700	2.86783600	-0.47949500
C	0.39504600	1.63194700	-0.02179900
C	-0.58847900	0.72029500	0.48402300
C	-0.10067500	-0.58354900	0.80841100
C	1.23126100	-0.91250600	0.76947100
C	2.21544000	0.05099100	0.36276600
N	3.53842000	-0.23146500	0.36178500
C	4.01448200	-1.57410500	0.68720000
C	4.47988300	0.75224200	-0.19546800
C	1.73520000	1.32487500	-0.06931700
H	-3.29191900	2.54007700	-0.53001600
H	-0.81482500	-1.35683100	1.08900600
H	1.52435300	-1.92573700	1.03828200
H	5.04352800	-1.48838900	1.05275300
H	3.42868300	-1.96275200	1.52952700
H	4.20678900	0.92639000	-1.25050700
H	4.31509100	1.70676000	0.32717400
H	2.40383300	2.09170100	-0.45538200
C	-3.02560300	0.43037100	1.23342000
O	-2.56723900	-1.47525200	-1.40863900
C	-2.68063900	-2.60575000	-0.96934000
O	-2.94673600	-2.85264800	0.31543800
C	-2.54142400	-3.85427900	-1.77956300
H	-1.70048300	-4.44542000	-1.38956500
H	-3.44926400	-4.46411700	-1.67222400
H	-2.37088300	-3.60365800	-2.83147300
C	-4.43519600	0.67119800	0.75467400
H	-4.51678000	0.47901800	-0.32758500
H	-5.14391700	0.02070800	1.28460600
H	-4.74454900	1.71574900	0.91953800
C	3.94982000	-2.51683800	-0.50655500
H	4.32704700	-3.50833400	-0.21920500

H	2.91484200	-2.62782400	-0.86373700
H	4.56409500	-2.13950200	-1.33778700
C	5.94521500	0.38368100	-0.09992400
H	6.27790800	0.27375900	0.94196500
H	6.18619500	-0.53630900	-0.65096200
H	6.52454700	1.20185400	-0.54943100
O	-1.46089300	4.18393000	-1.44678200
C	-2.82464500	-0.40341500	2.29790100
H	-1.84342900	-0.55897800	2.75069400
H	-3.68211600	-0.86992700	2.79064700
H	-2.99539900	-2.00155100	0.81590700

5. k_2 diffusion barrier estimation through R^2 maximization

The DFT-calculated barriers in the excited state shown below (table S3) were used (kcal/mol): [1]

Compound	**1**	**2**	**3**	**4**	**5**	**6**
$\Delta G^{\ddagger}_{k1}$	12.00	9.63	6.82	7.18	6.78	10.04
$\Delta G^{\ddagger}_{k-1}$	2.23	3.27	12.51	13.74	15.60	9.82
$\Delta G^{\ddagger}_{k2}$	x	x	x	x	x	**9.36**
$\Delta G^{\ddagger}_{k-1} / (\Delta G^{\ddagger}_{k1} * \Delta G^{\ddagger}_{k2})$	0.186/x	0.340/x	1.834/x	1.914/x	2.301/x	**0.104**

Table S 3. The DFT-calculated energy barriers of the photolysis of coumarins **1** – **6** in S1 in kcal/mol**.**

Only for tertiary coumarin **6**, a $\mathbf{k_2}$ barrier of deprotonation was known (calculated by TD-DFT, see section 4). The diffusion barrier for PPGs **1** - **5** was left as a variable. For all compounds **1** - **6**, the ratio of $\Delta G^{\ddagger}_{k-1} / (\Delta G^{\ddagger}_{k1} * \Delta G^{\ddagger}_{k2})$ was calculated. For compound **6** this yielded a value of 0.104. For the other compounds, this yielded a value that was still to be divided by a variable x. The energy barrier ratios were plotted against the Ln QY[1], with the diffusion barrier height initially being estimated at 10 kcal/mol. (x = 10 kcal/mol).

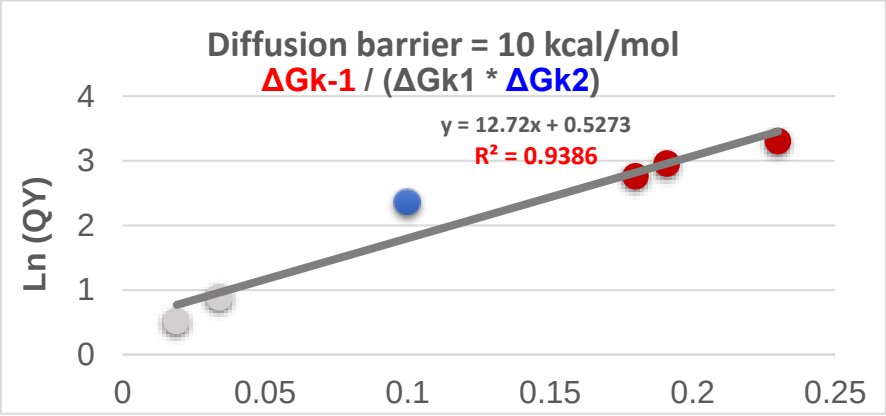

Figure S 128. The correlation of the energy barrier ratio and the Ln QY for coumarins **1 – 6**, when the k_2 diffusion barrier is estimated at 10 kcal/mol.

The quantum yield of tertiary coumarin **6** could be found above the linear correlation (figure S128, blue point), indicating that the estimated diffusion barrier was too low. When the diffusion barrier was estimated at 20 kcal/mol, the QY of **6** could be found below the linear fit (figure S129, blue point).

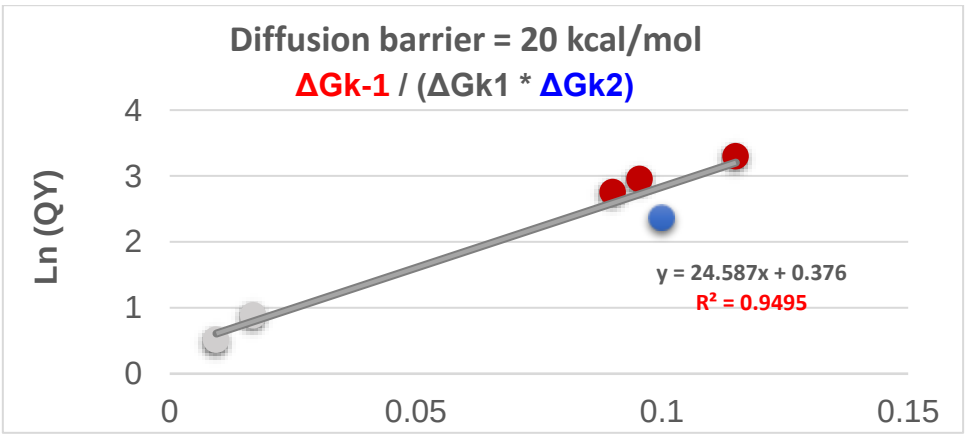

Figure S 129**.** The correlation of the energy barrier ratio and the Ln QY for coumarins **1 – 6**, when the k_2 diffusion barrier is estimated at 20 kcal/mol.

Using the plugin solver from MS Excel, the R^2 of the correlation could be maximized numerically through varying x (the $\mathbf{k_2}$ diffusion barrier), yielding the following correlation (figure S130)

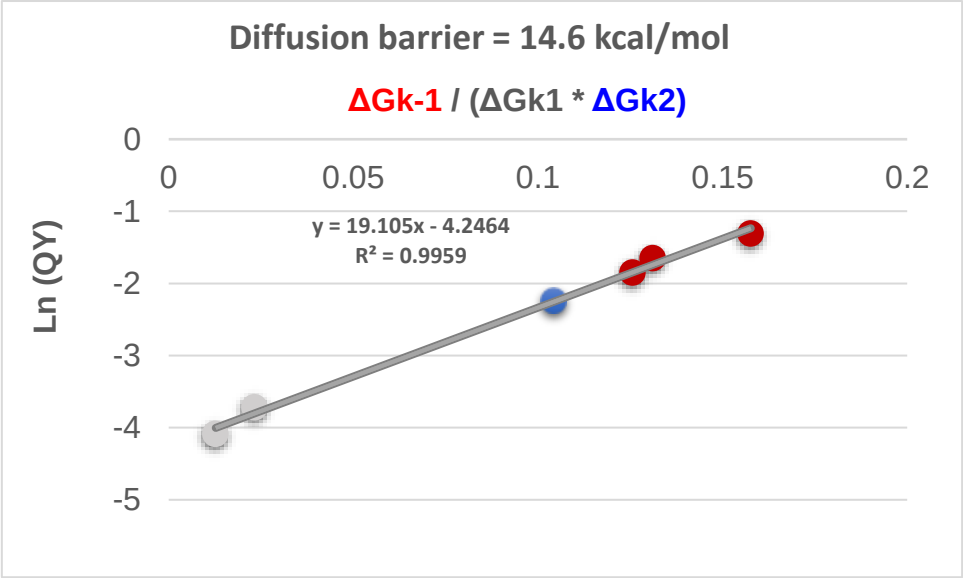

Figure S 130. The correlation of the energy barrier ratio and the Ln QY for coumarins **1 – 6**, when the k_2 diffusion barrier is optimized at 14.6 kcal/mol.

Using only the $\mathbf{k_{-1}}$ / $\mathbf{k_2}$ ratio and maximizing R^2 numerically through using Solver, a lower $\mathbf{k_2}$ diffusion barrier of 10.3 kcal·mol^{-1} was found (figure S131).

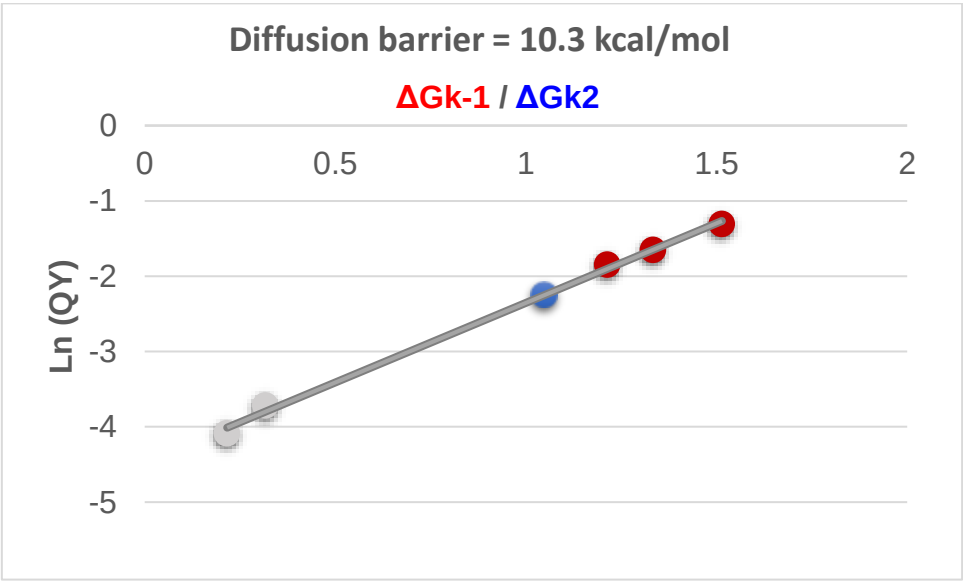

Figure S 131**.** The correlation of the energy barrier ratio and the Ln QY for coumarins **1 – 6**, when excluding the calculated values for k_1. The k_2 diffusion barrier is optimized at 10.3 kcal/mol.

Despite the strong correlation, it seems incomplete to leave one of the barriers of coumarin photolysis out of the analysis, although the magnitude of the $\mathbf{k_1}$ barrier might be of less importance since it could be partially overcome through excitation to a higher vibrational state in S_1. Nonetheless, the actual $\mathbf{k_2}$ diffusion barrier might lie somewhere between the two found values of 10.3 and 14.6 kcal·mol^{-1}.

6. Prediction of the Quantum Yield of 6-D_6

The obtained strong correlation of the QYs to the energy barrier ratios yielded the following formula (equation S1).

$$Ln\ QY = 19.105\ x - 4.2464 \qquad in\ which\ x = \frac{\Delta \boldsymbol{G}^{\ddagger}_{\boldsymbol{-1}}}{\Delta \boldsymbol{G}^{\ddagger}_{\boldsymbol{1}} \times \Delta \boldsymbol{G}^{\ddagger}_{\boldsymbol{2}}}$$

Equation S1. Formula correlating Ln QY to the energy barrier ratio x

This formula was rewritten by raising both sides through the power of e (equation S2).

$$Ln\ QY = 19.105\ x - 4.2464\ \rightarrow\ \ QY = e^{19.105\ x - 4.2464}$$

$$\rightarrow\ QY = 0.0143 \times e^{19.105x}$$

Equation S2. Rewritten formula correlating the QY to the energy barrier ratio x

Using this formula, from the calculated energy barrier x the Quantum Yield could be predicted. For Coumarin PPG **6-D_6**, the following energy barriers were calculated by DFT (Table S4).

Compound	**6-D_6**
$\Delta G^{\ddagger}_{k1}$	10.12
$\Delta G^{\ddagger}_{k-1}$	9.72
$\Delta G^{\ddagger}_{k2}$	11.49
$\Delta G^{\ddagger}_{k-1}$ / ($\Delta G^{\ddagger}_{k1}$*$\Delta G^{\ddagger}_{k2}$)	0.0836

Table S 4**.** The DFT-calculated energy barriers of the photolysis of coumarin **6-D_6** in S1**.**

From the calculated energy barriers, the energy barrier ratio **$\Delta G^{\ddagger}_{k-1}$ / ($\Delta G^{\ddagger}_{k1}$*$\Delta G^{\ddagger}_{k2}$)** could be determined at 0.0836. Filling in this value into equation S2 yielded a predicted QY of 7.06 % (equation S3), a value very close to the measured QY of 7.0 ± 0.4 % (see figure S112).

$$QY = 0.0143 \times e^{19.105\ *0.0836}\ = 0.0706$$

Equation S3. Prediction of the photolysis QY of **6-D_6** through filling in the calculated energy barrier ratio into equation S2.

7. References

1. Schulte, A. M., Alachouzos, G., Szymański, W. & Feringa, B. L. Strategy for Engineering High Photolysis Efficiency of Photocleavable Protecting Groups through Cation Stabilization. *J Am Chem Soc* **144**, 12421–12430 (2022).

2. Weinrich, T., Gränz, M., Grünewald, C., Prisner, T. F. & Göbel, M. W. Synthesis of a Cytidine Phosphoramidite with Protected Nitroxide Spin Label for EPR Experiments with RNA. *European J Org Chem* **2017**, 491–496 (2017).

3. Stranius, K. & Börjesson, K. Determining the photoisomerization quantum yield of photoswitchable molecules in solution and in the solid state. *Sci Rep* **7**, 1–9 (2017).

4. Marenich, A. V., Cramer, C. J. & Truhlar, D. G. Universal solvation model based on solute electron density and on a continuum model of the solvent defined by the bulk dielectric constant and atomic surface tensions. *Journal of Physical Chemistry B* **113**, 6378–6396 (2009).

5. Zheng, J., Xu, X. & Truhlar, D. G. Minimally augmented Karlsruhe basis sets. *Theor Chem Acc* **128**, 295–305 (2011).

6. Yu, H. S., He, X., Li, S. L. & Truhlar, D. G. MN15: A Kohn–Sham global-hybrid exchange–correlation density functional with broad accuracy for multi-reference and single-reference systems and noncovalent interactions. *Chem Sci* **7**, 5032–5051 (2016).